University of Montana
ScholarWorks at University of Montana

Graduate Student Theses, Dissertations, & Professional Papers

Graduate School

2019

MULTINUCLEATED GIANT CELL FORMATION AND PHENOTYPE

Kevin Lewis Trout
University of Montana - Missoula

Let us know how access to this document benefits you.

Follow this and additional works at: https://scholarworks.umt.edu/etd

Recommended Citation

Trout, Kevin Lewis, "MULTINUCLEATED GIANT CELL FORMATION AND PHENOTYPE" (2019). *Graduate Student Theses, Dissertations, & Professional Papers*. 11448.
https://scholarworks.umt.edu/etd/11448

This Dissertation is brought to you for free and open access by the Graduate School at ScholarWorks at University of Montana. It has been accepted for inclusion in Graduate Student Theses, Dissertations, & Professional Papers by an authorized administrator of ScholarWorks at University of Montana. For more information, please contact scholarworks@mso.umt.edu.

MULTINUCLEATED GIANT CELL FORMATION AND PHENOTYPE

By

KEVIN LEWIS TROUT

B.S. Biochemistry & Biology, The College of Saint Scholastica, Duluth, MN, 2011

Dissertation

presented in partial fulfillment of the requirements
for the degree of

Doctor of Philosophy
in Biomedical Sciences

University of Montana
Missoula, MT

August 2019

Approved by:

Scott Whittenburg,
Graduate School Dean

Andrij Holian, Ph.D., Chair
Department of Biomedical and Pharmaceutical Sciences

Keith Parker, Ph.D.
Department of Biomedical and Pharmaceutical Sciences

Howard Beall, Ph.D.
Skaggs School of Pharmacy

Elizabeth Putnam, Ph.D.
Department of Biomedical and Pharmaceutical Sciences

Horst von Recum, Ph.D.
Department of Biomedical Engineering
Case Western Reserve University, Cleveland, OH

© COPYRIGHT

by

Kevin Lewis Trout

2019

All Rights Reserved

Abstract

Trout, Kevin, Ph.D., August 2019 Biomedical Sciences

Multinucleated Giant Cell Formation and Phenotype

Chairperson: Holian, Andrij, Ph.D.

Multinucleated giant cells (MGC) are homotypic macrophage syncytia associated with granulomas. Despite their correlation with pathology, MGC functional contributions to inflammation are relatively unknown. The objective of this work was to gain an understanding of MGC phenotype. First, techniques were developed to better enable the study of these cells *in vitro*. Second, inorganic particles known to cause inflammation were observed to cause MGC formation in the lungs. Finally, the particle that resulted in the highest macrophage fusion was used together with the *in vitro* system to compare MGC and macrophage phenotype in response to stimulation. The results contribute to fundamental MGC cell biology knowledge that is important toward developing approaches to control the foreign body response and understanding the role of MGC in granulomatous disease.

Acknowledgements

I was fortunate to have such a great advisor for my graduate research. Dr. Holian leads with professionalism and works hard to always be available when his students need help. Thanks for supporting my independence, valuing my scientific ideas, and believing in me to finish the PhD.

I appreciate the time spent by other members of my advisory committee to assist in my progress and assessment. I would like to thank Dr. Migliaccio and Dr. Jessop (co-authors on published book chapters) for their involvement with my research. Thanks to the Department of Biomedical & Pharmaceutical Sciences and the Center for Environmental Health Sciences for research and administrative support. Also, it is important to recognize financial support from the University of Montana and federal funding for science.

I enjoyed working alongside and learning from the other researchers in the department, especially those in the Holian laboratory group. Members of the lab group create a great culture of teamwork and maintain high spirits even when experiments get frustrating. Other fellow students in the department have made my entire experience much more enriching and enjoyable. I would also like to give a special thanks to the past participants in our summer undergraduate research program.

There are others that I would like to thank for influencing my decision to attend graduate school in the first place. The College of St. Scholastica faculty and McNair Scholars program played an important role in my professional development and motivation to pursue research. My first in-depth experience working on a biomedical research project was during the Research in Science and Engineering (RiSE) and Research Experience for Undergraduates in Cellular Bioengineering (REU-CB) programs at Rutgers/UMDNJ. Thank you to my mentor there, Dr. Langrana, and members of his laboratory.

Thanks to my friends for the good times and fun trips exploring the natural beauty of Montana. Thanks to my girlfriend for providing some balance in life and encouraging me to get my work done. Thanks to my family members for dealing with me often being away. Lastly, I am immensely grateful for the two most important mentors in my life: my parents.

Additional Acknowledgements:
Refer to the end of each Chapter 2, 3, and 4 for acknowledgements specific to each project.

Contents

List of Figures

List of Tables

Chapter 1

Introduction

Multinucleated giant cell (MGC):
a homotypic macrophage syncytium
associated with granulomas.

This chapter provides an introduction to multinucleated giant cells (MGC) and the macrophages from which they are formed. First, macrophage biology, developmental origins, and functional classification will be described. Next, MGC will be introduced with an overview of morphological identification, phenotype, and pathological associations. The role of these cells in the foreign body response is discussed, particularly in response to particulate exposures.

1.1 Macrophages

It is important to note that macrophage behavior *in vivo* cannot be fully explained by studies *in vitro*. From all that has been learned, we know that the macrophage is a complex cell in a very complex environment. The environment defines the cell, and the macrophage is altered when the environment is perturbed either by a toxic exposure or by any manipulation to study the tissue. Consequently, our best information always has room for error. In addition, there is much that we do not know about the macrophage response to toxic exposures and the macrophage's role in pathogenesis.

Macrophages are derived from bone marrow stem cells. The monoblasts mature to promonocytes and then to monocytes. Monocytes remain in the bone marrow for a short period and move into the circulatory system where they remain for 36-104 h [1]. From there monocytes enter the tissue and mature into macrophages. Once in the tissue, macrophages are relatively long-lived cells with a lifetime in the order of months [2]. Maturation of monocytes to macrophages is driven by a combination of at least three factors: (i) genetic programming, (ii) growth factors/cytokines, and (iii) the environment of the tissue. The extent of the effect of the environment on cell maturation is a recent area of research. Current thought is that the environment, growth factors and cytokines all contribute to the macrophage phenotype.

The term "big eater" was coined by Metchnikoff in 1892 to describe the phagocytic function of the macrophage, which is still considered one of the most important functions of the macrophage. This includes recognition and, if possible, degradation of foreign material. The macrophage is well suited for this activity, as it possesses a large number of receptors functionally linked to phagocytosis, such as immunoglobulin, complement, and scavenger receptors. Since macrophages are relatively large cells, they can accommodate ingested material. Macrophages are mobile cells capable of responding to various chemotactic factors. They can release superoxide anion and proteolytic enzymes to kill and/or digest microbes, and can present digested peptide fragments with the major histocompatibility complex (MHC) to trigger an immune response [3–6]. Finally, they can release various mediators to: (i) recruit additional phagocytic cells (polymorphonuclear neutrophils, monocytes, and macrophages); (ii) stimulate maturation of phagocytic cells; and (iii) modulate the function of other local cells to respond to the adverse condition. A major function of macrophages is regulatory in nature, in that as a front-line immune responder, it affects the subsequent nature of the response. Therefore, the nature, or phenotype, of the macrophage can have a profound effect on the outcome of an immune

response. In the context of exposure to foreign material (i.e particles), the outcome is dictated by the local macrophage content, which may be dominated by one or several different subsets at any given time.

The term macrophage has occasionally been used to describe monocytes and monocyte-derived cells in culture. This is a misnomer that can create confusion. The term macrophage should be used to describe tissue mononuclear phagocytic cells, and monocytes should be used to describe the circulating mononuclear precursor cells. Since mononuclear-derived cells *in vitro* may not adequately describe the true macrophage [7, 8] in part for the preceding reasons, they should be clearly distinguished.

Blood monocytes are larger than lymphocytes, have a rounded shape and have a nuclear/cytoplasmic ratio of approximately one. They often present with a bean-shaped nucleus with considerable margination of heterochromatin. Macrophages are larger cells, have many lamellapodia, many subsurface vacuoles and an irregularly indented nucleus with little heterochromatin. Macrophages also have more rough endoplasmic reticulum, coated vesicles, lysosomes, and microtubules than monocytes. The macrophage nuclear/cytoplasmic volume ratio is less than one. Consequently, the cells are easily distinguished morphologically.

1.2 Developmental origins

Originally, tissue macrophages were thought to solely be derived from bone marrow stem cells. In this process, pluripotent hematopoietic stem cells (HSC) in the bone marrow differentiate into multiple precursors, one of which, the common myeloid progenitor, gives rise to granulocytes and monocytes. A continuum of monocyte translocation from the circulation and differentiation within the target tissue was considered the primary mechanism responsible for replacement of resident tissue macrophages. New evidence reporting resident tissue macrophages in multiple organ systems originating from the yolk sac during

embryonic development has caused a paradigm shift in our understanding of macrophage biology [9, 10]. Furthermore, macrophages have recently been shown to self-maintain resident tissue populations by local proliferation [11]. A summary of macrophage origin is shown in Fig. 1.

1.2.1 Bone marrow-derived

HSC derived macrophages remain an important contributor to immunity as well as responses to toxic exposure. In the bone marrow, macrophage-dendritic progenitors mature to committed monocyte progenitors and then to monocytes. Monocytes remain in the bone marrow for a short period and move into the circulatory system where they remain for 36-104 h [12]. Circulating monocytes, which constitute about 5-10% of circulating leukocytes, were originally described by the surface expression of CD14 [13]. However, multiple monocyte populations are currently described in humans and animals based on additional surface marker expression and generally fall in to one of two categories: inflammatory monocytes and resident monocytes [14]. From the circulation, monocytes enter tissue and mature into macrophages. Specialized HSC-derived macrophages can be recruited to tissues following infection or toxic exposure, where they play a critical role in the inflammatory and immune response.

1.2.2 Yolk sac-derived

Recent studies using Cre-loxP-based fate-mapping and parabiotic mice have shown that HSC-derived macrophages contribute very little to maintaining resident tissue macrophage populations during “steady state” homeostasis [15, 16]. During embryonic development, hematopoiesis occurs in the yolk sac in two phases: the primitive stage, which is primarily myeloerythroid development, and the definitive stage, which includes generation of HSC.

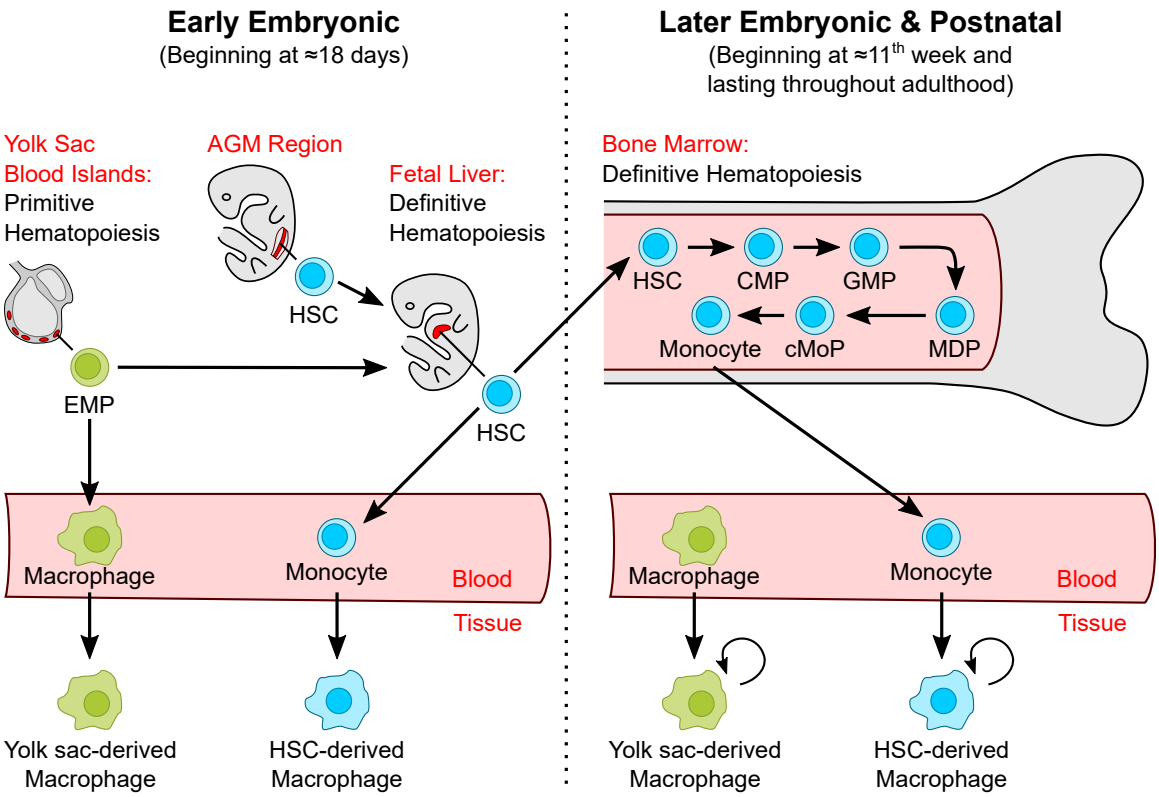

Fig. 1. Macrophage origins. Primitive hematopoieses begins in the yolk sac blood islands at approximately 18 days estimated gestational age, during which erythro-myeloid progenitors (EMP) differentiate into macrophages [19]. EMP from yolk sac and hematopoietic stem cells (HSC) from the aorta-gonad-mesonephros (AGM) region colonize the fetal liver. Other embryonic hematopoietic sites may exist that are not shown here, such as large arteries and the placenta. Early definitive hematopoiesis occurs in the fetal liver, where HSC differentiate into monocytes. Monocytes differentiate into macrophages as they move from blood into tissue. HSC from the fetal liver colonize bone marrow, where hematopoiesis begins during approximately the 11th week [20] and continues throughout adulthood. Several unique myeloid progenitor cell intermediates have been identified, including common myeloid progenitors (CMP), granulocyte-macrophage progenitors (GMP), macrophage-dendritic progenitors (MDP), and committed monocyte progenitors (cMoP). Eventually, monocytes formed in the bone marrow exit into the circulation. Monocytes differentiate into macrophages as they move from blood into tissue. Relative populations of yolk sac-derived and HSC-derived macrophages in the tissue vary depending on the organ system. Both macrophage types have the capacity for self-replication, but their extent of replication varies with certain factors such as the inflammatory environment.

Author's own work; reprinted/adapted by permission from Elsevier. 15.07 - Inflammatory Cells of the Lung: Macrophages by Forrest Jessop, Kevin L. Trout, Andrij Holian, and Christopher Migliaccio 2018. https://doi.org/10.1016/B978-0-12-801238-3.95651-4.

At mouse embryonic day 10 (E10), yolk sac hematopoietic progenitors cells colonize the fetal liver, which then becomes a central hematopoietic tissue for all lineages [17, 18]. The majority of adult tissue macrophages, for most tissues including the liver, brain, epidermis, and lung originate from erythro-myeloid progenitors coming from the fetal liver and not HSCs from the bone marrow. Resident adult tissue macrophages from fetal yolk sac origin are considered more specialized to the physiological function of the organ. For example, alveolar macrophages express high levels of pattern-recognition receptors and scavenger receptors, and are more adapt to surveillance of the alveolar spaces, phago-cytosis, and particle clearance. Furthermore, there is evidence that yolk sac derived tissue macrophages maintain lung resident populations independent of factors that cause bone marrow recruitment of monocytes such as CCR2 [15].

In support of the *in situ* proliferation mechanism, colony stimulating factors have been reported to induce proliferation of macrophages *in vitro* [21, 22]. In addition, Bitterman *et al*. [23] have shown that 0.5% of alveolar macrophages incorporate ^{3}H-thymidine which could increase under chronic inflammation. This is a low frequency event and therefore difficult to capture at one time point. It may also vary in importance between humans and animal models. There is evidence that under steady state conditions, pulmonary macrophages self-renew without addition from circulating monocytes, and there is a slow turn over rate (40-60% replacement in one year) [24, 25]. Some studies designed with specific irradiation protocols further support the self-renewel hypothesis [26].

Maturation of monocytes to macrophages or progenitor resident macrophages to tissue specific macrophages is driven by a combination of at least three factors: (i) genetic programming, (ii) growth factors/cytokines, and (iii) the environment of the lung tissue. Tissue macrophages adapt specialized functions based on the tissue of residence [27]. The extent of the effect of the environment on cell maturation is not certain. It can be speculated, however, that the environment, growth factors and cytokines all contribute to the lung

macrophage phenotype.

1.3 'M' classification

Just a few decades ago macrophages were considered to have a relatively homogeneous phenotype. Macrophages were defined as mediators and regulators of inflammation, and that inflammation was generally considered to be Th1. This is characterized by a response involving classic inflammatory mediators: IFN-γ, TNF-α, IL-6, and IL-1β. However, recent research has determined that macrophages are subject to their environment and macrophage functions are altered by the local mix of signaling factors. Macrophages are now categorized based on phenotypes that are defined by the expression of surface markers, intracellular pathways, and soluble mediators.These categories are described using an 'M' nomenclature system [28–32]. There is no general consensus on macrophage polarization prior to induction of an inflammatory response. Original naming created the M1 and M2 macrophage subsets where the M1 was considered the Classic subset and the M2, by default, the alternatively-activated. Over time more subsets were defined when the M2 was further divided to account for different phenotypes, mechanisms of activation, and additional pathologies associated with atherosclerosis.

1.3.1 M1: classic

The "classical" nomenclature, labeled as the M1 subset, refers to the phenotype typically associated with macrophages: inflammatory cytokines, Th1-association, and antigen-presentation capability. This subset is most commonly generated with either IFN-γ or TLR-agonists [30, 31] (Table 1). Recent reports identify GM-CSF stimulation as a partial M1 agonist, specifically through its ability to enhance antigen presentation and many other M1 macrophage functions [33].

Subset	Activating Signals	Markers	References
M1	IFN-γ TLR signal	TNF-α IL-1β IL-6 IL-12 ROS, iNOS CD80/86 MHC II CXCL9 CXCL10 GM-CSF	[30, 33–37]
M2a	IL-4 IL-13	Ch3l3/Ym1 (mouse) FIZZ1/RELM (mouse) IL-1ra Arg-1 IL-10 CD206	[38–44]
M2b	FcγR ligation TLR signal	IL-1β IL-6 IL-10 TNF-α CD86 MHC II	[30, 37, 45]
M2c	TGF-β IL-10 glucocorticoids	TGF-β IL-10 CD163 TLR1 TLR8	[46–52]
M2d/TAM	IL-6 LIF M-CSF	VEGF	[44, 53–57]

Table 1. Macrophage subsets. Common activating signals and markers for each macrophage M-classification. This listing is not exhaustive.

Reprinted/adapted by permission from Springer Nature Customer Service Centre GmbH: Springer. Macrophage and Multinucleated Giant Cell Classification by Kevin L. Trout, Forrest Jessop, Christopher T. Migliaccio 2016. https://doi.org/10.1007/978-4-431-55732-6_1.

Function/phenotype

The M1 subset has a pro-inflammatory phenotype. This manifests in both the types of soluble mediators and surface proteins expressed upon activation. *Ex vivo* polarization of alveolar macrophages with IFN-γ induced changes in approximately 41 genes, specifically including increased expression of Toll Like Receptors and multiple CXCL chemokines [36]. In addition to the classic cytokines of IFN-γ, TNF-α, IL-6, and IL-1β, the M1 has been associated with production and release of IL-12p70, reactive oxygen species (ROS) and nitric oxide (NO) [34, 35]. This subset has also been described to express both MHC II and CD86 on the surface which are key for T lymphocyte activation (Table 1).

Disease associations

The M1 subset has been found to increase renal cell damage [50], as well as increase disease in the *mdx* mouse model of muscular dystrophy [58]. M1 is the dominant macrophage phenotype in infection (acute and chronic), and is thought to play a critical role in granuloma formation in tuberculosis [34]. In addition, the M1 has been described as the predominant phenotype associated with non-malignant tumor-associated macrophages (TAM) [59, 60], and aspects of the phenotype have been shown to prevent HIV-1 infection [61].

Interaction with particulates

In animal exposure models to particulates such as silica or nanomaterials, an initial Th1 response has been implicated in the pathology, specifically through IL-1 signaling [62, 63]. In addition, recent studies have described a role of M1 macrophages in the inflammatory response to joint replacement wear debris [64–67]. The usage of replacement joints leads to the generation of particulates that are categorized as wear products. Some have proposed skewing toward an M2a phenotype as a potential treatment for inflammation in worn joint replacement [65, 67].

1.3.2 M2a: Th2-associated

This subset was originally designated as the M2 or alternatively activated macrophage. However, as more phenotypes were characterized this subset was given the nomenclature of M2a and was described as being activated by the Th2-associated cytokines IL-4 and IL-13 [29–31, 44, 68]. The dependence of this subset on Th2 immunity was confirmed by studies using IL-4Rα null mice, where this protein is a key functional component of both the IL-4 and IL-13 receptors [69].

Function/phenotype

The M2a subset has a Th2-promoting phenotype. The production of several soluble mediators have been associated with the M2a phenotype and promoting of Th2 type of inflammation. While IL-10 and IL-1ra are more associated with an anti-Th1 inflammation type of activity, the release of Ym1/Chi3l3 has been found to induce Th2 responses [43]. In addition, the surface expression of CD206 is greatly increased in the M2a [44]. The M2a are also associated with increased intracellular expression of Arg-1 and FIZZ1, both of which had been a couple of the original markers used for identification of these cells [28, 70, 71] (Table 1).

Disease associations

Both M2a and M2c subsets have been found to increase type VI collagen and fibrosis in an adipocyte model [72]. Furthermore, the M2a phenotype has also been associated with pulmonary and renal fibrosis [50].

Interaction with particulates

Th2 immunity plays a well-accepted role in models of lung fibrosis. This is entirely consistent with the observed function of M2a macrophages in fibrosis and the therapeutic

rationale for targeting this subset. In studies comparing wild-type mice and IL-4Rα null mice, a significant increase in the M2a in wild-type, corresponded with the development of silica-induced pulmonary fibrosis. However, IL-4Rα null mice that lack the ability to generate the M2a had a significant decrease in the pathology [69].

1.3.3 M2b: alternatively activated

This subset is generated by the presence of antibody-antigen complexes [30, 45, 73]. Because these are also a pro-inflammatory type of macrophage their activation is via FcγR ligation in conjunction with a TLR signal.

Function/phenotype

The M2b subset has a pro-inflammatory phenotype that is similar to the M1. These macrophages produce the classic inflammatory cytokines IL-1β, TNF-α, and IL-6 in addition to the surface proteins MHC II and CD86 [30, 74] (Table 1). These markers suggest an ability and propensity to activate nearby immune cells either by contact or within the vicinity. However, a key difference between the M2b and the M1 is the finding that M2b also produces IL-10 [30, 74].

Disease associations

The M2b subset has been found to play a key role in the pathology in the murine model of lupus, and shifting macrophages to the M2a phenotype was shown to alleviate the disease [75]. M2b have also been found in circulation and peripheral tissues following severe burns, supporting a systemic activity for this subset [76, 77].

Interaction with particulates

Silicosis and asbestosis have been associated with autoimmune comorbidities, including lupus, which involve TLR signling and FcyR ligation [78, 79]. Though there are no reports on the M2b phenotype in particle exposure and associated disease, their involvement is likely.

1.3.4 M2c: regulatory

This subset is generated by the presence of classic anti-inflammatory mediators: TGF-β, IL-10, or glucocorticoids [51].

Function/phenotype

The M2c are categorized as regulatory, but have anti-inflammatory or immunosuppressive activity. This subset is a good example of a macrophage being a product of its environment. Because the M2c is activated/generated by known immunosuppressive mediators, it follows that they possess the same qualities. They have been shown to produce TGF-β and IL-10 [47–49]. In addition, surface expression of CD163 is associated with this subset [52] (Table 1).

Disease associations

The M2c, or "anti-inflammatory," subset has been shown to be induced by apoptotic cell uptake and promote epithelial and vascular repair [46, 50], as well as play a modulating role to the M1 activity in the *mdx* mouse model [58]. Both M2a and M2c subsets have been found to increase type VI collagen and fibrosis in an adipocyte model [72].

Interaction with particulates

To date there have been no studies focused on the specific interaction between the M2c macrophage subset and particulates. Because the phenotype is considered to have regulatory activity, the potential role these cells could play in disease is evident. Some groups have hypothesized (personal communications) that deletion of this subset would result in a loss of regulation, which may be a key event in developing particle-induced pathologies (i.e. nanomaterials, silica). In addition, the use of this subset as a type of cellular therapy could be beneficial in chronic inflammatory pathologies induced by particulates.

1.3.5 M2d: tumor-associated

While the M1 subset is considered to have antitumor activity, the M2d subset are generated by the local environment and associated with tumor growth [55]. The factors involved in the generation of the M2d include IL-6, leukemia inhibitor factor (LIF), and M-CSF [53].

Function/phenotype

The general definition of the M2d/TAM subset is that it promotes the growth of tumors [80]. It is thought that these cells possess an immunosuppressive phenotype [53, 55]. This activity has been found to be antagonized by the M1 macrohages [54].

Disease associations

This subset is rare and is associated with tumors.

Interaction with particulates

While particles such as asbestos have been associated with cancer [56, 81], the link between particulates and TAM is not clear. Especially with such cancers as lung or gastrointestinal

tumors, where exposures to environmental particulates is relatively consistent, the role of the M2d/TAM as a potential mediator in this process is ripe for investigation. In addition, current research in oncology treatments has started focusing on the use of nanomaterials [57, 82, 83]. The use of particulates to treat tumors could take advantage of the phagocytic capacity of macrophages in a targeted therapy.

1.3.6 M4 and Mhem/Mox: atherosclerotic-associated

Macrophages and their contribution to atherosclerosis, as an inflammatory disease, has been an area of interest in cardiovascular research [84–86]. There are two to three types of macrophages that have recently been described in association with atherosclerosis: M4 and Mhem/Mox [87–89]. The M4 appear to be generated by activation with the chemokine CXCL4 [88]. The atheroprotective macrophages are generated by the presence of either heme (Mhem) or oxidized phospholipids (Mox) [87, 89].

Function/phenotype

The roles and functions of these subsets are areas of active research. While the M4 appears to fall into a role of promoting atherosclerosis, it is the Mhem/Mox subset(s) that are described as having atheroprotection activities. The M4 is a classical-type macrophage that is proinflammatory and, therefore, promotes atherosclerotic pathology through this mechanism. The protective activity of the Mhem/Mox subset(s) involves the stabilization of plaques [89].

Disease associations

As described in the above section regarding the generation of these subsets, these cells are associated with the environment that is responsible for their generation: atherosclerosis.

Interaction with particulates

To date no studies have investigated, let alone linked, the activities of these subsets with particulate exposures and pathology. However, the association between particulate exposure and cardiovascular disease has been shown [90], as has the effect of air pollution particulates on macrophage functions [91, 92]. With the contradictory functions of these subsets in the pathology, and the known influence of particulates on the disease progression, it is a potential area of research to evaluate a possible connection.

1.4 Multinucleated giant cells

Cells with more than two nuclei within a common cytoplasm are described as multinucleated or polykaryotic. Multinucleated cells formed by cell fusion are called syncytia, while multinucleated cells formed by repeated mitoses without cytokinesis are called coenocytes. Multinucleated cells are formed by cell-cell fusion in select human tissues as part of normal physiological processes. These include the fusion of macrophages into osteoclasts, myoblasts into myotubes, cytotrophoblast cells into syncytiotrophoblast, and sperm with oocyte [93]. Additionally, recent discoveries suggest bone marrow stem cells fuse with several cell types as a mechanism of tissue regeneration [94, 95].

Multinucleated giant cells (MGC) are typically defined as macrophage syncytia associated with granulomas (Fig. 2). MGC are distinct from osteoclasts, which are associated with bone and are present in normal, non-inflammatory conditions. The concept that MGC are formed by macrophages fusing together is supported by fluorescent- and radio-labeling studies [96, 97]. This is in contrast to the mechanism of megakaryocyte formation. Megakaryocytes become polyploid by endomitosis, resulting in a single polylobulated nuclei with a histological appearance similar to MGC [98].

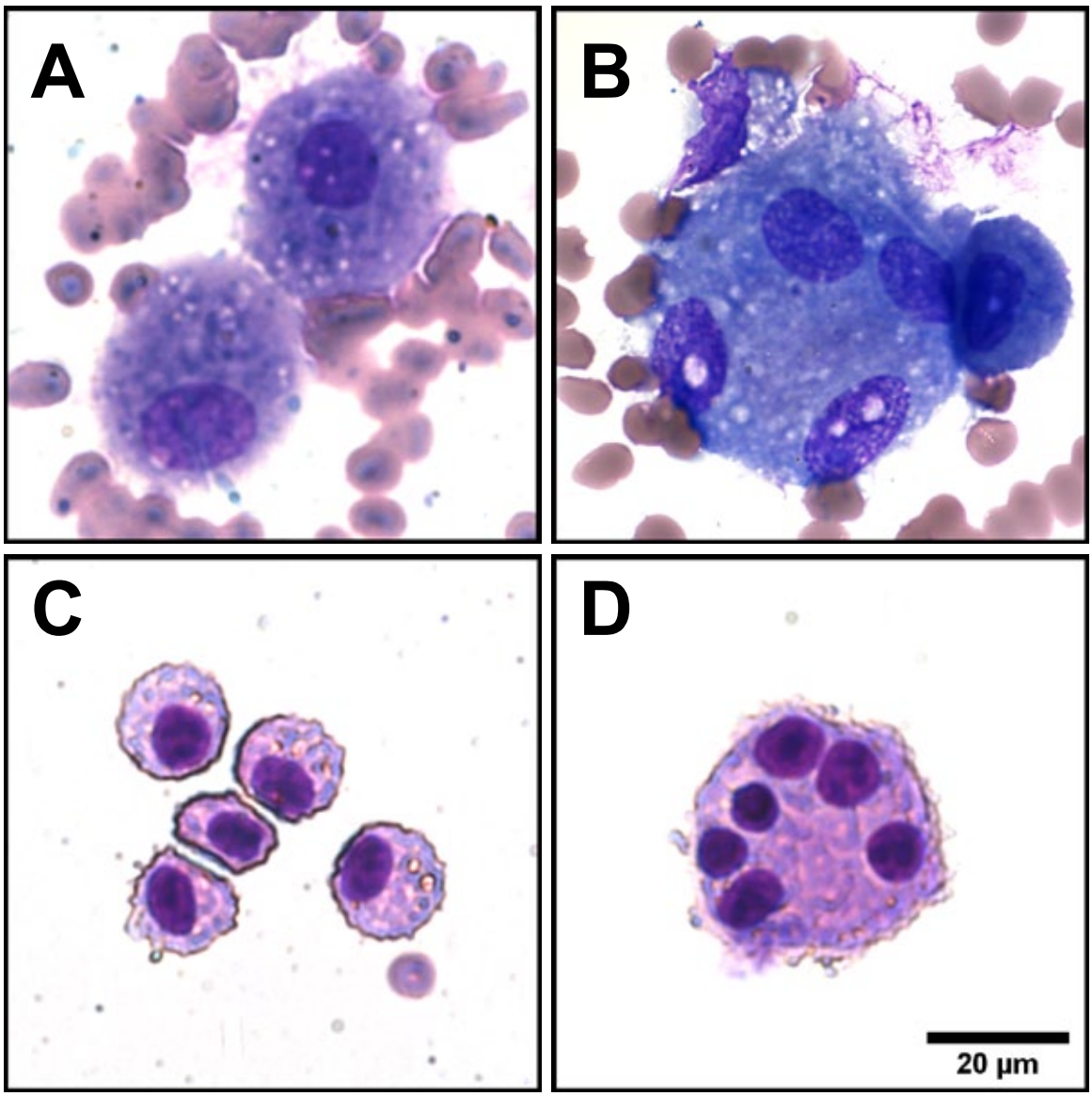

Fig. 2. Macrophage and MGC comparison. Photomicrographs (630x) of (A) human alveolar macrophages, (B) human multinucleated giant cell, (C) mouse macrophages, and (D) mouse multinucleated giant cell.
Experimental protocols were approved by the University of Montana Institutional Animal Care and Use Committee, University of Montana Institutional Biosafety Committee, and St. Patrick Hospital/Community Medical Center Institutional Review Board.

Author's own work; Reprinted/adapted by permission from Elsevier. 15.07 - Inflammatory Cells of the Lung: Macrophages by Forrest Jessop, Kevin L. Trout, Andrij Holian, and Christopher Migliaccio 2018. https://doi.org/10.1016/B978-0-12-801238-3.95651-4

Usage of the phrase “giant cell” is occasionally generalized to include cells of non-monocytic origin that become multinucleated in certain pathological conditions (Table 2). These giant cells are less commonly observed than giant cells of monocytic origin and are not necessarily formed by cell fusion in association with granulomas. For the remainder of this chapter, the phrase “multinucleated giant cell” (MGC) will refer to macrophage syncytia associated with granulomas. These macrophage-derived MGC can be classified as Langhans giant cells, foreign-body giant cells, and Touton giant cells.

1.4.1 MGC morphology

Multinucleated giant cells are classified into three morphological variants. Langhans giant cells and foreign-body giant cells are the most common variants and are observed in a range of granulomatous conditions. Touton giant cells are less common because they are usually only observed lesions with high lipid content.

The eponym of the Langhans giant cell is Theodor Langhans, who was the first to describe their unique nuclear arrangement in 1868 [99, 100]. The nuclei of Langhans giant cells are arranged near the periphery of the cell in a circular pattern or in a semi-circular pattern accumulating at one or two pole(s) of the cell (Fig. 3). Langhans giant cells usually contain less than 20 nuclei and have a spherical or slightly ovoid shape with a diameter of less than 50 μm. Langhans giant cells should not be confused with Langerhans cells and Islets of Langerhans.

The nuclei of foreign-body giant cells are diffuse throughout the cytoplasm with no well-defined spatial pattern (Fig. 3). Foreign-body giant cells may have a spherical or irregular shape. The number of nuclei and cell size fluctuates greatly (Fig. 4), with some cells containing over 100 nuclei and exceeding one mm in diameter.

Aschoff cells are formed by fusion of Anitschkow cells (occasionally called caterpillar cells), which are pathognomonic for rheumatic fever [102]. Anitschkow cells are likely to be of macrophage origin, but a potential myocyte origin has been a source of controversy [103, 104].
Balloon cells are pathognomonic for Type IIb focal cortical dysplasia (also called Taylor dysplasia) and are found in subependymal giant cell astrocytomas, subependymal nodules, and cortical tubers [105]. Balloon cell (not to be confused with multinucleated melanocytes) origin is suggested to be neuronal or glial [106].
Floret giant cells have been observed in various neoplasms including multinucleate cell angiohistiocytoma, pleomorphic lipoma, giant cell fibroblastoma, giant cell collagenoma [107], neurofibroma [108], pleomorphic fibroma [109], and dermatofibroma [110]. The name "floret" reflects the unique nuclear arrangement around the periphery of the cell, similar to petals on a flower. Although fibroblast or dendritic cell origins have been suggested [108], floret giant cell etiology is unknown.
Multinucleated epithelial giant cells are most often observed adjacent to the epithelial surface or lumen in pathological conditions of the epidermis, gastrointestinal tract, vulva, epididymis, and lungs [111–113].
Multinucleated erythroblasts are pathognomonic for congenital dyserythropoietic anemia III and may be formed by incomplete cytokinesis of proerythroblasts [114].
Multinucleated fibroblasts were recently discovered *in vitro* to form as either syncytia or coenocytes, depending on whether the culture contained cell lines or primary fibroblasts, respectively [115].
Multinucleated hepatocytes are found in neonatal giant cell hepatitis and autoimmune hepatitis [116, 117].
Multinucleated melanocytes found in nevi and melanomas are described as having a balloon appearance due to large vacuoles or a starburst appearance due to nuclear arrangement in lentigo maligna [118, 119].
Reed-Sternberg cells are pathognomonic for Hodgkin's lymphoma and are formed by multinucleation of the B cell-derived Hodgkin cell [120]. They become multinucleated by a unique mechanism: mitosis with incomplete cytokinesis followed by re-fusion of daughter cells [121].
Warthin-Finkeldey cells associated with measles, HIV, and Kimura lymphadenopathies are suggested to be derived from T cells [122] or dendritic cells [123].

Table 2. Other multinucleated cells. Miscellaneous cells that become multinucleated in pathological conditions. These cells may not necessarily be of monocytic origin, associated with granulomas, or formed by fusion.

Author's own work; reprinted/adapted by permission from Springer Nature Customer Service Centre GmbH: Springer. Macrophage and Multinucleated Giant Cell Classification by Kevin L. Trout, Forrest Jessop, Christopher T. Migliaccio 2016. https://doi.org/10.1007/978-4-431-55732-6_1.

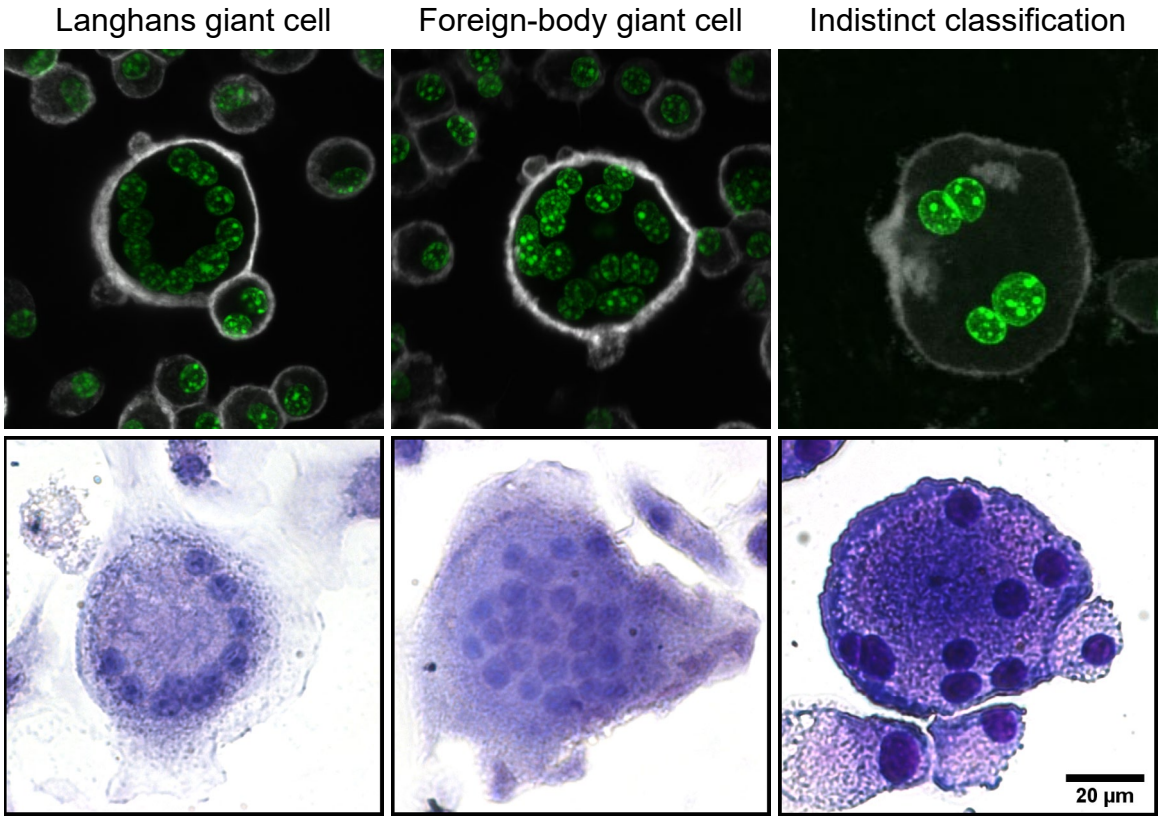

Fig. 3. MGC morphology. Two frequently observed morphological variants of MGC are the Langhans giant cell (left column) and foreign-body giant cell (center column). MGC with less distinct nuclear patterns (right column) can lead to subjectivity or uncertainty when classifications are based upon morphology alone. Not shown is the less common Touton giant cell. MGC were generated *in vitro* by IL-4 treatment of mouse bone marrow-derived macrophages (see Chapter 2).

Author's own work; Three panels (top left two and bottom right) were reprinted/adapted by permission from Springer Nature Customer Service Centre GmbH: Springer. Macrophage and Multinucleated Giant Cell Classification by Kevin L. Trout, Forrest Jessop, Christopher T. Migliaccio 2016. https://doi.org/10.1007/978-4-431-55732-6_1.

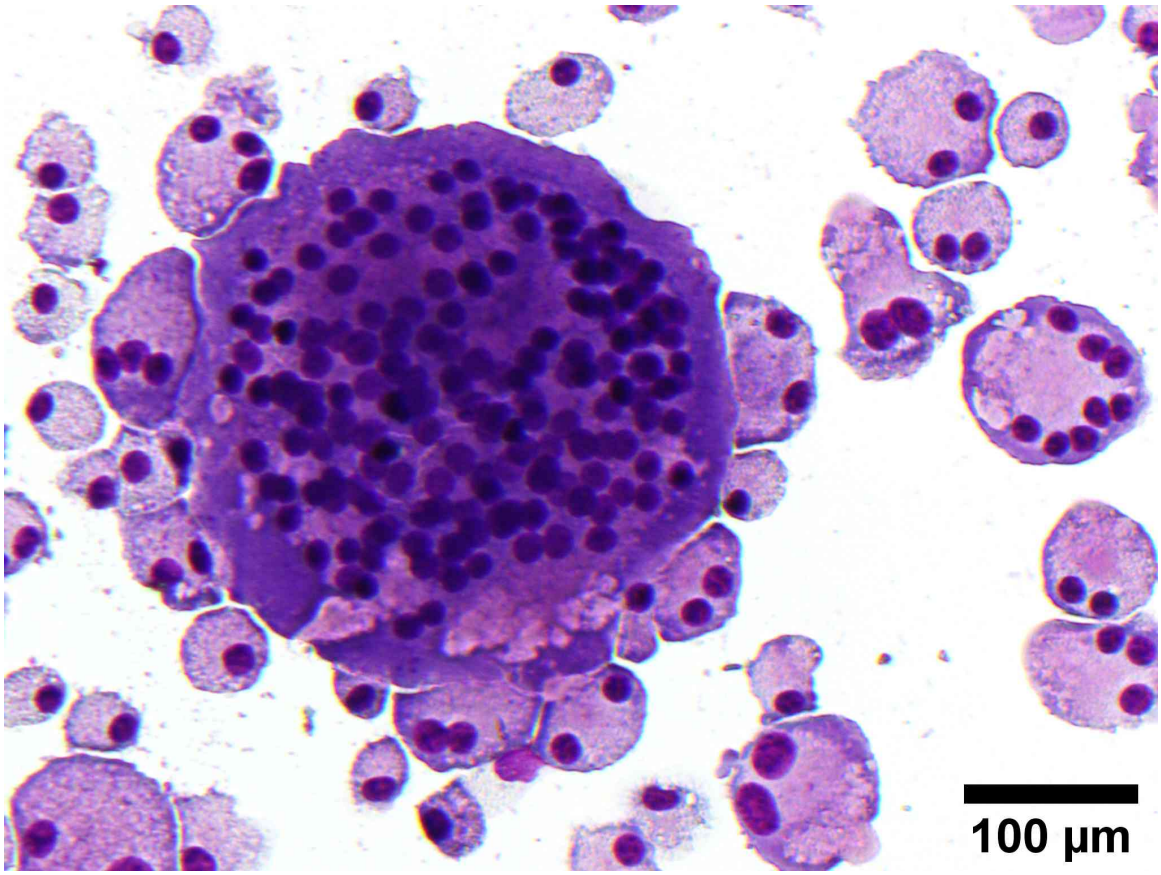

Fig. 4. MGC size. A relatively large MGC with >100 nuclei and >300 µm diameter. MGC were generated *in vitro* by IL-4 treatment of mouse bone marrow-derived macrophages (see Chapter 2).

Author's own work.

The eponym of the Touton giant cell is Karl Touton, who originally called them "xanthelasmatic giant cells" in 1885 [100, 101]. The Touton giant cell size, number of nuclei, and arrangement of nuclei is similar to that of Langhans giant cells, except the nuclei in Touton giant cells are surrounded by a foamy cytoplasm. This suggests that these cells may be formed by fusion of foam cells, which are lipid-laden macrophages.

The morphology-based classification of these variants can lead to uncertainty in their identification, especially when MGC have relatively few nuclei or unclear patterns of nuclear arrangement. This gray area is augmented because MGC are usually observed at only one timepoint during the continuum of the multinucleation process. For example, it is possible that Langhans giant cells are precursors to foreign-body giant cells, or vice versa.

1.4.2 Environment/generation

One of the environments in which MGC are generated is in granulomas surrounding implanted medical devices or biomaterials. This particular environment provides a useful model system to characterize the dynamics of MGC formation. MGC begin to form within the first three days following biomaterial implantation in rodents, reach a peak population at 2-4 weeks, and slowly decrease in population until reaching a steady-state [124, 125]. The relatively short lifespan of an individual MGC is estimated to be approximately one week, at this point the MGC is thought to undergo apoptosis [126]. The MGC population at the implant site is maintained by continuous recruitment and differentiation of monocytes from the circulation until the foreign body has been degraded or removed [127]. These MGC populations have been observed to persist beyond 15 years post-implantation [128].

Well-known stimulators of macrophage fusion into MGC include IL-4 [129], IL-13 [130], and IFN-γ [131]. In some *in vitro* models, MGC formation is increased when these fusion stimulators are combined with macrophage maturation factors: GM-CSF, M-CSF,

or IL-3. The macrophage maturation factors alone do not induce fusion [132, 133]. Stimulation with IL-4 or IL-13 *in vitro* results predominantly in foreign-body giant cell formation, while stimulation with IFNγ results predominantly in Langhans giant cell formation [134]. Other factors suggested to stimulate MGC formation include α-tocopherol (a form of vitamin E) [135], calcitriol (1,25-dihydroxyvitamin D3) [136], phorbol 12-myristate 13-acetate [137], and T-cell mitogenic plant lectins concanavalin A and phytohemagglutinin [138].

Progress in MGC research within the previous two decades has begun to elucidate the mechanism of macrophage fusion. An overview of this mechanism is provided here. For a more comprehensive description of proteins and signaling pathways implicated in MGC formation, excellent summaries have been published as book chapters [128, 139, 140] and reviews [141, 142]. The mechanism of macrophage fusion into MGC can be divided into three major steps [143]:

1. Competence. Fusion stimulating factors such as IL-4 increase macrophage fusogenicity or "fusion-competency." Programming into a fusion-competent state usually involves endogenous or exogenous signals that increase transcription of key proteins such as MMP9 [144], E-cadherin [145], dendritic cell-specific transmembrane protein (DC-STAMP), and osteoclast stimulatory transmembrane protein (OC-STAMP) [146].

2. Commitment. The fusion-competent macrophage must migrate into proximity with a fusion partner. A chemokine that induces this migration during MGC formation is chemokine (C-C motif) ligand 2 (CCL2), also called monocyte chemoattractant protein 1 (MCP-1) [147]. Cell-cell and cell-substrate adhesion are part of macrophage commitment to fusion. For example, engagement of β1 and β2 integrins regulates MGC formation[148].

3. Fusion. Finally, the membranes merge and the cell undergoes a series of cytoskeletal rearrangements. As an example of a membrane merging event, ATP activation of purinergic receptor P2X7 results in exposure of phosphatidylserine in the plasma membrane [149],

which is recognized by class B scavenger receptor CD36 in the fusion partner [150]. Cytoskeletal rearrangements are important during migration as well as post-fusion. A known factor involved in actin polymerization and reorganization during MGC formation is Rac1 [147].

1.4.3 Function/phenotype

Due to their macrophage origin, it is suspected that MGC share some of the same functions as macrophages. Also, similarly to macrophages, it is likely that MGC possess heterogeneous phenotypes based upon tissue location, pathological association, and stimulating factors (e.g., IL-4 versus IFNγ). Another factor that may affect MGC phenotype is the cell maturation stage. This alteration of activity is evident in MGC capacity for phagocytosis. A MGC is capable of internalizing approximately the same number of particles as a mononuclear macrophage [151, 152], but phagocytosis decreases as the number of MGC nuclei increases [124, 153].

MGC can phagocytose larger particles than macrophages [145]. When a foreign body is too large to be engulfed, MGC attempt to degrade them extracellularly. MGC form adhesive structures called podosomes that are localized to the ventral cell periphery, forming a compartment between the MGC and foreign body [154]. A degradative microenvironment is formed within this sealed compartment, likely as a result of lysosomal exocytosis. This microenvironment contains degradative enzymes, an acidic pH, and reactive oxygen species generated predominantly by NADPH oxidase [142]. In the context of medical implants, MGC can degrade biomaterials through a mechanism similar to osteoclast degradation of bone [155]. Specific enzymes released by MGC that have been implicated in foreign body degradation include MMP9 [144, 156] and cathepsin K [157]. It has been hypothesized that this MGC degradative activity may eventually be down-modulated [128]. If this is the case, it is possible that MGC may reach a inactive phase, during which their primary function is

to protect the host by sequestering the foreign material or pathogen.

1.4.4 Disease associations

MGC are most commonly associated with granulomas of diverse etiology (Table 3). Multinucleated cells have also been described in giant cell tumor of bone and soft tissues; however, these cells exhibit features more characteristic of osteoclasts [158, 159].

1.4.5 Interaction with particulates

The most well-known lung conditions associated with MGC include tuberculosis infection [153] and sarcoidosis [97]. There is a growing body of studies that describe MGC formation in response to particle inhalation. MGC are frequently observed in response to inhalation of antigens that cause hypersensitivity pneumonitis [160, 161] and inhalation of other organic materials such as a mycobacteria and fungi (Table 3). Inhalation of inorganic particles is also known to induce MGC formation. MGC have been observed in the lungs of rodents after exposure to silica [162, 163], asbestos [162, 164], sepiolite nanoclay [163], silver nanowires [165], or multi-walled carbon nanotubes [166]. Giant cell interstitial pneumonitis is a pathological pattern of hard metal lung disease that is characterized by the presence of MGC [167, 168]. This interstitial lung disease is usually observed as a result of occupational exposure tungsten carbide and cobalt alloys. Inhalation of other metals have also been reported to induce formation of MGC, such as beryllium [169].

1.5 Research motivation

Macrophages function as a first-line agent of immunity by phagocytosis of foreign material and generation/regulation of subsequent immune responses. Numerous macrophage

Classification	Disease or pathogenic material
Autoimmune/Idiopathic	Annular elastolytic giant cell granuloma, granuloma annulare [170] Crohn's disease, ulcerative colitis [171] Langerhans cell histiocytosis [172] Rheumatoid Disease [173] Sarcoidosis [97] Vasculitides (e.g. Giant Cell Arteritis [174])
Endogenous materials	Keratin [175] Lipids [100], cholesterol crystals [176] Monosodium urate crystals [177]
Exogenous materials	Engineered nanomaterials (e.g. Ag nanowires [165], carbon nanotubes [166]) Medical implants [178] Metals (e.g. Al [179], Be [169], Zr [180], Co/WC alloys [181]) Minerals (e.g. asbestos [182], silica [182], talc [183]) Plant materials (e.g. cactus spines, corn starch, wood splinters [184])
Infection – Bacteria	Brucellosis [185] Cat-Scratch Disease [186] Mycobacteria infection (e.g. Leprosy [187], Tuberculosis [153]) Syphilis [188]
Infection – Fungus	African histoplasmosis [189] Aspergillosis [190] Cryptococcosis [191]
Infection – Parasite	Filariasis (e.g. dirofilariasis [192], onchocerciasis [193]) Leishmaniasis [194] Schistosomiasis [195]

Table 3. MGC disease associations. Granulomatous conditions in which macrophage-derived multinucleated giant cells are found. This list of example conditions is not exhaustive.

Author's own work; reprinted/adapted by permission from Springer Nature Customer Service Centre GmbH: Springer. Macrophage and Multinucleated Giant Cell Classification by Kevin L. Trout, Forrest Jessop, Christopher T. Migliaccio 2016. https://doi.org/10.1007/978-4-431-55732-6_1.

phenotypic subsets have been identified. However, less is know about MGC phenotype and function. Although MGC association with granulomas has been known for many years, determining whether or not they significantly contribute to formation of the granuloma requires an increased understanding of their biology. Studies of MGC are frequently conducted in the context of medical implants, but few have examined macrophage fusion in response to inhaled particles.

In recent years, various molecular mediators of macrophage fusion have been described. Interleukin (IL)-4 is a well-known inducer of MGC formation and is commonly used to study macrophage fusion *in vitro*. However, culture conditions used for models of IL-4-induced macrophage fusion vary widely among different laboratories. Developing reproducible methods to study MGC will help to define MGC function and response to foreign materials such as environmental or engineered particles. These methods will be used to test the hypothesis that significant quantities of MGC can form in response to inhaled particles and the MGC phenotype is unique from their macrophage precursors. The following describes the specific aims of each chapter.

Chapter 2 aims to determine the effects of varying culture conditions on mouse bone marrow-derived macrophage (BMdM) fusion into multinucleated giant cells (MGC). Previous studies have used multiple different culture methods without systematic comparison or justification. First, the efficiency and objectivity of morphological quantification methods will be improved by developing methods using fluorescent nuclear and plasma membrane stains with automated image segmentation. Then, the effects of varying *in vitro* conditions will be assessed using a model of IL-4-induced fusion in BMdM from C57Bl/6 mice. The following culture conditions will be examined: growth timeline, cell seeding density, growth surface, and addition of granulocyte-macrophage colony-stimulating factor (GM-CSF) or macrophage colony-stimulating factor (M-CSF). Finally, the most effective method for enrichment of MGC populations from mixed cultures will be

determined.

Chapter 3 aims to quantitatively compare MGC formation resulting from exposure to a spectrum of environmental particles and engineered nanomaterials, both *in vivo* and *in vitro*. The particles for these experiments are selected to represent a wide variety of micron- and nano-sized particles of both environmental and anthropogenic origin. These particles include crystalline silica, multiwalled carbon nanotubes, titanium nanobelts, and crocidolite asbestos. C57Bl/6 mice will receive particles by oropharyngeal aspiration and cells will be collected by lavage after seven days for differential counts. *In vitro* experiments will be performed as described in Chapter 2, except with the addition of particles at the same time as IL-4. The capacity for MGC to engulf particles will be determined by qualitative cytological observations.

Chapter 4 aims to demonstrate that the phenotype of MGC are unique from their macrophage precursors. An i*n vitro* BMdM model of IL-4-induced fusion will be used to establish mixed cultures of macrophages and mGC. These cells will be separated by methods determined in Chapter 2, then purified macrophage and MGC populations will be compared at baseline or when stimulated by addition of particles as described in Chapter 3. A multiplex immunoassay will be used to determine macrophage and MGC secretion of the following cytokines: Interferon (IFN)-γ, tumor necrosis factor (TNF)-α, IL-1β, IL-6, IL-10, IL-13 and IL-33. Flow cytometry will be used to determine macrophage and MGC expression of surface markers: cluster of differentiation (CD)11b, CD11c, F4/80, and major histocompatibility complex (MHC) class II.

Overall, this research contributes to the standardization and replicability of methods to study MGC, quantitatively demonstrates MGC presence in response to particles in the lung, and leads to a new understanding of the unique MGC phenotype. This fundamental cell biology knowledge will help to develop methods to control the foreign body response and provide insight into other granulomatous conditions in which the role of MGC is unclear.

Chapter 2

Factors influencing multinucleated giant cell formation *in vitro*

2.1 Abstract

Macrophages fuse together to form multinucleated giant cells (MGC) in granulomas associated with various pathological conditions. Improved *in vitro* methods are required to better enable investigations of MGC biology and potential contribution to disease. There is a need for standardization of MGC quantification, purification of MGC populations, and characterization of how cell culture variables influence MGC formation. This study examined solutions to address these needs while providing context with other current and alternative methods. Primary mouse bone marrow-derived macrophages were treated with interleukin-4, a cytokine known to induce fusion into MGC. This model was used to systematically assess the influence of cell stimulant timing, cell seeding density, colony stimulating factors, and culture vessel type. Results indicated that MGC formation is greatly impacted by alterations in certain culture variables. An assessment of previously published research showed that these culture conditions varied widely between different laboratories, which may explain inconsistencies in the literature. A particularly novel and unexpected observation was that MGC formation appears to be greatly increased by silicone, which is a component of a chamber slide system commonly used for MGC studies. The most

successful quantification method was fluorescent staining with semi-automated morphological evaluation. The most successful enrichment method was microfiltration. Overall, this study takes steps toward standardizing *in vitro* methods, enhancing replicability, and guiding investigators attempting to culture, quantify, and enrich MGC.

2.2 Introduction

Multinucleated giant cells (MGC) are homotypic macrophage syncytia associated with granulomas. Occasionally, other cell types that become multinucleated in pathological conditions are referred to as giant cells (see Chapter 1); however, the focus of this study is on multinucleated cells of monocyte/macrophage origin. These MGC are found in some autoimmune or idiopathic conditions, but are most commonly formed as a result of exposure to persistent foreign microorganisms or materials. Recent *in vitro* studies have led to many new discoveries about MGC, such as their mechanism of formation [141]. However, many of these studies are completed using a range of methods with little systematic comparison or justification.

Investigators have observed fusion of monocyte/macrophage cells into MGC *in vitro* using primary cells and cell lines from a variety of tissue sources and species. Species include human [196], mouse [197–199], rat [198], rabbit [200], and pig [201]. Primary cells include bone marrow-derived macrophages (BMdM) [197, 199], blood monocytes [196], peritoneal macrophages [198, 200], alveolar macrophages [198, 200], splenic macrophages [199], and microglia [201]. Cell lines include RAW264.7 [197], UG3 [202], and J774 [198]. While it is useful to make observations using a variety of model systems, results can be difficult to compare. Cell lines present a unique challenge because multinucleation due to rapid divisions of immortalized cells could lead to artifacts, though they may be particularly useful for studying MGC in the context of cancer. The two most commonly published *in vitro* MGC models are human monocytes and mouse BMdM. There are certain

advantages to mouse BMdM: availability of transgenic models, replicability gained from genetic and environmental interindividual similarity, ethical considerations, and ability to obtain high yields of relatively pure monocyte/macrophage primary cell populations using simple methods.

It is common for *in vitro* studies involving BMdM fusion into MGC to first use macrophage colony-stimulating factor (M-CSF) for BM cell maturation, followed by treatment with interleukin (IL)-4 to stimulate MGC formation. Osteoclasts have been formed *in vitro* using similar methods, except that receptor activator of nuclear factor kappa-B ligand (RANKL) is used instead of IL-4. IL-13 signaling has some overlap with IL-4, and both cytokines each result in similar rates of MGC formation [130]. Monocytes/macrophages have also been stimulated to fuse into MGC *in vitro* by other means: live microbes, microbial components, concanavalin A with/without interferon-γ in older publications, genetic manipulations, and stimulating factors released from other cells. Some researchers use co-stimulatory factors together with IL-4, the most common of which is granulocyte-macrophage colony-stimulating factor (GM-CSF). One laboratory group (Table 4, Kyriakides) reports quite high fusion with Fms-related tyrosine kinase 3 ligand (Flt3L) when delivered together with IL-4. GM-CSF and Flt3L are often used to generate dendritic cells with phenotypes distinct from each other [203] and from M-CSF-dependent macrophages [204, 205]. MGC are traditionally considered to be more macrophage-like, but some suggest dendritic cells can also fuse [206–208]. Because these cell types have many overlapping features, more studies are needed to examine phenotypes as they relate to MGC.

Experimental models of IL-4-induced BMdM fusion vary widely in terms of *in vitro* conditions, such as media composition, stimulant concentrations, culture timing, and cell seeding density (Table 4). Another important variable is the cell growth surface. These surfaces may include untreated polystyrene (PS), tissue culture-treated PS (TCPS), glass,

(A) Overview and BM maturation

Laboratory	# of articles	Media	%FBS	Antibiotic	M-CSF, ng/mL	Flt3L, ng/mL	Days
Aderem	1	DMEM	10	Yes	50	No	4
Gordon	5	αMEM,RPMI,OptiMEM	10	Yes	50*	No	3-10
Keegan	2	αMEM	10	Yes	20	No	1-5
Kyriakides	6	IMDM	10-20	Yes	1.5	100	10**
Miyamoto	6	αMEM	10	No	50	No	2-3
Morrison	2	αMEM	10	Yes	30	No	2
Park	1	DMEM	10	No	10	No	7

(B) MGC formation and quantification

Laboratory	Cell seeding, $x10^5/cm^2$	Growth surface	IL-4, ng/mL	CSF, ng/mL	Days	Primary quantification	MGC definition	%Fusion estimate
Aderem	Unspecified	Unspecified	50	No	6	Ploidy	>16n ploidy	8
Gordon	1.3-2.5	Permanox	100*	±GM 100	1-4	%Fusion	>2 nuclei	0-64
Keegan	Unspecified	Glass	10	M 20	5	%Fusion	>2 nuclei	46***
Kyriakides	2.6-5.3	Untreated PS	10	±GM 10	3-7**	%Fusion	>2 nuclei	29-77
Miyamoto	1.6	Microplate	50	±GM 50, other	2-10	MGC/well, $/cm^2$	>3 nuclei	0.2-10
Morrison	0.15	Microplate	50	GM 50	4-8	MGC/view	>3 nuclei	N/A
Park	Unspecified	Permanox	25	No	7	MGC number	>1 nucleus	N/A

Table 4. Methods in literature. Assessment of culture variables during IL-4-induced fusion of mouse BMdM into MGC. All studies used a two-part process: maturation of BM cells using M-CSF (A), followed by fusion into MGC using IL-4 (B). Notes for specific parameters are indicated by asterisks. *Stimulating proteins were occasionally sourced from cell line supernatants rather than recombinant proteins. **Media was changed periodically throughout culture period. ***%Fusion estimated from BALB/c mice rather than C57Bl/6.

Author's own work; reprinted/adapted from Elsevier: Immunobiology. Factors Influencing Multinucleated Giant Cell Formation *In Vitro* by Kevin L. Trout and Andrij Holian 2019. https://doi.org/10.1016/j.imbio.2019.08.002.

various biomaterials, or various coatings. MGC formation has been reported to be enhanced on chamber slides made from Permanox™ plastic [96]. Also, a culture dish coating of particular interest is Arginine-Glycine-Aspartate (RGD) [196], which is a tripeptide sequence present in extracellular matrix proteins (e.g. fibronectin) that can coat implanted foreign bodies and are bound by integrins for cell attachment.

One of the most widely used MGC quantification metrics is the percent fusion of MGC defined morphologically, usually via microscopy, as containing three or more nuclei within a common cytoplasm. Although binucleated cells could be MGC precursors, they could also arise from cells undergoing mitosis without yet completing cytokinesis, so binucleated cells are often excluded from MGC calculations to avoid artifacts that may especially occur in cell line or cancer studies. A fusion index is calculated by dividing the total number of nuclei within MGC by the total nuclei in all cells within the field of view or sample, which can then be converted to a percent. This normalized metric provides a meaningful number that can be used for comparisons between multiple studies, while other limited relative metrics (i.e. MGC number per field of view) only allow for comparisons within a single study. The percent fusion metric is also more objective than semi-quantitative scoring. However, counting all the nuclei can be tedious. High content imaging methods have recently been described [209], but automated methods may require specialized equipment such as a laser scanning cytometer and can be less accurate when it comes to distinguishing MGC from clumped macrophages.

Enrichment of MGC from mixed cultures would allow for more effective analysis of these cells. Cells with unique surface proteins can be targeted by antibodies for sorting using methods such as magnetic-activated or fluorescence-activated cell sorting (MACS or FACS). Certain surface proteins are upregulated in MGC (e.g. dendritic cell–specific transmembrane protein [210]), but whether the magnitude of upregulation is sufficient for effective sorting has not yet been determined. Due to the lack of MGC-specific

markers, nuclear fluorescence has been used with flow cytometry to distinguish MGC from macrophages [151, 211]. However, these methods may have undesired effects on subsequent *in vitro* assays due to cell stress during handling and interference from stains or antibodies. Manual isolation methods such as laser capture microdissection [212] or picking with a micromanipulator [213, 214] are damaging to cells and are not feasible for large scale experiments. Some investigators propose that a short incubation with trypsin or other proteases allows mononucleated cells to be removed by washing while multinucleated cells remain [215, 216], but this technique can result in low purity and artificially selects for a phenotype of cells containing more adhesion proteins. Density gradient centrifugation is suggested to result in partial purification of osteoclasts [217], so testing this method for MGC separation would be valuable. Finally, a simple approach without the need for stains is to sort based on size, which may be possible using differential centrifugation [218], microfluidics, microfiltration [219], or light scatter signals from flow cytometry.

The objective of this study was to evaluate how these various *in vitro* conditions influence IL-4-induced fusion of primary mouse BMdM into MGC, as well as improve methods for MGC quantification and enrichment. Experimental variables were selected which we hypothesized would have the greatest impact on MGC formation, including treatment timeline, seeding density, CSF treatment, and growth surface. A quantification method was developed using fluorescent staining for a semi-automated approach to morphological evaluation using routine microscope equipment and freely available software. Finally, enrichment methods which we expected to be most promising were tested for sorting MGC based on size or density. Results will help guide investigators attempting to study MGC, enhance replicability, and elucidate factors critical to MGC formation. Furthermore, observations such as fusion kinetics or reactions to different materials/surfaces have implications in understanding granuloma formation in response to foreign materials or biomaterials.

2.3 Methods

2.3.1 Analysis of methods in literature

Primary research involving IL-4-induced fusion of mouse BMdM into MGC was assessed. Related published research methods were grouped according to articles sharing a common author, as shown in each row of Table 4. The "Laboratory" column contains the last name of this author, which is often the senior or corresponding author on the cited publication(s). The articles examined include: Aderem [220], Gordon [96, 150, 219, 221, 222], Keegan [145, 223], Kyriakides [144, 147, 197, 224–226], Miyamoto [199, 210, 227–230], Morrison [231, 232], and Park [233]. Seeding density during the MGC formation step was calculated to a universal unit of cells/cm^2 where possible. The quantification method most widely used in all MGC literature, including *in vivo* studies, is %fusion of MGC defined as containing >2 nuclei. However, some BMdM publications deviated from this standard. Estimates of %fusion were calculated using data graphs and/or representative images from these publications where possible. Accuracy of these estimates may vary depending on the amount of information provided in the article.

2.3.2 Cell culture materials and methods

Cells were grown in a humidified, water jacketed incubator (Thermo Fisher Scientific, Waltham, MA) at 37°C and 5% CO_2. Sterile 0.2 μm filtered culture media consisted of RPMI-1640 with 10% heat-inactivated fetal bovine serum (FBS), 25 mM HEPES, 2 mM L-glutamine, 1 mM sodium pyruvate, 100 I.U./mL penicillin, and 100 μg/mL streptomycin (FBS: VWR Seradigm, Radnor, PA; all others: Corning subsidiary Mediatech, Manassas, VA). Cells were suspended by using 0.05% trypsin with 0.53 mM EDTA in HBSS (Corning) or Accutase® with 0.5 mM EDTA in Dulbecco's PBS (BioLegend, San Diego, CA), followed by physical dislodging of cells as necessary using a cell scraper or

pipette action. When specified, cells were fixed by 4% paraformaldehyde in PBS for 10 min at room temperature. Treatment concentrations for all recombinant murine proteins was 30 ng/mL, including M-CSF (R& D Systems, Minneapolis, MN), GM-CSF (PeproTech, Rocky Hill, NJ), and IL-4 (R& D Systems). Centrifugations of cells in tubes were performed at RCF_{avg} 300 x *g* for 5 min. Cytocentrifugations of cells onto slides were performed at approximately RCF_{avg} 250 x *g* for 5 min. Cell counting was completed using a Beckman Coulter (Indianapolis, IN) Z2 cell counter.

Permanox is a trademarked (Nalge Nunc International, Rochester, NY) polymethylpentene (TPX RT18XB; Mitsui Chemicals, Tokyo, Japan) tissue culture-treated growth surface. Permanox slides have a silicone gasket (MDX4-4210; Dow Corning, Midland, MI) that connects removable natural polystyrene chamber walls. Media working volumes per chamber or vessel were as follows: 8-chamber permanox slides (Thermo Fisher) at 0.4 mL, 60x15mm permanox dishes (Thermo Fisher) at 5 mL, 8-chamber borosilicate glass slides with non-removable wells (Thermo Fisher) at 0.4 mL, 24-well PS or TCPS plates (Greiner Bio-One, Monroe, NC) at 0.5 mL, and T75 TCPS flasks at 20 mL. Designated plates were coated with 5 $\mu g/cm^2$ RGD protein polymer (F5022; Sigma-Aldrich, St. Louis, MO) for 30 min, then washed twice with PBS and used immediately.

2.3.3 Mice

Male and female C57Bl/6 mice (Jackson Laboratories, Bar Harbor, ME) aged 9 to 20 weeks were used for all experiments. Mice were housed in microisolator cages with *ad libitum* access to food and water in a specific-pathogen-free facility maintained at 22 ± 2°C, 30–40% humidity, and 12-hour light/12-hour dark cycle. Mice were euthanized by intraperitoneal injection of sodium pentobarbital followed by a secondary mechanical means of euthanasia

prior to removal of rear legs for bone marrow isolation in a tissue culture hood. Experimental protocols were approved by the University of Montana Institutional Animal Care and Use Committee.

2.3.4 Multinucleated giant cell (MGC) culture

BMdM methods were similar to those previously used in our laboratory [69]. BM was flushed from the tibiae and femora in a sterile environment, pooled, centrifuged, resuspended in media, and seeded at 4 x 10^5 cells/cm^2 in a T75 flask. Cells were incubated at 37°C overnight. Adherent stromal cells were discarded, and suspended macrophage progenitor cells were collected. In culture timeline evaluation experiments, these suspended progenitor cells were seeded at 6 x 10^5 cells/cm^2 in Permanox slides with M-CSF until the media was replaced with IL-4-containing media at varying time points (Fig. 6). In other experiments after the timeline was optimized, suspended progenitor cells were added to T75 flasks at 2 x 10^5 cells/cm^2 with M-CSF for four days to mature into BMdM. Then, mature BMdM were seeded at 9 x 10^5 cells/cm^2 (established in Fig. 7) in specified culture vessels with IL-4 for four days.

2.3.5 Staining and microscopy

Cells in initial experiments (Fig. 5, A and B) were stained using a method similar to Wright-Giemsa (PROTOCOL™ Hema 3™; Fisher Scientific, Kalamazoo, MI) by submerging slides in a methanol-based fixative for 90 sec, “Solution I” for 120 sec, “Solution II” for 30 sec, and water for 90 sec. Cells in remaining experiments were stained with HCS NuclearMask Blue followed by CellMask Orange Plasma Membrane according to manufacturer (Thermo Fisher) recommendations. When necessary, FluorSave™ (Calbiochem, MilliporeSigma, Burlington, MA) medium was used to mount coverslips on slides. Images

for MGC quantification were collected using a routine transmitted light and epifluorescent Zeiss Axioskop upright microscope with AxioCamMR3 camera (Carl Zeiss, Jena, Germany) at 200x magnification with DAPI and TRITC filters. At least five random, independent (non-overlapping) images were acquired per sample chamber. Fluorescent images used to illustrate differences among staining methods (Fig. 5, C and D) were collected using an Olympus FluoView FV1000 IX81 confocal microscope.

2.3.6 Quantification

MGC were defined morphologically as containing three or more nuclei within a common cytoplasm. The number of MGC nuclei were manually counted, while the total nuclei were counted by an automated method developed in the freely available, open-source ImageJ v1.51-1.52 software (https://imagej.nih.gov/ij/index.html) (Appendix A). The number of nuclei within MGC was divided by total nuclei within all cells to calculate a fusion index for each image field. Fusion indices of all image fields within a sample were combined into a mean, then multiplied by 100 to be expressed as percent fusion.

2.3.7 Enrichment

Cultures of mature mouse BMdM treated with IL-4, as described above, contain a mixture of MGC and macrophages. Separation of this cell mixture into purified populations was attempted using three enrichment methods. First, the mixed cell suspension was layered on sterile isotonic Percoll™ colloid (GE Healthcare, Uppsala, Sweden) diluted with cell culture medium to densities of 1.02, 1.05, and 1.08 g/mL to form a discontinuous gradient. The gradient was centrifuged at RCF_{avg} 400 x *g* for 30 min in a swinging bucket rotor with slow acceleration/deceleration. Fractions were collected with a sterile Pasteur pipette at gradient interfaces for staining and analysis. Second, the mixture of cells was stained with NuclearMask for measuring nuclear fluorescence, forward scatter (FSC), and side

scatter (SSC) with an Attune NXT flow cytometer (Thermo Fisher). Third, the mixture of cells was suspended in 2 mL media, transferred onto a pre-rinsed cell strainer (PluriStrainer by PluriSelect; Leipzig, Germany), and washed twice with 4 mL/wash into a tube. Then, the strainer was inverted and washed twice with 4 mL/wash into a new tube. The first tube contained cells that were small enough to pass through the sieve, while the other tube contained larger cells that were blocked by the sieve. The number of MGC relative to macrophages in each tube was assessed for various cell strainer sizes.

2.3.8 Statistics

Graphs display mean and standard error for $n \geq 3$ independent replicate mice in each condition. M-CSF groups in culture timing experiments were analyzed by linear regression to assist interpretation of MGC formation over time (Fig. 6). Effects of CSF on IL-4-induced fusion was assessed by one-way ANOVA (Fig. 8). Fusion data from cell seeding density (Fig. 7) and culture vessel (Fig. 9) experiments included some sample groups with a normal underlying distribution and some groups with a nonsymmetric, bimodal distribution due to the large number of zero values. This was confirmed by Shapiro-Wilk tests. This violates assumptions of normality required by parametric methods and violates assumptions that all sample distributions are approximately the same form required by the nonparametric Kruskal-Wallis test. Therefore, a one-sample sign-test with one-sided alternative was selected to determine whether % fusion of each group was significantly different from zero. The Holm-Bonferroni correction was applied to p-values to counteract increased type I error due to multiple comparisons. All analysis was completed in R v3.4.0 statistical software. Statistical significance was defined as a probability of type I error occurring at less than 5%.

2.4 Results

2.4.1 Analysis of methods in literature

Primary literature was systematically assessed to determine which culture variables may have the most potential to influence IL-4-induced fusion of mouse BMdM into MGC (Table 4). Most studies used BM from C57Bl/6 mice ranging in age from 4 (Keegan) to 30 weeks (Gordon). Mouse sex, BM growth surface, and seeding density during the BM maturation step were rarely reported. Methods for elimination of stromal cells widely varied or were not reported. Determining correlations between culture variables and effects on fusion was difficult because the methods were so widely varied. However, this literature synthesis demonstrates the importance of investigating these variables because results show a very broad range of % fusion outcomes.

2.4.2 Quantification method

Non-standard MGC quantification methods in the literature create challenges when attempting to compare and evaluate results. The normalized and most objective metric is the percent fusion of macrophages into MGC, which are defined morphologically as containing three or more nuclei within a common cytoplasm. These cells are typically visualized using brightfield microscopy with traditional histological stains, but manually counting nuclei to calculate %fusion is tedious and impractical for larger scale studies. Faster, more automated analysis methods are possible by segmenting, or partitioning, images into regions representing nuclei and cell borders. However, segmentation of these images was challenging due to inconsistencies in staining quality (Fig. 5, A and B) that often resulted in poor contrast and unclear distinctions between nuclei, cytoplasm, and cell borders. Also, MGC cytoplasm tended to stain darker than macrophage cytoplasm, which obscured MGC nuclei during counting.

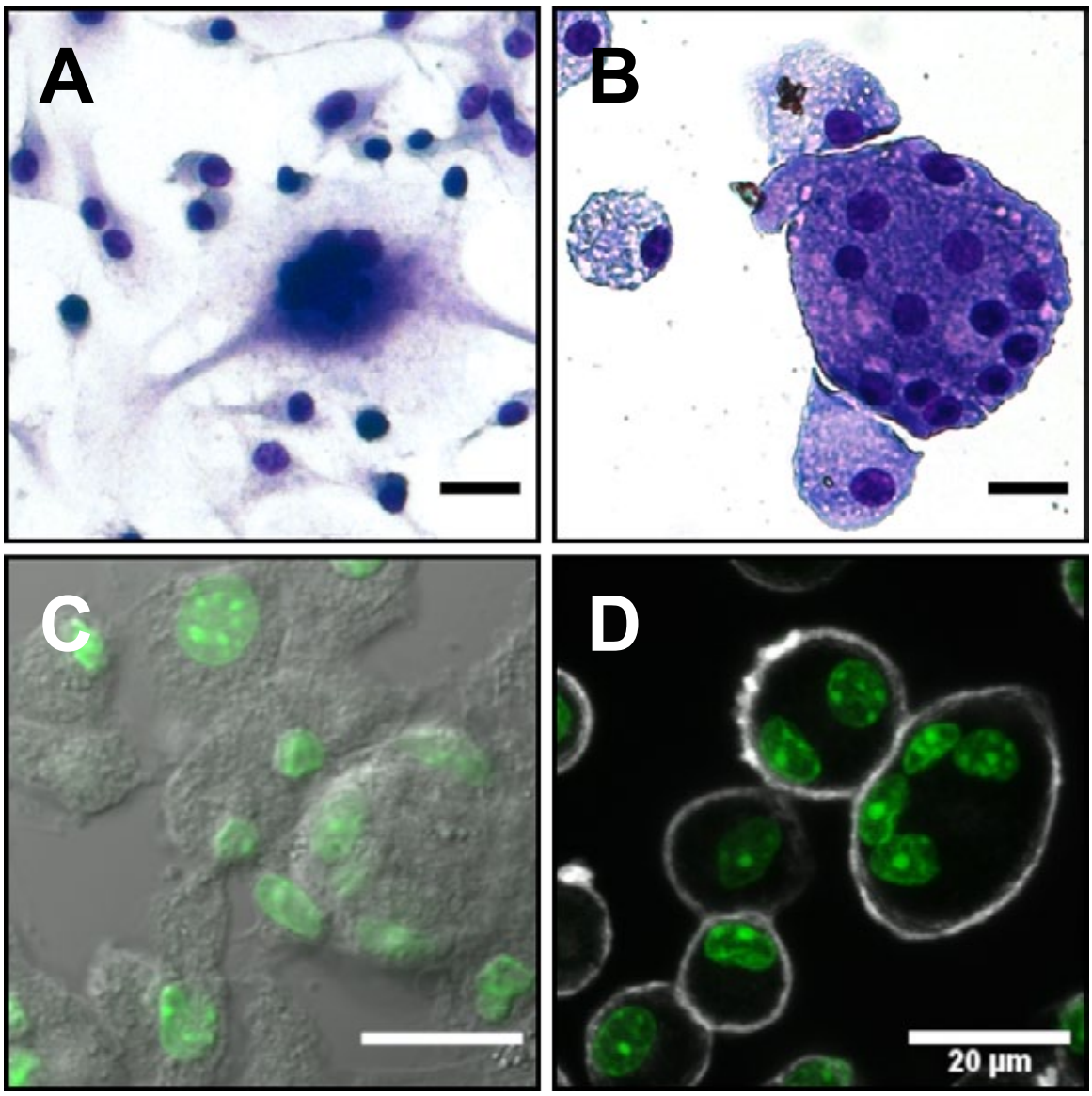

Fig. 5. Quantification method. Comparison of staining methods for morphological quantification of MGC. Brightfield images show cells stained with Hema 3, a method similar to Wright-Giemsa. Pseudo-color fluorescent images show cells stained with NuclearMask (green) and a second channel consisting of either differential interference contrast (DIC) or CellMask Plasma Membrane stain. (A) Example of lower-quality staining with adherent cells. (B) Example of higher-quality staining with cytocentrifuged cells. (C) NuclearMask + DIC. (D) NuclearMask + CellMask. Scale bars 20 µm.

Author's own work; reprinted/adapted from Elsevier: Immunobiology. Factors Influencing Multinucleated Giant Cell Formation *In Vitro* by Kevin L. Trout and Andrij Holian 2019. https://doi.org/10.1016/j.imbio.2019.08.002.

In an attempt to improve image segmentation based on nuclei, a fluorescent nuclear stain was used together with differential interference contrast (DIC; Fig. 5C). This method allowed for automated counting of nuclei, but cell borders in the DIC channel were unclear in regions where other cells were within close proximity. Therefore, a plasma membrane stain was added to improve visualization of cell outlines and more accurately determine whether a particular nucleus was within a macrophage or MGC (Fig. 5D). The resulting images were well-suited for semi-automated analysis with freely available software (ImageJ) to calculate % fusion. Furthermore, this stain combination is compatible with routine fluorescent microscopes, which promoted simple, rapid acquisition of images in subsequent experiments.

2.4.3 Culture timing

Primary mouse bone marrow cells treated with macrophage colony-stimulating factor (M-CSF) mature into bone marrow-derived macrophages (BMdM), which then fuse into MGC when treated with interleukin-4 (IL-4). An evaluation of studies using this *in vitro* model shows that various permutations of culture conditions can have a range of effects on BMdM fusion outcomes (Table 4). In order to make a more systematic assessment of these variables, we first compared cell stimulation timelines to determine kinetics of MGC formation and effects of BMdM maturity on percent fusion.

As expected, BM cells that received M-CSF for only one day (x=1) were immature compared to cells in extended cultures. The average total number of nuclei per image field on the first day after IL-4 treatment was 157 for the x=1 group, while all other groups were 286±19 (standard error). Although the total number of nuclei in this group remained consistent throughout all IL-4 treatment durations (range 132 to 157), the rates of fusion were highly variable (Fig. 6, x=1). This suggests MGC death, detachment, or splitting may have been occurring. Many of these MGC had a morphology that was different from those

generated from mature BMdM *in vitro* or the MGC that are typically observed *in vivo*. They appeared in localized regions of the culture and often consisted of vast cytoplasm containing clustered areas of packed nuclei.

More consistent MGC results were observed with mature BMdM (Fig. 6). In all cases, at least two days with IL-4 was required for high levels of MGC. A relatively early timepoint with consistently high fusion (M-CSF for 4d, then IL-4 for 4d) was selected for subsequent experiments. The shorter culture period allows for more rapid sequential experiments while still having sufficient number of MGC and avoiding unexpected effects on primary cell condition when they are maintained in culture for extended periods of time.

2.4.4 Cell seeding density

The next *in vitro* variable examined was mouse BMdM seeding density prior to IL-4-induced fusion into MGC. High cell density resulted in high fusion, which peaked at 9 x 10^5 cells/cm^2 (Fig. 7). Fusion was reduced in the highest seeding density, 12 x 10^5 cells/cm^2. This culture contained overlapping/clumping cells. Likely, MGC formation was reduced due to the number of cells exceeding available space for attachment to the growth surface. Therefore, the seeding density with consistently high fusion, 9 x 10^5 cells/cm^2, was used for subsequent experiments.

2.4.5 Colony stimulating factors

As in previous experiments, BM cells were differentiated M-CSF. Then, the BMdM were treated with IL-4 alone or in combination with M-CSF or GM-CSF to examine the potential influence on fusion into MGC. Results show that neither CSF significantly alters IL-4-induced fusion (Fig. 8).

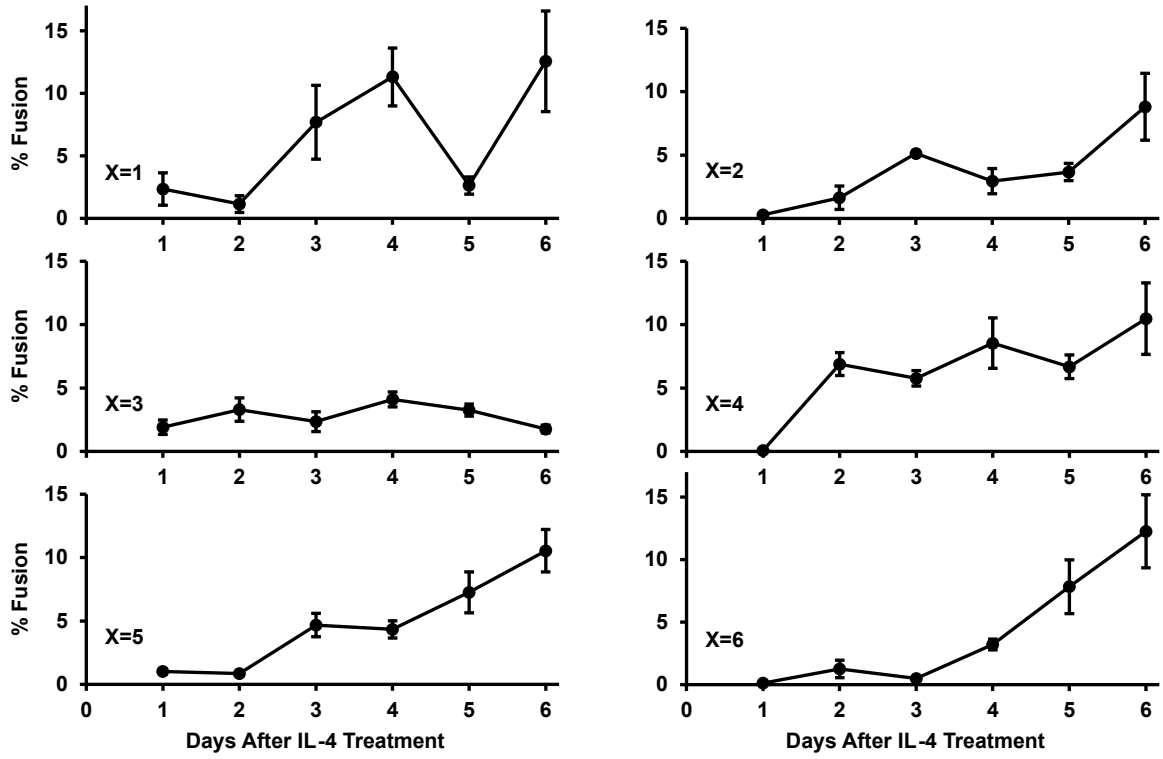

Fig. 6. Effects of culture timing. Time-course examining fusion kinetics of immature and mature BMdM. BM on Permanox slides were treated with M-CSF for x days until media was replaced with IL-4-containing media. Then, groups of cells were fixed daily for 6 days to be analyzed for % fusion. Regression lines with y-intercepts set to zero had slopes of 1.8, 1.2, 0.6, 1.8, 1.5, and 1.4 corresponding to groups x=1, 2, 3, 4, 5, and 6 (regression not displayed on graphs). Higher slopes reflect fast and consistent increases in % fusion.

Author's own work; reprinted/adapted from Elsevier: Immunobiology. Factors Influencing Multinucleated Giant Cell Formation *In Vitro* by Kevin L. Trout and Andrij Holian 2019. https://doi.org/10.1016/j.imbio.2019.08.002.

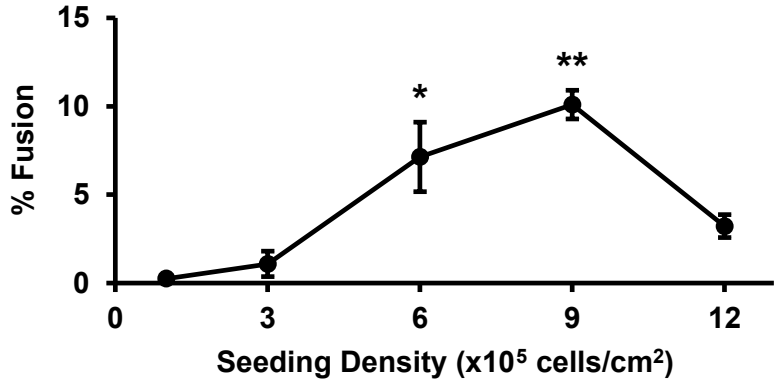

Fig. 7. Effects of cell seeding density. BMdM were added to Permanox slides at the specified seeding density and treated with IL-4. After four days, cells were analyzed for % fusion. Samples with % fusion significantly greater than zero by one-sample sign-test are shown as *$p<0.05$ and **$p<0.01$.

Author's own work; reprinted/adapted from Elsevier: Immunobiology. Factors Influencing Multinucleated Giant Cell Formation *In Vitro* by Kevin L. Trout and Andrij Holian 2019. https://doi.org/10.1016/j.imbio.2019.08.002.

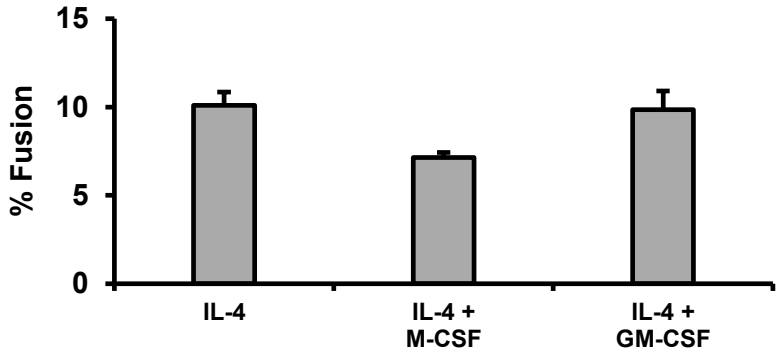

Fig. 8. Effects of colony stimulating factor. BMdM were added to Permanox slides at 9 x 10^5 cells/cm^2 and treated with IL-4 alone or in combination with M-CSF or GM-CSF. After four days, cells were analyzed for % fusion. No significant effects were observed by one-way ANOVA at $p<0.05$ level.

Author's own work; reprinted/adapted from Elsevier: Immunobiology. Factors Influencing Multinucleated Giant Cell Formation *In Vitro* by Kevin L. Trout and Andrij Holian 2019. https://doi.org/10.1016/j.imbio.2019.08.002.

2.4.6 Culture vessel

The final *in vitro* variable examined was the influence of common culture vessels on MGC formation. IL-4-induced fusion was highest on Permanox chamber slides (Fig. 9A). MGC were observed in small numbers on all other surfaces: glass, untreated polystyrene (PS) plates, tissue culture-treated PS (TCPS) plates, and RGD-treated PS or TCPS.

Next, we investigated whether increased MGC formation on Permanox slides was a result of the plastic surface (polymethylpentene) or another component of the chamber slide system, particularly the silicone gasket used by the manufacturer to attach the media chamber to the slide base. Cells cultured on intact Permanox slides containing gaskets were compared to cells on round 60x15mm Permanox dishes that did not contain gaskets. As an additional control, cells grown in PS wells were compared to cells in PS wells containing pieces of gasket that were cut from disassembled Permanox chamber slides.

In both cases, significant MGC formation was only observed in the presence of the silicone gasket (Fig. 9B). Similar results were observed in the presence of an alternative piece of silicone (ring gasket from a cryogenic vial; data not shown). This shows that presence of silicone in the culture has a greater influence on MGC formation than the growth surface itself.

2.4.7 Enrichment

Exploratory experiments were completed to enrich MGC from mixed macrophage-MGC cultures. A pre-formed, discontinuous density centrifugation did not provide distinct separation between macrophages and MGC. This indicates that the buoyant densities of these cells are similar, likely as a result of similar ratios of nuclei to cytoplasm. The similar ratios suggest that cytoplasm is conserved during macrophage fusion. More extensive studies are needed to further test this hypothesis, such as continuous density gradients and

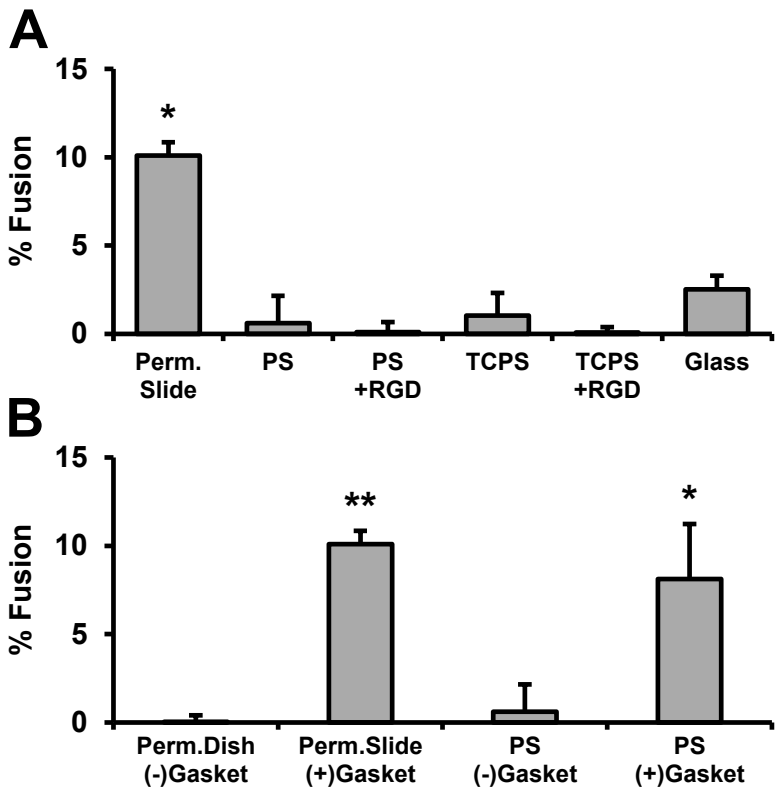

Fig. 9. Effects of culture vessel. BMdM were added to the specified culture vessels at 9 x 10^5 cells/cm^2 and treated with IL-4. After four days, cells were analyzed for % fusion. (A) Culture vessels included Permanox chamber slides, glass, untreated polystyrene (PS), tissue culture-treated PS (TCPS), and RGD-treated PS or TCPS. The Permanox slides are manufactured with chambers attached via silicone gasket, which was hypothesized to be causing increased MGC formation. (B) Therefore, fusion was compared for cells on Permanox dishes without gaskets, Permanox slides containing gaskets, PS wells without gaskets, and PS wells containing gasket pieces cut from the slides. Samples with % fusion significantly greater than zero by one-sample sign-test are shown as *$p<0.05$ and **$p<0.01$.

Author's own work; reprinted/adapted from Elsevier: Immunobiology. Factors Influencing Multinucleated Giant Cell Formation *In Vitro* by Kevin L. Trout and Andrij Holian 2019. https://doi.org/10.1016/j.imbio.2019.08.002.

live cell imaging.

When cell nuclei were fluorescently stained for analysis by flow cytometry, the cells could be distinguished into groups of mononucleated macrophages, binucleated macrophages, and MGC. However, the stain may interfere with experiments requiring cells to be cultured after sorting, so forward scatter (FSC) and side scatter (SSC) parameters were considered as a potential stain-free method of discrimination. MGC tended toward slightly higher FSC and SSC than macrophages, but the overlap in the populations would prevent sufficient separation of highly pure MGC without losing many cells (Fig. 10).

The best enrichment was achieved using microfiltration. Sieve mesh sizes 10, 15, 20, 30, and 35 μm were tested. The enriched population from the 20 μm size had the highest average purity (number of MGC divided by total cells), which was over 20-fold purer than the average filtrate population. Enrichment efficiency would likely be further increased by protocol optimization (i.e. adjusting filter washing procedures) or by using microfiltration in combination with another purification method. This simple approach would be useful for future studies, allowing MGC populations to be compared with macrophage control groups derived from the same source culture while avoiding potential interference from cell stains or cell stress due to extensive handling.

2.5 Discussion

This study shows IL-4-induced fusion into MGC *in vitro* is greatly impacted by alterations in certain culture conditions. This was demonstrated by systematic assessment of cell stimulant timing, cell seeding density, colony stimulating factors, and culture vessel type. A particularly novel discovery is that MGC formation appears to be greatly increased by silicone. MGC culture methods vary widely between different research laboratories, creating challenges when critically comparing results in the literature. Another challenge

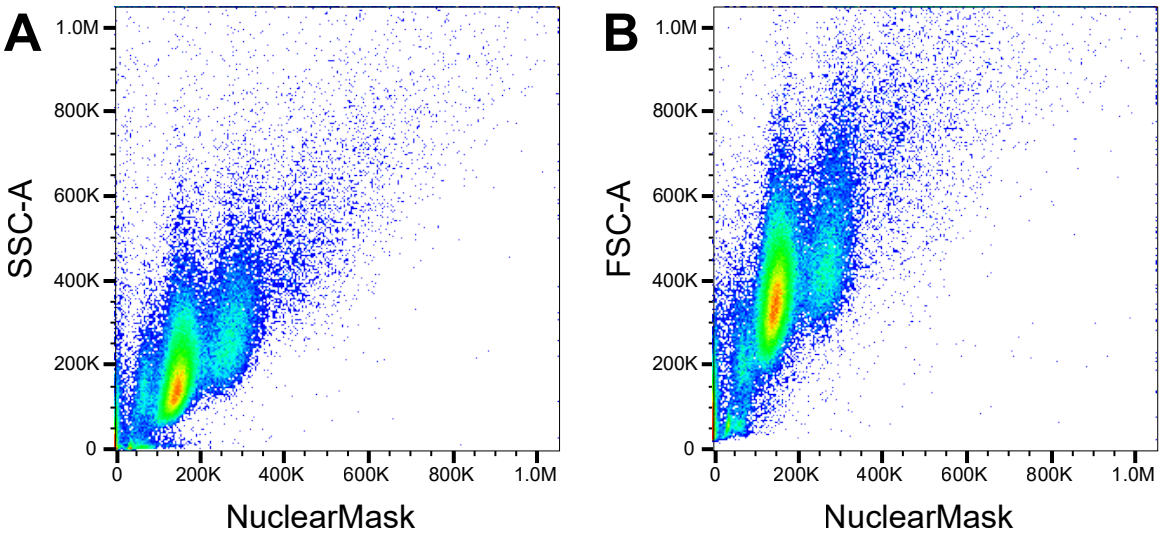

Fig. 10. Flow cytometry. Cells stained with NuclearMask can be identified by flow cytometry as mononucleated macrophages (fluorescent intensity ≈100K-225K), binucleated macrophages (≈225K-325K), or MGC (>325K). Further binary subclassification of MGC based on number of nuclei may be possible, but a large quantity of cells would be required for accuracy. Dot plots show that side scatter (A) and forward scatter (B) tend to increase with nuclear fluorescence. However, scatter alone would not be sufficient to separate MGC from macrophages with high purity. Results concatenated from n=3 true replicates.

Author's own work; reprinted/adapted from Elsevier: Immunobiology. Factors Influencing Multinucleated Giant Cell Formation *In Vitro* by Kevin L. Trout and Andrij Holian 2019. https://doi.org/10.1016/j.imbio.2019.08.002.

for researchers attempting to study MGC is the ability to obtain relatively pure populations of these cells together with appropriate macrophage control populations. Solutions to this enrichment problem were explored, with microfiltration emerging as a successful method. Finally, this study was enabled by our improved quantification methods, which provided the means for accurate and efficient analysis of MGC formation.

Morphological analysis to calculate %fusion using brightfield microscopy and traditional histological stains was less suitable for large scale studies, varied in accuracy with stain quality, and became more subjective when cells are densely packed together. Image segmentation was facilitated by using fluorescent nuclear and cell membrane stains, which was more conducive to automation. Quantification could be completed using routine laboratory microscopes and freely available image analysis software, such as ImageJ or CellProfiler. This stain combination would be adaptable to high-throughput automation as necessary. When attempting to distinguish MGC from clumped macrophages, a stain specific for plasma membranes was more effective than stains that diffuse throughout the entire cell. The CellMask plasma membrane stain usually yielded well-defined cell outlines but is not compatible with experiments requiring permeabilization. Alternatives may include lipid, cholesterol, protein, or other novel membrane stains [234].

BMdM cell maturity and culture density were important variables affecting fusion. IL-4 treatment of more mature BMdM (at least four days with M-CSF) resulted in more consistent MGC formation than immature BMdM. High cell seeding densities resulted in high % fusion, which is in agreement with previous results by Moreno et al [145] and follows logically with the idea that cells are more likely to fuse when less migration is required to reach proximity. These culture parameters were used for subsequent experiments. No significant difference in fusion was observed when mature BMdM were treated with IL-4 + M-CSF versus IL-4 + GM-CSF, which has also been shown by Yagi et al [199]. To our knowledge, our report is the first to compare fusion of mature BMdM treated with

IL-4-only versus CSF co-treatment. No differences were observed, likely because BM were already sufficiently differentiated and cultured at a density optimal for MGC formation. If IL-4 was added to immature BM at a lower culture density, we would hypothesize CSF co-treatment to increase fusion as an indirect side effect of CSF-stimulated proliferation and differentiation.

IL-4-induced fusion of BMdM grown on Permanox slides was over twice as high compared to other culture dishes, including: PS, TCPS, glass, and RGD-modified polystyrene. This was expected based on previous studies with mouse thioglycolate-elicited peritoneal macrophages [96, 235]. However, previous reports have not included control experiments to determine which component of the Permanox slide system causes increased fusion. Surprisingly, we found that this occurred due to the presence of a silicone gasket that attaches the media chamber to the slide, rather than the Permanox surface itself. Future studies are needed to determine how cellular events related to macrophage fusion are impacted by silicone. It is possible that culture medium composition or surface properties are altered as a result of adsorption, leachables, or release of by-products from manufacturing or degradation. Clinically, MGC are commonly found surrounding breast implants and in other silicone granulomas [236]. Understanding these mechanisms are important because of the variety of implantable silicone medical devices with prolonged tissue contact, including those with applications in ophthalmology, otology, cardiology, gastroenterology, orthopedics, and aesthetics.

Many of the culture variables found to be important during fusion of BMdM would likely influence other *in vitro* MGC models as well. For example, we hypothesize that treatment timing and seeding density would also affect fusion in human blood monocyte cultures, which is another frequently published MGC model. Other variables such as CSF treatment effects may differ, as these monocytes are often supplemented with autologous serum instead of additional M-CSF stimulation [196]. It would be valuable to repeat

methods used in this study with other cell models, particularly the experiments examining effects of silicone on MGC formation. Additionally, other future investigations should compare phenotype and function of MGC from various monocyte/macrophage sources, including MGC that have formed *in vivo*. Standardization of *in vitro* methods will facilitate these comparisons. However, isolating large quantities of MGC for *ex vivo* experiments remains challenging, and different methods used to induce MGC formation *in vivo* may result in diverse phenotypes.

Overall, this study demonstrates macrophage fusion is influenced by many experimental variables, which need to be considered to improve *in vitro* study replicability within a laboratory or between different laboratories. It is important for authors to provide detailed methods in publications, such as culture vessel type and cell seeding density. Including an IL-4-only positive control is helpful for interlaboratory comparisons, reduction of false negatives, and troubleshooting when% fusion is outside the typical range. Although we have assessed many major factors affecting MGC formation, there are other possible variables that could be influential. Some examples include hormone variability between serum lots, serum source [237], stimulating factor source, endotoxin levels [227], microbial contamination [238], and interindividual differences among organisms used for primary cell collection. This study provides a step toward standardization of major parameters influencing macrophage fusion, and we hope it will serve as a guide for new investigators attempting to culture, quantify, and enrich MGC.

2.6 Acknowledgements

Samantha Couture (Summer Undergraduate Research Program) helped gather preliminary data that contributed to early development of this project. Technical laboratory support was provided by Center for Environmental Health Sciences core facilities and staff: Lou Herritt, Molecular Histology and Fluorescence Imaging; Pam Shaw, Fluorescence Cytometry.

Research funding was provided by an Institutional Development Award (IDeA) from the National Institute of General Medical Sciences (NIGMS) of the National Institutes of Health (NIH) under grant number P30GM103338. Contents of this publication are solely the responsibility of the authors and do not necessarily represent the official views of NIGMS or NIH.

Chapter 3

Macrophage fusion caused by particle exposure

3.1 Abstract

Background: Multinucleated giant cells (MGC) are formed by fusion of macrophages in pathological conditions. These are often studied in the context of the foreign body response to biomaterial implants, but MGC formation is rarely assessed in response to inorganic particles in the lungs. Therefore, a major objective of this study was to quantitatively compare *in vivo* macrophage fusion resulting from exposure to a spectrum of micron- and nano-sized particles from both environmental and engineered origin, including crystalline silica, multiwalled carbon nanotubes, titanium nanobelts, and crocidolite asbestos.

Methods: Groups of C57Bl/6 mice were instilled with inorganic particles or PBS control. Lung cells were collected by lavage after one week for cell differentials, quantification of macrophage fusion, and microscopic observation of particle uptake.

Results: MGC were present in lungs of all mice exposed to particles; no MGC were found in control mice. Asbestos exposure resulted in significant macrophage fusion, which coincided with significantly increased total lavage cells and percent neutrophils. Microscopic observations show particle internalization in MGC and a unique case of potential heterotypic fusion of macrophages with neutrophils.

Conclusion: MGC can form in the lungs of mice within a relatively short one-week time period after particle exposure. Observations of particles within MGC warrants further investigation of MGC involvement in inflammation and particle clearance. It is important for inhalation toxicologists to be aware that MGC appear in sufficient numbers for quantification, rather than appearing simply as a chance occurrence.

3.2 Introduction

Multinucleated giant cells (MGC) are macrophage syncytia associated with granulomas in various tissues. In the lung, they are found in interstitial lung diseases caused by unknown (idiopathic) reasons, infection, or inhaled substances (Chapter 1). One of these inhaled substances is inorganic particles from environmental or occupational exposures. Increased MGC have been observed in bronchoalveolar lavage from humans with pneumoconiosis after inhalation of asbestos [182, 239], silica [182], coal [182], and hard metals [168, 240]. Among these small number of studies assessing MGC formation in response to inorganic particle inhalation, some include only a limited number of case examples. Other challenges with human studies are that they rely on environmental exposures with uncontrolled doses, durations, confounding co-exposures (e.g. smoking), and other inter-individual variabilities.

There have been thousands of lung toxicology studies using laboratory animals exposed to environmental and anthropogenic inorganic particles, but the potential for these particles to cause macrophage fusion into MGC is rarely assessed. We identified seven *in vivo* studies that quantitatively assessed MGC formation in lungs in response to inorganic particle exposure, all of which showed an increase in MGC. The particles of interest and animals used in these studies are: amosite asbestos in rats [164, 241], chrysotile asbestos in rats [242, 243], crocidolite asbestos in mice [162], multiwalled carbon nanotubes in mice [244], ultrafine titanium dioxide in rats [163], and silica in mice [162] and rats [163]. The

chrysotile studies by Lemaire were the only to quantify MGC using fusion index, which is a commonly used metric to normalize MGC in relation to macrophages while also considering MGC size in terms of nuclei number (Chapter 2, [141]). Comparing relative effects of different particles on MGC formation can be challenging due to nonstandard quantification methods and varying experimental conditions (e.g. exposure timelines) between studies. If lung exposure to certain inorganic particles causes MGC formation, a logical next step is to determine whether MGC directly interact with the particles. Microscopic images of MGC containing particles has been used as evidence of phagocytosis in lung cells from mice exposed to multiwalled carbon nanotubes [166, 245] and humans with occupational exposure to coal [182] or hard metals [240, 246]. To our knowledge, there are no published reports containing images with discernable MGC uptake of asbestos, silica, or other inorganic particles.

The objective of the current study is to demonstrate that significant numbers of macrophages fuse into MGC in mouse lungs within a relatively short time (7 days) after exposure to inorganic particles. Particles for these experiments were selected to represent a wide variety of micron- and nano-sized particles of both environmental and anthropogenic origin. They include crystalline silica (SiO_2), multiwalled carbon nanotubes (CNT), titanium nanobelts (TNB), and crocidolite asbestos (Asb). Each particle type was hypothesized to result in quantitatively different macrophage fusion rates. Particles were observed to be engulfed by MGC, suggesting an active role in uptake. Finally, we present a case of potential macrophage heterotypic fusion with neutrophils, a unique phenomenon that has not yet been described in response to inorganic particle exposure.

3.3 Methods

3.3.1 Particles

The particles for this study were selected to represent a wide variety of micron- and nano-sized particles of both environmental and anthropogenic origin. The selected particles have been shown previously by our laboratory group to be pro-inflammatory in mice. SiO_2, CNT, and Asb particles were obtained from Pennsylvania Glass Sand Company (Pittsburgh, PA), Sun Nano (Fremont, CA), and Research Triangle Institute (Research Triangle Park, NC), respectively. SiO_2 was washed in 1 M HCl as previously described [247]. TNB was synthesized as previously described [248]. Particle characteristics are shown in Table 5, including references for further detail. For illustration purposes, relative sizes are shown in Fig. 11. Endotoxin levels were determined to be negligible by Limulus Amebocyte Lysate assay (Cambrex, Walkersville, MD).

3.3.2 Particle suspension

Particles were prepared into homogenous dispersions in phosphate-buffered saline (PBS, pH 7.4) immediately prior to each *in vivo* exposure. The following were added to PBS for adequate dispersion of engineered nanomaterials (CNT and TNB): 5.5 mM D-glucose, 0.6 mg/mL mouse serum albumin, and 0.01 mg/mL 1,2-dipalmitoyl-sn-glycero-3-phosphocholine (Sigma-Aldrich, St. Louis, MO). This dispersion medium has previously been shown to not significantly alter pulmonary responses compared to PBS alone [249]. TNB were suspended by mechanical stirring for one hour to avoid potential fracture by sonication [250]. Remaining particles were sonicated for one minute with a 500W, 20 kHz Qsonica Q500 (Newtown, CT) cup-horn system at 30

Abbr	Particle	Identifier	Shape	Diameter (nm)	Length (μm)	Ref
SiO_2	Crystalline silica	MIN-U-SIL5	Sphere, Irregular	200 to 2500	N/A	[251]
CNT	Carbon nanotube	FA21	Tube, Multiwall	27	5 to 15	[252]
TNB	Titanium nanobelt	NB-2 Long	Belt, Anatase	10 x 200	7	[250]
Asb	Crocidolite asbestos	N/A	Fiber, Amphibole	160	5	[253]

Table 5. Particle characteristics. Properties of particles used in this study.

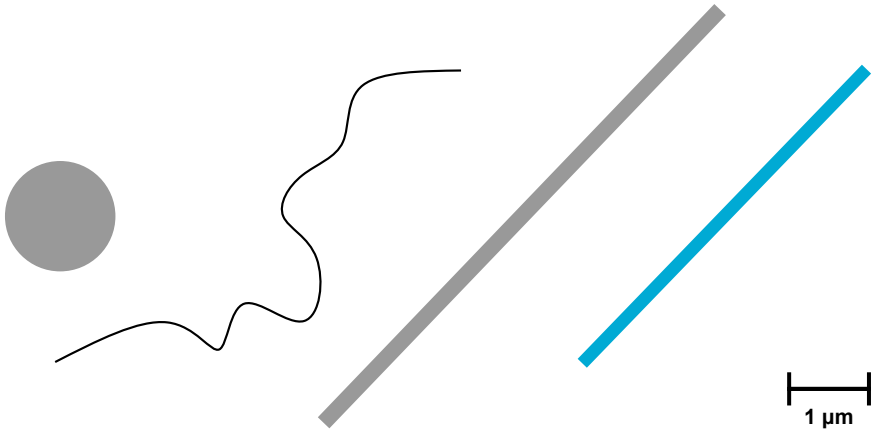

Fig. 11. Particles to scale. Illustration depicting relative size of particles (left to right): crystalline silica (SiO_2), multiwalled carbon nanotube (CNT), titanium nanobelt (TNB), and crocidolite asbestos (Asb).

3.3.3 Mice

Male and female C57Bl/6 mice (Jackson Laboratories, Bar Harbor, ME) aged 8 to 12 weeks were used for all experiments. Mice were housed in microisolator cages with *ad libitum* access to food and water in a specific-pathogen-free (SPF) facility maintained at 22 ± 2°C, 30–40% humidity, and 12-hour light/12-hour dark cycle. Euthanasia was performed by intraperitoneal injection of sodium pentobarbital. Experimental protocols were approved by the University of Montana Institutional Animal Care and Use Committee (IACUC).

3.3.4 *In vivo* experiments

Mice were anesthetized by isoflurane inhalation and exposed to 30 µl of particle suspension or sterile PBS control by oropharyngeal aspiration. Doses were 1 mg/mouse for SiO_2 or 50 µg/mouse for other particles. These doses were selected to induce similar ranges of inflammatory responses as observed during previous dose escalation experiments in our laboratory and to enable comparisons with our existing published data [247, 254, 255]. Mice were euthanized after 7 days and cells were collected by lung lavage with PBS. Cell counting was completed using a Beckman Coulter (Indianapolis, IN) Z2 cell counter. Cytocentrifugation of cells was performed at approximately RCF_{avg} 250 x *g* for 5 min. Slides were stained using a Hematek 2000 autostainer (Bayer Diagnostics, Dublin, Ireland) with a modified Wright-Giemsa (PROTOCOL™; Fisher Scientific, Kalamazoo, MI).

3.3.5 Microscopy analysis

Differential cell counting was completed by manual morphological evaluation. Multinucleated giant cells (MGC) were defined as containing three or more nuclei. Macrophage fusion into MGC was quantified as previously described (Chapter 2) by counting MGC and macrophage nuclei in at least five independent (non-overlapping), random 100x to 200x

magnified image fields per treatment. MGC quantification results are expressed as percent fusion by dividing the number of nuclei within MGC by the total macrophage and MGC nuclei, then multiplying by 100. Images showing particle uptake were acquired using an Axioskop microscope with AxioCamMR3 camera (Carl Zeiss, Jena, Germany). The image of potential heterotypic cell fusion was acquired using an Eclipse E800 (Nikon, Melville, NY) microscope with DP26 (Olympus, Waltham, MA) camera.

3.3.6 Statistics

Multiple comparisons of means from cell differential counts was completed by one-way ANOVA followed by Tukey's HSD test. The MGC % fusion dataset contained sample groups with many zero values (e.g. in PBS group), violating ANOVA assumptions of normality and homogeneity of variance. The nonparametric Kruskal-Wallis test was not appropriate because the shape of each sample distribution was very different. Therefore, a one-sample sign-test with one-sided alternative was selected to determine whether % fusion of each treatment group was significantly different from zero. The Holm-Bonferroni correction was applied to p-values to counteract increased type I error due to multiple comparisons. Statistical significance was defined as a probability of type I error occurring at less than 5%. Graphs display mean and standard error for $n \geq 3$ independent replicate mice in each condition. All analysis was completed in R v3.4.0 statistical software.

3.4 Results

3.4.1 MGC in lavage

An objective was to determine whether macrophages fuse into MGC within a relatively short, 7-day time period after exposure to inorganic particles. C57Bl/6 mice were instilled with a representative selection of micron- and nano-sized particles of both environmental

and anthropogenic origin, including crystalline silica (SiO_2), multiwalled carbon nanotubes (CNT), titanium nanobelts (TNB), and crocidolite asbestos (Asb). As expected, MGC were not found in the lung lavage when mice were not exposed to particles (Fig. 12; PBS control). Measurable numbers of MGC appeared in all particle-treated mice. MGC formation is quantified by % fusion, which reflects both MGC size and abundance relative to macrophages. Asbestos exposure resulted in the higher number of MGC, with statistically significant % fusion. (Fig. 12).

3.4.2 Cell differentials in lavage

Lavage cell differentials were evaluated 7 days after particle exposure in order to provide a more complete assessment and explore potential correlations with MGC formation (Fig. 13). The total number of cells per mouse was significantly higher in response to asbestos exposure compared to control. This increase in total cells was largely attributed to neutrophil influx. The percentage of neutrophils in the lavage from mice exposed to asbestos was significantly increased compared to control. Lung cell differentials from mice exposed to other particles had similar increasing trends in total cells and neutrophils, though not statistically significant.

3.4.3 Particle uptake

MGC appeared to actively interact with particles in the lung. Larger particles and nanomaterial aggregates became visible in the interior of MGC cells at increased magnification (630x) with careful adjustment of microscope focus. MGC were found to contain particles of all types examined (Fig. 14).

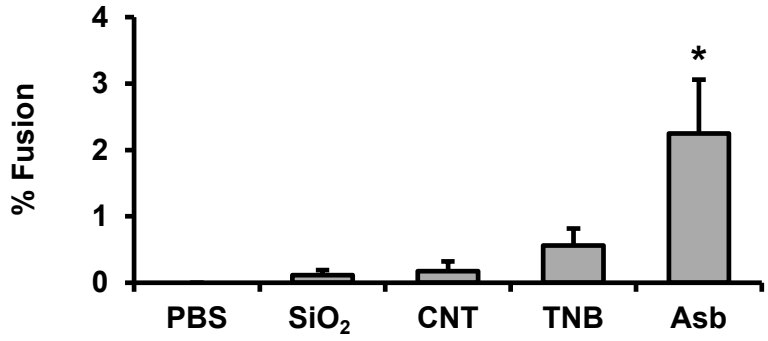

Fig. 12. Fusion *in vivo*. Quantification of MGC in mouse lung lavage 7 days after in vivo exposure to specified inorganic particles. The % fusion of asbestos-treated group was significantly greater than zero. *$p<0.05$.

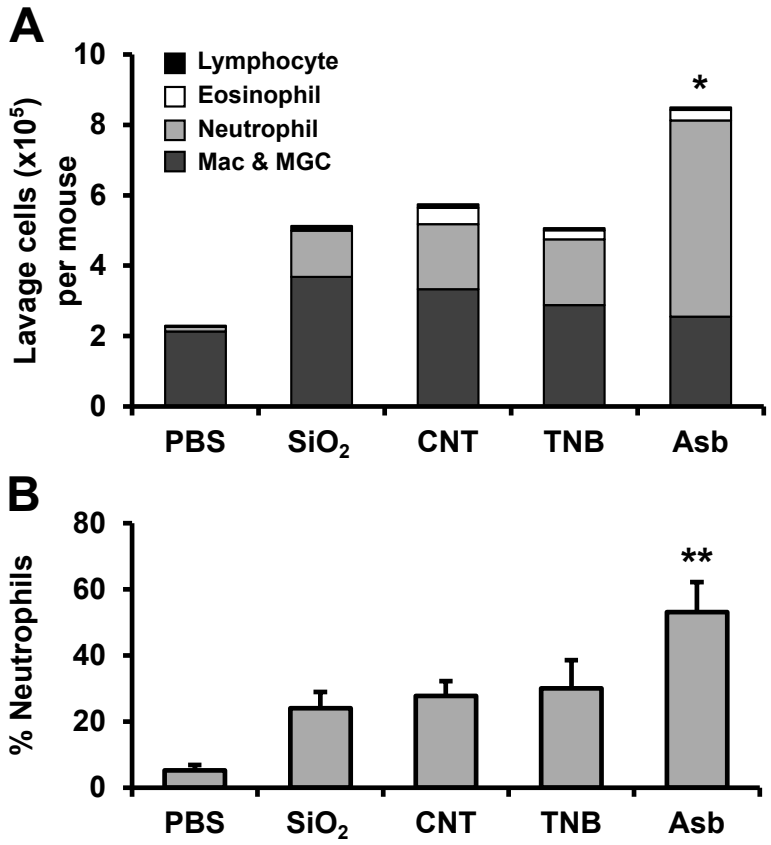

Fig. 13. Cell differential. (A) Lavage cell differentials and (B) % neutrophils in mouse lung lavage 7 days after *in vivo* exposure to specified inorganic particles. The total cells per mouse ($x10^5$) and % neutrophils of asbestos-treated group were significantly greater than PBS control. *$p<0.05$, **$p<0.01$.

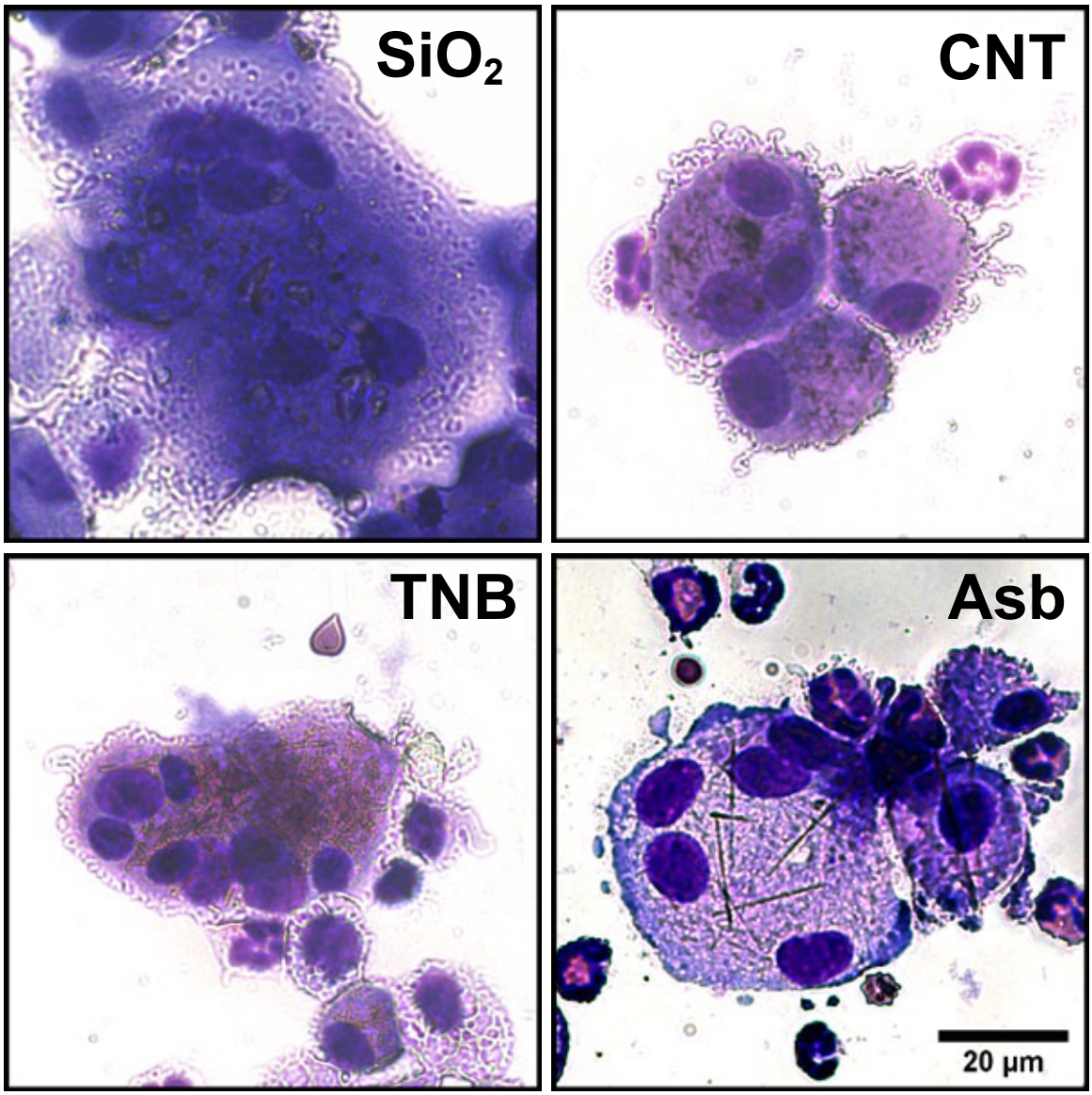

Fig. 14. Particle uptake. MGC observed 7 days after *in vivo* exposure to particles specified in image labels. Scale equal for all images, bar 20 µm.

3.4.4 Possible heterotypic fusion

A unique cell was discovered in the lung lavage from a mouse exposed to asbestos. This was a multinucleated cell containing nuclei from both macrophages and neutrophils within a common cytoplasm (Fig. 15). No visible membranes surround the neutrophil nuclei, suggesting this large cell was formed by heterotypic fusion rather than MGC engulfing whole neutrophil cells. Other cells of this type may have been present in the lung lavage from asbestos-treated mice, but they unfortunately could not be identified with confidence due to less clear staining and overlapping clumps of nuclei.

3.5 Discussion

Particle and fiber toxicology publications often neglect to assess macrophage fusion into MGC. However, this study shows that measurable numbers of MGC do appear in the lungs of mice exposed to a variety of inorganic particles. MGC formation could be directly compared in response to different particles because appropriate quantification methods were used. Exposure to crocidolite asbestos resulted in the highest % fusion. The number of MGC were not as exceedingly high as commonly observed in response to biomaterial implants, but this is a difficult comparison when considering the relative size of implants versus particles. It is noteworthy that MGC appeared within only a short, 7-day time period following particle exposure. Additional studies are necessary to determine why asbestos caused more macrophage fusion than other particles. This outcome could be a direct consequence of particle physical properties, such as size or aspect ratio, or an indirect consequence of asbestos influencing other inflammatory processes.

Macrophage fusion tended to correlate with neutrophil influx, which may provide evidence toward beginning to understand the cause of MGC formation in response to certain

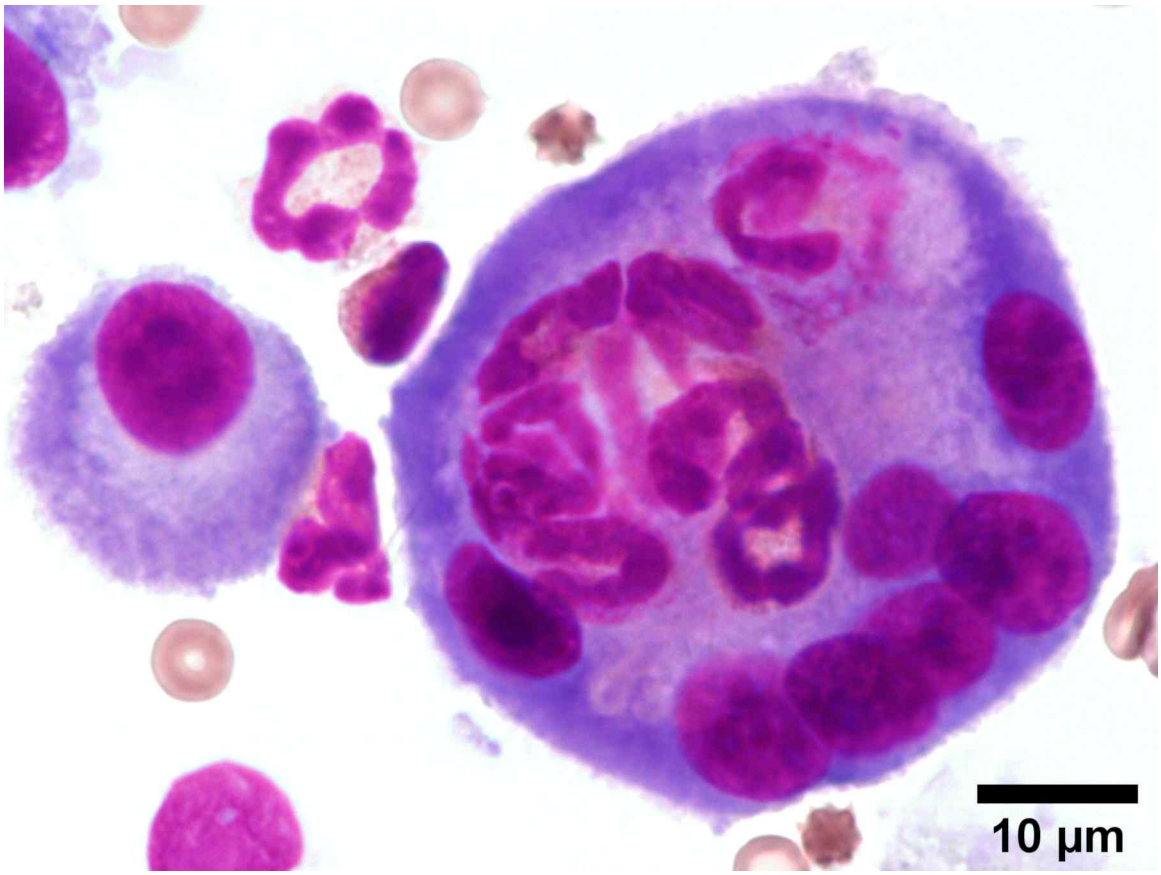

Fig. 15. Heterotypic fusion. Unique case of potential macrophage heterotypic fusion with neutrophils. This cell was observed 7 days after *in vivo* exposure to asbestos. Scale bar 10 µm.

particles. Similar factors that stimulate neutrophilia may also contribute to fusion, such as cytokines and chemokines present in the inflammatory lung environment. An example experiment to test the impact of soluble factors would be to prepare a cell-free supernatant of lung lavage from mice exposed to asbestos, then add it to bone marrow-derived macrophages *in vitro* to observe MGC formation.

An interesting case of potential heterotypic fusion of macrophages and neutrophils was observed. Another publication [256] claimed that *Burkholderia thailandensis* caused heterotypic fusion of RAW264.7 macrophage cell line with neutrophils from human blood *in vitro*. It is unclear in these images whether it is a clump of cells or a common cytoplasm is shared. It is also likely that bacteria cause fusion by a separate mechanism. To our knowledge, our study shows the first case of macrophage and neutrophil fusion *in vivo* and in response to inorganic particles. It is important to note that only one obvious cell of this type was observed, so additional confirmatory studies would be important. Other cells types have been considered for potential heterotypic fusion with macrophages as well, including T lymphocytes in response to HIV-1 [257] and somatic cells in tumor pathogenesis [143].

Microscopic observations of particle uptake were evidence of MGC interaction with particles in the lung after *in vivo* exposure to all types examined (SiO_2, CNT, TNB, and Asb). It is unknown whether phagocytosis occurred before or after macrophage fusion into MGC; this would be challenging to assess *in vivo*. Researchers have hypothesized that macrophages fuse as a result of attempting to phagocytose larger objects, which could explain why larger particles such as asbestos cause more MGC formation. *In vitro* studies using polystyrene beads have shown that MGC are capable of phagocytosis and can internalize larger particles than macrophages [145, 219, 258]. Additional studies are needed to compare macrophage and MGC phagocytic capacity for various environmental and engineered particles, as well as to compare expression of surface receptors related to phagocytosis.

In conclusion, this study shows that MGC can form in the lung within only 7 days after exposure to inorganic particles, with significant macrophage fusion after exposure to asbestos. Asbestos also resulted in significant increases in total lavage cells and percent neutrophils. Nano- and micron-sized particles of both environmental and anthropogenic origin were observed to be engulfed by MGC. Therefore, it is important for inhalation toxicology researchers to be familiar with MGC in order to identify them while completing routine cell differentials, as well as appropriately report quantification of fusion. Further investigations are warranted to determine the role of MGC in the inflammatory response and particle clearance.

3.6 Acknowledgements

Special thanks to Forrest Jessop for contributions toward the laboratory work. Microscopes, equipment, and laboratory animal assistance was provided by Center for Environmental Health Sciences core facilities: Molecular Histology and Fluorescence Imaging, Inhalation and Pulmonary Physiology, and Fluorescence Cytometry. Research reported in this publication was supported by an Institutional Development Award (IDeA) from the National Institute of General Medical Sciences (NIGMS) of the National Institutes of Health (NIH) under grant number P30GM103338 and National Institute of Environmental Health Sciences (NIEHS) R01ES023209. Contents of this publication are solely the responsibility of the authors and do not necessarily represent the official views of NIH.

Chapter 4

Multinucleated giant cell phenotype in response to stimulation

4.1 Abstract

Macrophages fuse into multinucleated giant cells (MGC) in many pathological conditions. Despite MGC correlations with granulomas, their functional contribution to inflammation is relatively unknown. An *in vitro* mouse model of IL-4-induced bone marrow-derived macrophage fusion and microfiltration were used to generate enriched MGC and macrophage populations. Phenotypes were compared in response to well-known inflammatory stimuli, including lipopolysaccharide and crocidolite asbestos. Surface markers were assessed by flow cytometry: CD11b, CD11c, F4/80, and MHC II. Secreted cytokines were assessed by multiplex immunoassay: IFN-γ, IL-1β, IL-6, TNF-α, IL-10, IL-13, and IL-33. Results show that MGC maintained macrophage surface protein expression but lost the ability to produce a cytokine response. This suggests a potentially beneficial role of MGC in isolating the host from a foreign body without contributing to excessive inflammation. This study and future research using other stimulants and environments are important to gaining a fundamental MGC cell biology understanding. This will inform approaches to controlling the foreign body response to particle exposure, medical implants, and many diseases associated with granulomas.

4.2 Introduction

Macrophage fusion into multinucleated giant cells (MGC) occurs in pathological events associated with granulomas. MGC most often form in response to persistent microorganisms or materials, but are also found in certain autoimmune or idiopathic conditions (Chapter 1). One example is medical implants, where MGC have been observed to persist on the device for over 15 years post-implantation [128]. The well-established correlation with granulomatous conditions may lead to the assumption that MGC actively contribute to inflammation and fibrosis, but their physiological role remains unclear [259, 260]. A better understanding of MGC functions in disease is important for future development of therapeutics and approaches to control the foreign body response.

Phagocytosis and extracellular degradation of foreign material are among the few MGC functions that are more commonly described. Studies using mouse cells *in vitro* have shown MGC can phagocytose larger polystyrene beads than macrophages [145, 219, 258]. Human clinical [182, 240, 246] and mouse *in vivo* ([166, 245], Chapter 3) particle inhalation toxicology studies have provided microscopic images of MGC with internalized coal, hard metals, asbestos, silica, multiwalled carbon nanotubes, and titanium dioxide nanoparticles. When macrophages encounter foreign bodies too large to be engulfed, it is hypothesized that they fuse into MGC to degrade or sequester them. Podosomes form a sealed compartment that is filled by lysosome exocytosis with degradative enzymes, reactive oxygen species, and an acidic pH (Chapter 1). This process, occasionally termed "frustrated phagocytosis," occurs in MGC and osteoclasts [232, 261]. Similar to MGC, osteoclasts are multinucleated cells formed by macrophage fusion. Osteoclasts are distinguished by their presence in non-pathological conditions where they function to resorb bone and are commonly identified by tartrate-resistant acid phosphatase (TRAP) expression. Some MGC express enzymes associated with degradation, including cathepsin K [157, 262] and matrix metalloproteinase-9 [144, 156], but levels in osteoclasts are usually higher, coinciding with

increased bone resorption capacity [261, 263]. It is possible that MGC degradative activity is similar to macrophages during initial formation, then diminishes shortly afterwards [128, 264].

There is a lack of research describing phenotypic differences between MGC and the macrophages from which they originate, especially in the context of their inflammatory activity. *In vivo* and *ex vivo* studies on this topic are limited because MGC are difficult to isolate in sufficient quantity and purity for successful analysis. Controlled *in vitro* environments are favorable for investigating effects of specific treatments directly on the cells and analyzing cells using a broader range of techniques (e.g. flow cytometry). The most frequently published *in vitro* MGC models use interleukin (IL)-4 to stimulate MGC formation from human blood monocytes or mouse bone marrow-derived macrophages (BMdM). We have identified two studies that assess immune profile differences between macrophage and MGC. Khan et al [263] compared macrophages, osteoclasts, and MGC using mouse BMdM. Although the focus was on osteoclasts and related markers, CC chemokine and CC receptor gene expression was also assessed. MGC expressed higher CCL3, CCL4, CCL5, and CCL9 than macrophages, while others were generally similar depending on timepoint. McNally and Anderson [265] compared macrophages and MGC derived from human monocytes. Western blots of whole cell lysates and cell immunostaining were used to detect lymphocyte co-stimulatory, osteoclast, and dendritic cell related markers. Results of interest include MGC displaying increased human leukocyte antigen (HLA-DR), slightly increased CD11c, and loss of CD14. A common limitation of these studies is that they do not control for confounding effects of IL-4 treatment. For example, HLA-DR in MGC may not necessarily be increased as a result of multinucleation, rather this is likely attributed the culture receiving IL-4, a known inducer of HLA-DR [266].

Questions remain about MGC phenotype and function. Ultimately, it is important to know whether the presence of MGC in granulomatous conditions is beneficial or damaging.

The answers would influence therapeutic approaches. The objective of this study was to determine how the phenotype of MGC unique from their macrophage precursors in the context of inflammation. This was investigated using our recently described model of IL-4-induced fusion of mouse BMdM and techniques for MGC enrichment and analysis (Chapter 2). Comparing enriched macrophages and MGC from the same original culture controlled for confounding effects. Inflammatory response was assessed by stimulation with conventional lipopolysaccharide (LPS) treatment methods and via the phagocytic pathway using crocidolite asbestos. Key macrophage-related surface markers and cytokines were analyzed: integrin alpha M (CD11b), integrin alpha X (CD11c), adhesion G protein-coupled receptor E1 (F4/80), histocompatibility 2 class II (MHC II), interferon (IFN)-γ, interleukin (IL)-1β, IL-6, tumor necrosis factor (TNF)-α, IL-10, IL-13, and IL-33.

4.3 Methods

4.3.1 Cell culture materials and methods

General methods for mouse BMdM macrophage and MGC culture, enrichment, and quantification have been previously described by our laboratory (Chapter 2). Cells were grown in a humidified, water jacketed incubator (Thermo Fisher Scientific, Waltham, MA) at 37°C and 5% CO_2. Sterile 0.2 µm filtered culture media consisted of RPMI-1640 with 10% heat-inactivated fetal bovine serum (FBS), 25 mM HEPES, 2 mM L-glutamine, 1 mM sodium pyruvate, 100 I.U./mL penicillin, and 100 µg/mL streptomycin (FBS: VWR Seradigm, Radnor, PA; all others: Corning subsidiary Mediatech, Manassas, VA). Cells were suspended by using 0.05% trypsin with 0.53 mM EDTA in HBSS (Corning) or Accutase® with 0.5 mM EDTA in Dulbecco's PBS (BioLegend, San Diego, CA), followed by physical dislodging of cells as necessary using a cell scraper or pipette action. Treatment concentrations of 30 ng/mL were used for recombinant murine proteins M-CSF (R& D

Systems, Minneapolis, MN) and IL-4 (R& D Systems). Centrifugations of cells in tubes were performed at RCF_{avg} 300 x *g* for 5 min. Cytocentrifugations of cells onto slides were performed at approximately RCF_{avg} 250 x *g* for 5 min. Cell counting was completed using a Beckman Coulter (Indianapolis, IN) Z2 cell counter.

Permanox is a trademarked (Nalge Nunc International, Rochester, NY) polymethylpentene tissue culture-treated growth surface with a silicone gasket connecting removable polystyrene chamber walls. Media working volumes per well or vessel were as follows: 8-chamber permanox slides at 0.4 mL, 96-well tissue culture-treated polystyrene (TCPS) plates (Greiner Bio-One, Monroe, NC) at 0.1 mL, and T75 TCPS flasks at 20 mL.

4.3.2 Mice

C57Bl/6 mice (Jackson Laboratories, Bar Harbor, ME) aged 10 to 13 weeks were used for all experiments. Mice were housed in microisolator cages with *ad libitum* access to food and water in a specific-pathogen-free facility maintained at 22 ± 2°C, 30–40% humidity, and 12-hour light/12-hour dark cycle. Mice were euthanized by intraperitoneal injection of sodium pentobarbital followed by a secondary mechanical means of euthanasia prior to removal of rear legs for bone marrow isolation in a tissue culture hood. Experimental protocols were approved by the University of Montana Institutional Animal Care and Use Committee.

4.3.3 Particle preparation

Asbestos was selected as a model treatment because it is well-established by our laboratory and others to be a stimulator of macrophage activity in rodents and humans. Crocidolite asbestos (diameter 160nm, length 5 μm) was obtained from Research Triangle Institute (Research Triangle Park, NC). Asbestos was prepared into a homogenous dispersion in phosphate-buffered saline (PBS, pH 7.4) immediately prior to *in vitro* exposure by

sonicating for one minute with a 500W, 20 kHz Qsonica Q500 (Newtown, CT) cup-horn system at 30% amplitude pulse.

4.3.4 Macrophage and MGC culture

BM was flushed from the tibiae and femora in a sterile environment, pooled, centrifuged, resuspended in media, and seeded at 4 x 10^5 cells/cm^2 in a T75 flask. Cells were incubated at 37°C overnight. Adherent stromal cells were discarded, and suspended macrophage progenitor cells were collected. Progenitor cells were added to T75 flasks at 2 x 10^5 cells/cm^2 with M-CSF for four days to mature into BMdM. Mature BMdM were collected using trypsin and were seeded at 9 x 10^5 cells/cm^2 in permanox chamber slides with IL-4 for four days. Media was replaced with fresh media containing IL-4, then cells were cultured for five more days. The culture now consisted of a mixture of BMdM macrophages and MGC.

Cell detachment was completed using Accutase instead of trypsin for the remainder of the experiment, with efforts to handle cells gently to better preserve cell surface protein integrity. The suspended macrophage and MGC mixture was transferred onto a pre-rinsed 20 μm cell strainer (PluriStrainer by PluriSelect; Leipzig, Germany) and washed twice with 4 mL/wash into a tube. The strainer was inverted and washed twice with 4 mL/wash into a new tube. Cells small enough to pass through the strainer into the first tube were designated as the macrophage-enriched population, while cells blocked by the strainer were designated as the MGC-enriched population. A sample of cells was used to confirm enrichment. Remaining cells were seeded at 2.5 x 10^5 nuclei/mL (≈7.8 x 10^4 nuclei/cm^2) in a 96-well plate. Specified wells were treated with 20 ng/mL LPS from *Escherichia coli* (MilliporeSigma) and 25 μg/mL asbestos. After 24 hours, cells were prepared for flow cytometry and supernatants were collected for multiplex immunoassay.

4.3.5 Quantification of microfiltration enrichment

Samples of macrophage-enriched and MGC-enriched populations were cytocentrifuged and stained using a method similar to Wright-Giemsa (PROTOCOL™ Hema 3™; Fisher Scientific, Kalamazoo, MI) by submerging slides in a methanol-based fixative for 90 sec, "Solution I" for 120 sec, "Solution II" for 30 sec, and water for 90 sec. At least five random, independent (non-overlapping) images were acquired per sample using a Zeiss Axioskop upright microscope with AxioCamMR3 camera (Carl Zeiss, Jena, Germany) at 100x magnification. MGC were defined morphologically as containing three or more nuclei within a common cytoplasm. MGC quantification results are expressed as percent fusion by dividing the number of nuclei within MGC by the total macrophage and MGC nuclei, then multiplying by 100. Alternatively, a purity index was calculated by dividing the number of MGC by total cells.

4.3.6 Flow cytometry

Combined live macrophage and MGC cells were stained with HCS NuclearMask Blue according to manufacturer (Thermo) recommendations. Antibody staining was performed in 100 µl buffer consisting of 1% w/v bovine serum albumin and 0.1% w/v sodium azide in PBS, sterile-filtered. Anti-mouse CD16/CD32 (Tonbo Biosciences, San Diego, CA) was added at 5 µg/mL for 10 minutes to block non-specific antibody binding. The following is a list of fluorochrome conjugated anti-mouse monoclonal antibodies obtained from BioLegend, staining concentrations (µg/mL), and corresponding wavelengths (nm) of lasers and filters: APC CD11b clone M1/70 at 2.5 (637, 670/14), PerCP/Cy5.5 CD11c clone N418 at 10 (488, 695/40), PE F4/80 clone BM8 at 10 (561, 585/16), and FITC MHC II (I-A/I-E) clone M5/114.15.2 at 2.5 (488, 530/30). Wavelengths for NuclearMask were 405, 440/50. Laser power was 100 mW for 637 nm and 50 mW for others. Cell staining time was 20

minutes, followed by two washes. Controls included unstained cells, cells with NuclearMask only, fluorescence minus one, and antibody-capture beads (Thermo) for multicolor compensation. At least 10,000 events per sample were analyzed using an Attune NxT (Thermo) flow cytometer with v2.6 software, with further analysis using FlowJo v10.4.2 software. Note that this acoustic-assisted hydrodynamic focusing cytometer had a configuration that accommodated large MGC cells, while other cytometers with small nozzles may clog.

Forward and side scatter gating was used to remove debris. Macrophages and MGC were separated according to nuclear fluorescence using methods described previously in our laboratory (Chapter 2), which is similar to methods used for analysis of osteoclasts [267] and megakaryocytes [268]. Preliminary experiments indicated that cells could be gated into categories of one nucleus (1N), two nuclei (2N), or three or more nuclei (≥3N) according to nuclear fluorescence, without the need for pre-enrichment by microfiltration. Therefore, MGC and macrophages were combined during staining to improve consistency. Flow cytometry data normalization was completed based on each individual event (e.g. cell) by dividing surface protein fluorescence by nuclear fluorescence. The median normalized ratio of all events within a sample was then used for graphing and statistical analysis.

4.3.7 Multiplex immunoassay

Cytokines secreted by macrophages and MGC were measured using a custom mouse U-PLEX Biomarker Group 1 kit (Meso Scale Discovery, Rockville, MD), which is a multiplex sandwich immunoassay consisting of biotinylated capture antibodies and SULFO-TAG conjugated detection antibodies. The 96-well plate assay was completed according to manufacturer protocol. The plate was washed with 300 µl/well using a Thermo Wellwash 4 MK 2 and shaken at approximately 715 RPM on a Thermo 4625 shaker. Electrochemiluminescence was measured using the MESO QuickPlex SQ 120 with Discovery Workbench 4.0

software. Secreted protein concentrations were calculated using a four-parameter logistic standard curve. Some concentrations were below the limit of detection and could not be estimated from the curves, particularly in unstimulated cells. These nondetect values were considered to be zero for graphing and statistical analysis.

4.3.8 Statistics

Statistical analysis involved comparison of means using a two-way ANOVA followed by multiple comparisons using Tukey's honest significant difference (HSD) test to compensate for increased type I error. Statistical significance was defined as a probability of type I error occurring at less than 5%. Significant simple contrasts of predetermined scientific interest are displayed on graphs, including treatment differences for each cell type and cell type differences for each treatment; complex and cross-group contrasts are not shown (e.g. Mac with LPS versus MGC control). Significant treatment differences compared to control of corresponding cell type are shown as *$p < 0.05$, **$p < 0.01$, and ***$p < 0.001$. The same p-value scheme is used for other contrasts indicated by daggers (†) with bars. Data is represented as the mean ± standard error of three independent replicate groups of mice for each condition. All analysis was completed in R v3.6.1 statistical software.

4.4 Results

4.4.1 Enrichment by microfiltration

Mature mouse BMdM were treated with IL-4 to induce macrophage fusion into MGC. Then, the mixed culture was separated into macrophage-enriched and MGC-enriched populations by microfiltration, as previously described (Chapter 2). A portion of these cells were collected for cytocentrifugation, staining, and morphological assessment of enrichment efficiency (Fig. 16). The percent fusion of each population was 33.1% for

MGC-enriched and 0.5% for macrophage-enriched. The purity index was increased 71-fold. Remaining cells from each population were seeded according to number of nuclei/well for subsequent experiments. Two groups of these cells received treatments known to stimulate macrophages: LPS and a combination of LPS and crocidolite asbestos. Supernatants containing secreted cytokines were collected after 24 hours and cells were prepared for flow cytometry.

4.4.2 Surface markers

Surface proteins on macrophages and MGC were analyzed by flow cytometry 24 hours after stimulation with LPS and asbestos. In order to compare marker expression between these two cell types, data normalization was required due to the difference in cell size. To illustrate the importance of normalization, cells were gated into categories of one nucleus (1N), two nuclei (2N), or three or more nuclei (≥3N) for comparisons. The increase in surface marker fluorescence correlates with an increase in the number of nuclei (Fig. 17). MGC are formed by the fusion of macrophages into a larger cell, so it is logical that the nucleus to membrane ratio remains proportional (Fig. 18). Evidence of this has been shown by live cell imaging of fusion [235] and results suggesting similar buoyant densities (Chapter 2). Therefore, surface protein fluorescence was normalized according to nuclear fluorescence of each individual cell.

Normalized surface marker expression in macrophages and MGC was compared for unstimulated cells, stimulated with LPS, and stimulated with LPS and asbestos (Fig. 19). Results of a two-way ANOVA indicate that cell-type effects were not significant. Treatment with LPS resulted in significant increases in F4/80 and a slightly increasing trend in CD11b and CD11c, consistent with previous BMdM studies [269, 270]. Macrophage activation by

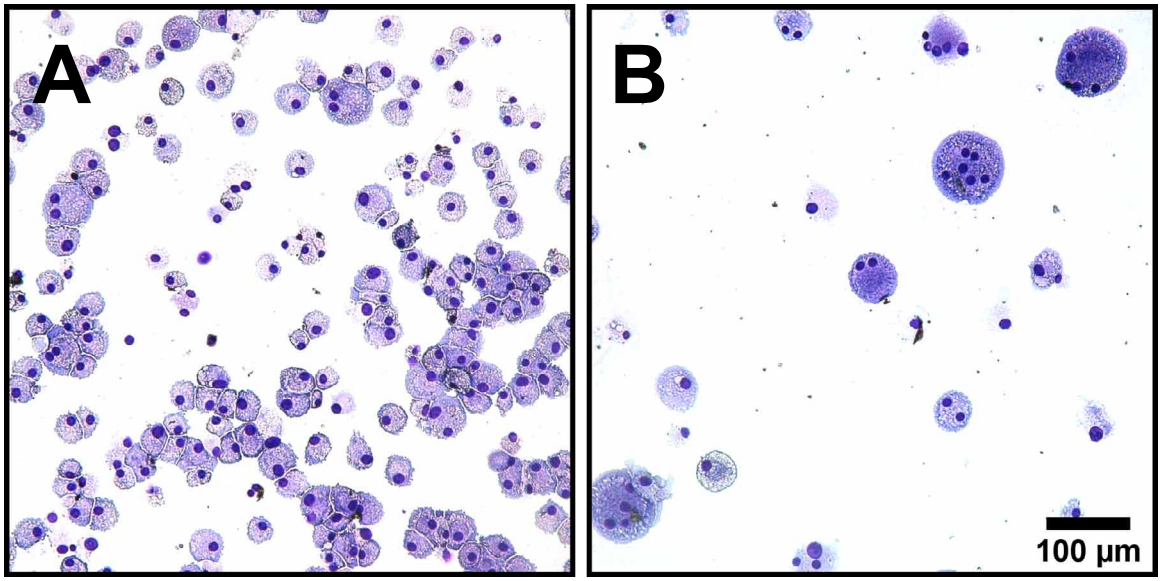

Fig. 16. Enrichment by microfiltration. Representative images of purified cell populations resulting from microfiltration separation. (A) Cells that passed through the filter were macrophage-enriched. (B) Cells blocked by the filter were MGC-enriched. After filtration, cell concentrations were adjusted to seed 96-well plates with equal numbers of nuclei/well for subsequent experiments. Scale is same for both images, bar 100 µm.

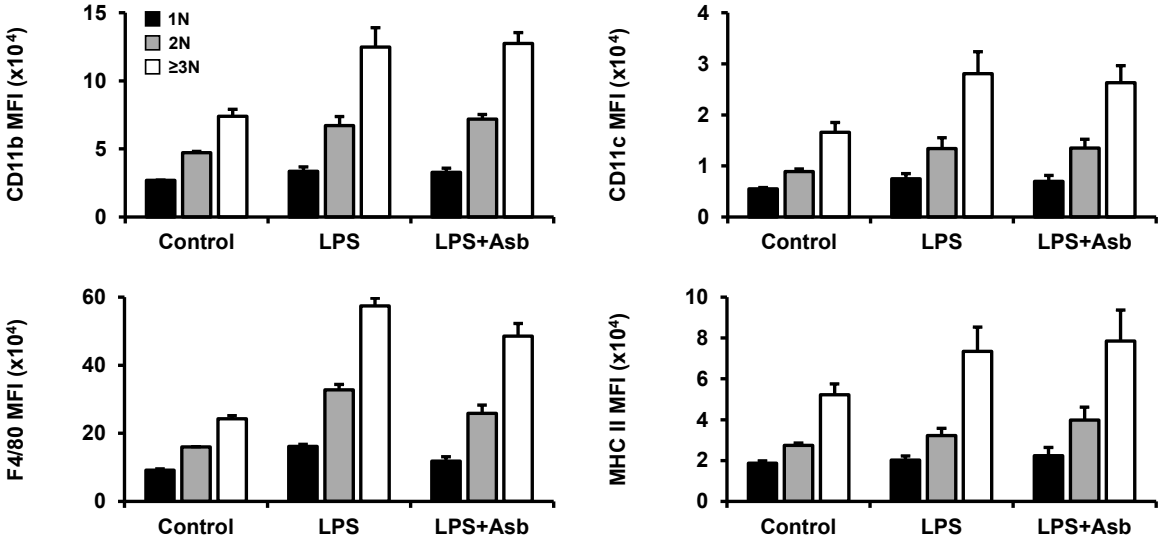

Fig. 17. Surface markers before normalization. Cells were gated according to nuclear fluorescence into three groups: one nucleus (1N; black bars), two nuclei (2N; gray), and three or more nuclei (≥3N; white). Median fluorescence intensity (MFI) of all surface markers increases in binucleated macrophages (2N) and MGC (≥3N), which may lead to the conclusion that marker expression is increased in these cells. However, the increase in fluorescence may simply be a result of larger cell size, with actual membrane density distribution of markers remaining unchanged. This demonstrates the importance of data normalization.

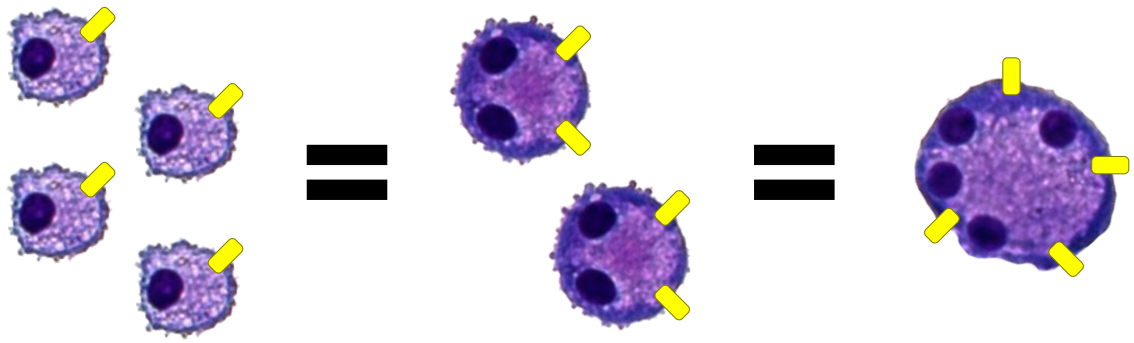

Fig. 18. Surface marker density illustration. Yellow rectangles indicate x number of surface markers. If x markers on each single-nucleated macrophage were conserved during fusion, then binucleated macrophages would each have 2x and an MGC with four nuclei would have 4x. This may lead to a false interpretation that surface marker expression is increased in MGC, when the actual membrane density distribution is equivalent. Therefore, data should be normalized in proportion to the number of nuclei per cell.

particle exposure has been shown to increase antigen-presentation [6], so LPS and asbestos treatment results showing increased MHC II were expected, though the increase was not statistically significant.

4.4.3 Cytokine secretion

Cytokines secreted by enriched populations of macrophages and MGC were analyzed by multiplex immunoassay 24 hours after stimulation with LPS and asbestos. In contrast to surface marker data, cytokine results did not require normalization because this was already controlled by the experimental design: supernatants were collected from cells seeded at an equal number of nuclei per well with an equal volume of media per well. Baseline secretion of all cytokines was very low (Fig. 20), as expected. This is why it was important to include treatments known to stimulate macrophages. Results of a two-way ANOVA indicate that cell-type effects were significant ($p<0.05$) for all proteins analyzed. Therefore, MGC in this study have an impaired ability to either produce or secrete these cytokines compared to macrophages. Although certain cytokines secreted by stimulated MGC were slightly increased from baseline, only IL-6 from the LPS-treated group showed a statistically significant increase.

Macrophages secreted higher concentrations of multiple cytokines when stimulated compared to baseline macrophages (Fig. 20). Many increases resulted from LPS treatment alone, but other cytokines were further increased when asbestos was added. Particularly, IL-1β and TNF-α were significantly higher in the LPS plus asbestos group compared to LPS alone, consistent with our previous studies [271, 272]. It was anticipated that IL-6 would also be increased by asbestos, but levels remained the same as with LPS alone. This was likely because the response to LPS was already very high.

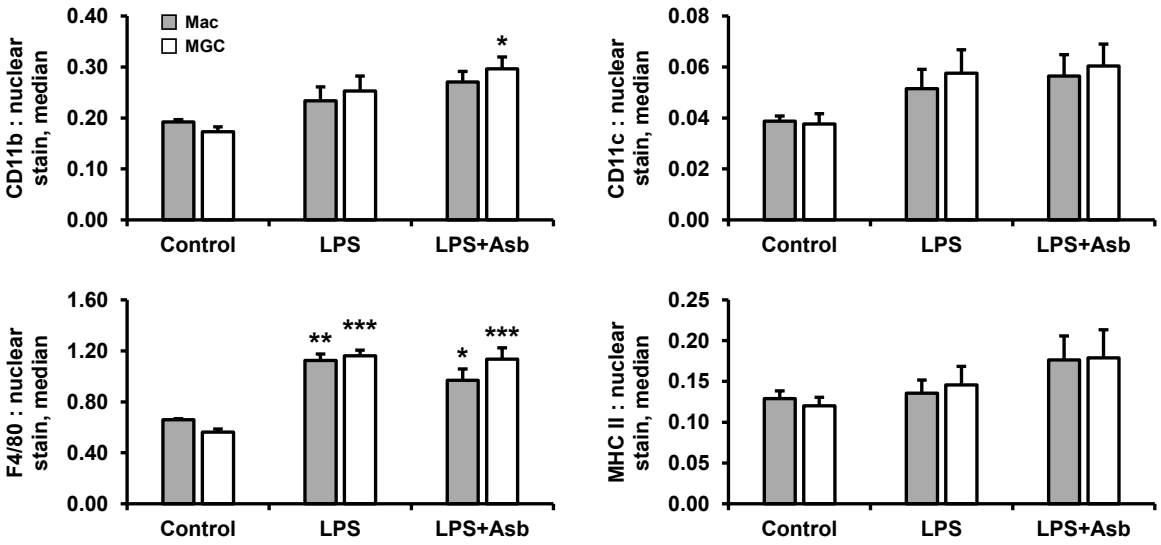

Fig. 19. Surface markers after normalization. Normalized protein expression by macrophages (gray bars) and MGC (white bars) that were unstimulated (control) or stimulated with LPS or LPS plus asbestos for 24 h. No significant differences in surface markers were observed between macrophages and MGC. Asterisks(*) indicate significant treatment effects versus corresponding cell-type control.

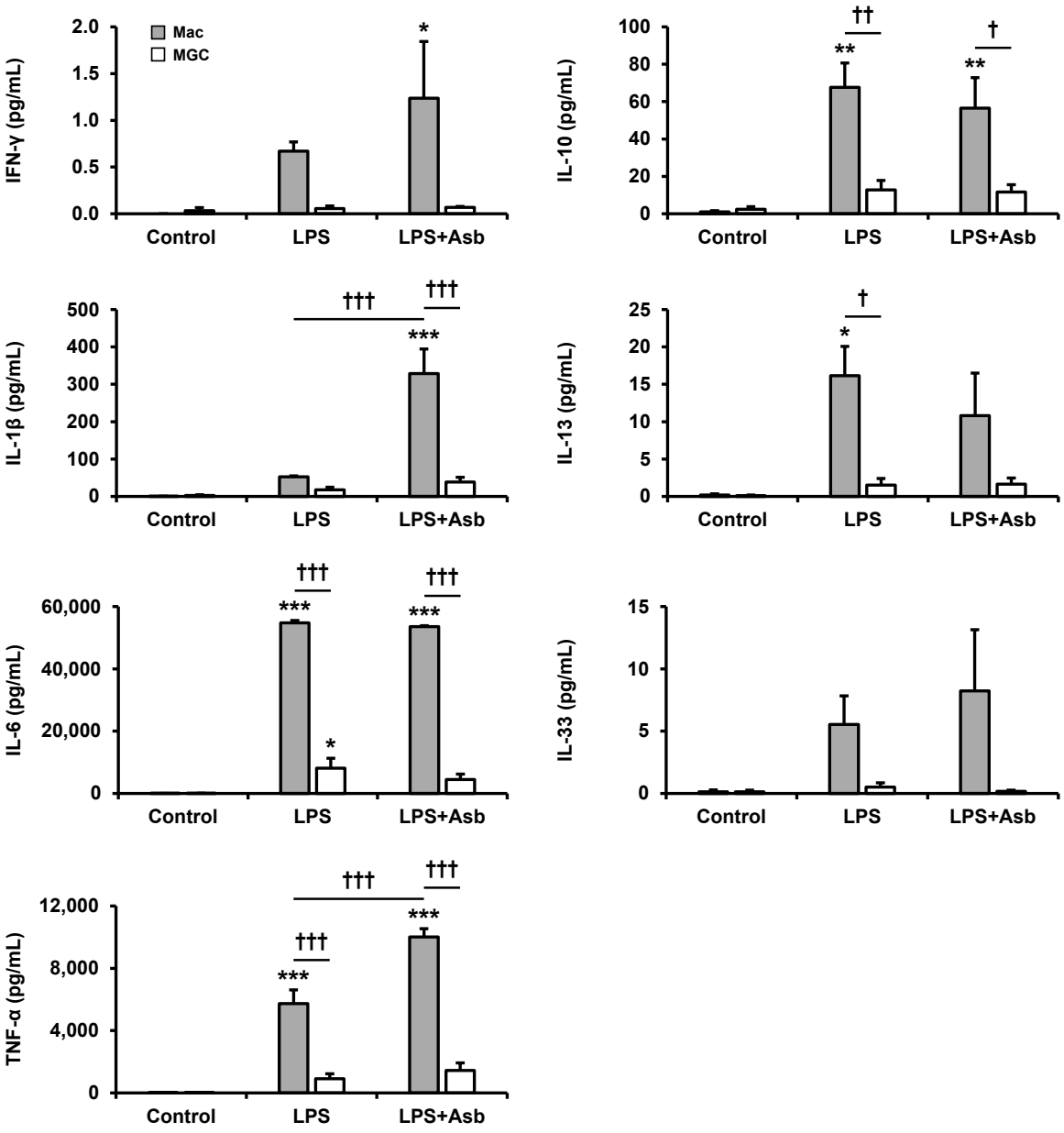

Fig. 20. Cytokine secretion. Supernatant protein concentrations from enriched populations of macrophages (gray bars) and MGC (white bars) that were unstimulated (control) or stimulated with LPS or LPS plus asbestos for 24 h. The immunoassay included cytokines generally associated with classical (M1; left column) and alternative (M2; right column) activation. Asterisks(*) indicate significant treatment effects versus corresponding cell-type control. Daggers(†) indicate other significant contrasts as shown by bars.

4.5 Discussion

Our recent investigation of *in vitro* MGC formation (Chapter 2) helped establish techniques that facilitated the completion of this study. Mouse BMdM were treated with IL-4 in permanox chamber slides to induce macrophage fusion into MGC. In order to effectively compare macrophages and MGC, it was important to purify populations arising from the same original culture. Purity was increased 71-fold by simple microfiltration, which allowed for continuation of the cell culture without stains or other treatments that would interfere with remaining experiments. Additional purification steps may have improved purity, but at the sacrifice of reduced total cell numbers. Enrichment allowed for more appropriate phenotype comparisons between macrophages and MGC. The main objective of this study was to assess common surface markers and cytokines at baseline and in response to stimulation. Stimulation was especially important for meaningful cytokine comparisons because both macrophage and MGC baseline secretions are very low.

Previous MGC phenotype studies [263, 265] used IL-4 to stimulate macrophage fusion into MGC, then compared these cultures with untreated macrophages. Results from using this experimental design cannot be used to distinguish whether any observed cell-type differences were a consequence of multinucleation or an artifact of IL-4 treatment. In the current study, enrichment methods allowed for macrophages and MGC to be sourced from the same IL-4-stimulated culture. Cell culture could be continued after enrichment by microfiltration without interfering factors present in other separation methods, such as stains required for fluorescence-activated cell sorting. This is the first MGC phenotype study, to our knowledge, that is controlled in a manner that removes confounding effects of treatment differences and other manipulations.

Normalized surface marker expression results indicate that common macrophage markers are present in a similar density on MGC. This was not surprising considering that MGC are formed by macrophage fusion and both cell types were sourced from the same

cultures. A particularly interesting result was that MGC-enriched cultures had a similar response to stimulation as macrophage-enriched cultures. For example, MGC had the capacity to respond to LPS by upregulating F4/80. This suggests that MGC have similar levels of toll-like receptor (TLR) 4 and functional LPS-TLR4 signaling pathways.

Baseline cytokine secretion was very low in both macrophages and MGC, as expected. However, the observation that MGC have a diminished ability to produce/secrete cytokines in response to stimulation was somewhat unexpected. Surface marker results suggested that MGC retain the capacity of reacting to LPS stimulation, indicating that those intracellular signaling pathways were not impaired. However, it is possible that those surface proteins were already loaded in intracellular vesicle pools, transferred from macrophages during fusion, that translocated to the plasma membrane during stimulation. Increased cytokine secretion is more dependent on *de novo* synthesis, followed by secretion via exocytosis. Notably, release of cytokines from both conventional and unconventional (e.g. IL-1β after LPS+Asb) secretion pathways were impaired in MGC.

One potential explanation of the impaired cytokine response in MGC is that the presence of multiple nuclei disrupts intracellular signaling and transcription factor localization. The organelle organization and nuclear coordination following fusion is not well understood. An osteoclast study claimed that only certain nuclei within the multinucleated cell are transcriptionally active [273], but another study said all nuclei were active [274]. Numerous cell functions could become disrupted throughout the complex pathway from cell signaling in response to stimulation to transcriptional upregulation, protein processing, and secretion. Further investigation is needed to determine how these mechanisms are altered in MGC. Some example approaches include flow cytometry to assess relevant membrane receptors, microscopic observation of transcription factor localization with nuclei, RT-qPCR, immunoassays using cell lysates, and fluorescence microscopy of organelles and secretory vesicles.

Overall, MGC appear to maintain certain macrophage surface protein characteristics, while losing the ability to promote an inflammatory response. These results fit with the theory that MGC form a "wall" to isolate the host from a foreign body without causing excessive inflammation. In this case, the presence of MGC would be beneficial. However, more research is needed to better understand how the MGC phenotype may differ in response to other stimulants and according to their environment. This fundamental cell biology knowledge will help to develop methods to control the foreign body response, as well as provide insight into several other granulomatous conditions in which the role of MGC is unclear.

4.6 Acknowledgements

Special thanks for technical laboratory support from Pam Shaw, Center for Environmental Health Sciences (CEHS) Fluorescence Cytometry core facility. Research funding was provided by an Institutional Development Award (IDeA) from the National Institute of General Medical Sciences (NIGMS) of the National Institutes of Health (NIH) under grant number P30GM103338. Contents of this publication are solely the responsibility of the authors and do not necessarily represent the official views of NIGMS or NIH.

Appendix A

ImageJ Macro

```
// Macro “CountAndConfirm” by Kevin Trout
// Add or remove "run("Fill Holes");" lines as appropriate for image conditions

macro "CountAndConfirm [q]" {
function PrimaryMethod() {
	roiManager("reset");
	run("Duplicate...", "title=[Counting Window]");
	run("Make Binary");
	// run("Fill Holes");
	run("Ultimate Points");
	run("Make Binary");
	run("Analyze Particles...", "size=0-Infinity circularity=0.00-1.00 show=Nothing summarize
add");
	close();
	roiManager("Show All");
	if(getBoolean("Satisfied with Result?\n  \"Yes\" to continue with next image in folder.\n
\"No\" to repeat analysis with manual threshold.\n  \"Cancel\" to end batch.")) {
		run("Open Next");
		PrimaryMethod();
	} else {
		n=Table.size("Summary");
		Table.deleteRows(n-1,n-1,"Summary");
		SecondaryMethod();
	}
}

function SecondaryMethod() {
	roiManager("reset");
	run("Duplicate...", "title=[Counting Window]");
	run("8-bit");
	run("Threshold...");
	title = "User Input Required";
	msg = "Manually threshold, then click \"OK\".";
	waitForUser(title, msg);
	run("Make Binary");
	run("Fill Holes");
	run("Ultimate Points");
	run("Make Binary");
	run("Analyze Particles...", "size=0-Infinity circularity=0.00-1.00 show=Nothing summarize
add");
	close();
	roiManager("Show All");
	if(getBoolean("Satisfied with Result?\n  \"Yes\" to continue with next image in folder.\n
\"No\" to repeat analysis with manual threshold.\n  \"Cancel\" to end batch.")) {
		run("Open Next");
		PrimaryMethod();
	} else {
		n=Table.size("Summary");
		Table.deleteRows(n-1,n-1,"Summary");
		SecondaryMethod();
	}
}
PrimaryMethod();
}
```

Appendix B

Rights and Permissions

The content of this dissertation is the work of author, Kevin L. Trout. Parts of this dissertation have been previously published, have been submitted for publication, or will be submitted in the future. Collaborative efforts contributed to work contained in this dissertation, as indicated in acknowledgements sections and in co-author listing within publications shown below.

B.1 Book Chapter: Elsevier

Jessop F, Trout KL, Holian A, Migliaccio C, 2018. 15.07 - Inflammatory Cells of the Lung: Macrophages, in: McQueen, C.A. (Ed.), Comprehensive Toxicology (Third Edition). Elsevier, Oxford, p.94–114. https://doi.org/10.1016/B978-0-12-801238-3.95651-4

Usage/Contribution
Body text was excerpted/modified from "Section 15.07.3 Macrophage Origins" and figures 1 and 3 were reprinted/modified. Kevin reviewed literature and contributed to writing this text. Kevin created figure 1 illustration and caption. Kevin acquired microscope images for figure 3.

B.2 Book Chapter: Springer

Trout KL, Jessop F, Migliaccio CT, 2016. Macrophage and multinucleated giant cell classification, in: Otsuki T, Yoshioka Y, Holian A (Eds.), Biological Effects of Fibrous and Particulate Substances, Current Topics in Environmental Health and Preventive Medicine. Springer Japan, Tokyo, p.1–26. https://doi.org/10.1007/978-4-431-55732-6_1

Usage/Contribution
The majority of this chapter was reproduced with modifications. Kevin wrote section "1.3 Multinucleated Giant Cells" and produced the associated figure 1.2, box 1.1, and table 1.2. Kevin also contributed to the remainder of the publication.

B.3 Journal Article

Trout KL, Holian A. Factors influencing multinucleated giant cell formation in vitro. Immunobiology. Available online 10 Aug 2019. https://doi.org/10.1016/j.imbio.2019.08.002

Usage/Contribution
This article was reproduced with only minor modifications. Kevin conducted the laboratory work and wrote the article with guidance from Andrij Holian.

SPRINGER NATURE LICENSE TERMS AND CONDITIONS

Aug 22, 2019

This Agreement between Mr. Kevin Trout ("You") and Springer Nature ("Springer Nature") consists of your license details and the terms and conditions provided by Springer Nature and Copyright Clearance Center.

License Number	4638320194864
License date	Jul 29, 2019
Licensed Content Publisher	Springer Nature
Licensed Content Publication	Springer eBook
Licensed Content Title	Macrophage and Multinucleated Giant Cell Classification
Licensed Content Author	Kevin L. Trout, Forrest Jessop, Christopher T. Migliaccio
Licensed Content Date	Jan 1, 2016
Type of Use	Thesis/Dissertation
Requestor type	academic/university or research institute
Format	electronic
Portion	full article/chapter
Will you be translating?	no
Circulation/distribution	<501
Author of this Springer Nature content	yes
Title	Multinucleated giant cell formation and phenotype
Institution name	n/a
Expected presentation date	Aug 2019

ELSEVIER LICENSE
TERMS AND CONDITIONS

Aug 22, 2019

This Agreement between Mr. Kevin Trout ("You") and Elsevier ("Elsevier") consists of your license details and the terms and conditions provided by Elsevier and Copyright Clearance Center.

License Number	4654380921144
License date	Aug 22, 2019
Licensed Content Publisher	Elsevier
Licensed Content Publication	Elsevier Books
Licensed Content Title	Comprehensive Toxicology
Licensed Content Author	F. Jessop,K.L. Trout,A. Holian,C. Migliaccio
Licensed Content Date	Jan 1, 2018
Licensed Content Pages	21
Start Page	94
End Page	114
Type of Use	reuse in a thesis/dissertation
Intended publisher of new work	other
Portion	excerpt
Number of excerpts	2
Format	electronic
Are you the author of this Elsevier chapter?	Yes
Will you be translating?	No
Title of your thesis/dissertation	Multinucleated giant cell formation and phenotype
Expected completion date	Aug 2019
Estimated size (number of pages)	150

ELSEVIER LICENSE
TERMS AND CONDITIONS

Aug 22, 2019

This Agreement between Mr. Kevin Trout ("You") and Elsevier ("Elsevier") consists of your license details and the terms and conditions provided by Elsevier and Copyright Clearance Center.

License Number	4654380824105
License date	Aug 22, 2019
Licensed Content Publisher	Elsevier
Licensed Content Publication	Elsevier Books
Licensed Content Title	Comprehensive Toxicology
Licensed Content Author	F. Jessop,K.L. Trout,A. Holian,C. Migliaccio
Licensed Content Date	Jan 1, 2018
Licensed Content Pages	21
Start Page	94
End Page	114
Type of Use	reuse in a thesis/dissertation
Intended publisher of new work	other
Portion	figures/tables/illustrations
Number of figures/tables/illustrations	2
Format	electronic
Are you the author of this Elsevier chapter?	Yes
Will you be translating?	No
Original figure numbers	Figures 1 and 3.
Title of your thesis/dissertation	Multinucleated giant cell formation and phenotype
Expected completion date	Aug 2019
Estimated size (number of pages)	150

References

1. Furth R van and Blusse van Oud Alblas A. The current view on the origin of pulmonary macrophages. Pathol Res Pract 1982;175:38–49.
2. Thomas ED, Ramberg RE, Sale GE, Sparkes RS, and Golde DW. Direct evidence for a bone marrow origin of the alveolar macrophage in man. Science 1976;192:1016–8.
3. Toews GB, Vial WC, Dunn MM, et al. The accessory cell function of human alveolar macrophages in specific T cell proliferation. J Immunol 1984;132:181–6.
4. Brodsky FM and Guagliardi LE. The cell biology of antigen processing and presentation. Annu Rev Immunol 1991;9:707–44.
5. Byersdorfer CA and Chaplin DD. Visualization of early APC/T cell interactions in the mouse lung following intranasal challenge. J Immunol 2001;167:6756–64.
6. Migliaccio CT, Hamilton Jr RF, and Holian A. Increase in a distinct pulmonary macrophage subset possessing an antigen-presenting cell phenotype and in vitro APC activity following silica exposure. Toxicol Appl Pharmacol 2005;205:168–76.
7. Strieter RM, Remick DG, Lynch J. P. 3, et al. Differential regulation of tumor necrosis factor-alpha in human alveolar macrophages and peripheral blood monocytes: a cellular and molecular analysis. Am J Respir Cell Mol Biol 1989;1:57–63.
8. Jabbour AJ, Holian A, and Scheule RK. Lung lining fluid modification of asbestos bioactivity for the alveolar macrophage. Toxicol Appl Pharmacol 1991;110:283–94.
9. Schulz C, Perdiguero EG, Chorro L, et al. A lineage of myeloid cells independent of myb and hematopoietic stem cells. Science 2012;336:86–90.
10. Perdiguero EG and Geissmann F. The development and maintenance of resident macrophages. Nat Immunol 2015;17:2–8.
11. Jenkins SJ, Ruckerl D, Cook PC, et al. Local macrophage proliferation, rather than recruitment from the blood, is a signature of TH2 inflammation. Science 2011;332:1284–8.
12. Furth R van, Cohn ZA, Hirsch JG, Humphrey JH, Spector WG, and Langevoort HL. The mononuclear phagocyte system: a new classification of macrophages, monocytes, and their precursor cells. Bull World Health Organ 1972;46:845–52.

13. Ziegler-Heitbrock HW, Fingerle G, Strobel M, et al. The novel subset of CD14+/CD16+ blood monocytes exhibits features of tissue macrophages. Eur J Immunol 1993;23:2053–8.

14. Tacke F and Randolph GJ. Migratory fate and differentiation of blood monocyte subsets. Immunobiology 2006;211:609–18.

15. Hashimoto D, Chow A, Noizat C, et al. Tissue-resident macrophages self-maintain locally throughout adult life with minimal contribution from circulating monocytes. Immunity 2013;38:792–804.

16. Yona S, Kim KW, Wolf Y, et al. Fate mapping reveals origins and dynamics of monocytes and tissue macrophages under homeostasis. Immunity 2013;38:79–91.

17. Ginhoux F, Schultze JL, Murray PJ, Ochando J, and Biswas SK. New insights into the multidimensional concept of macrophage ontogeny, activation and function. Nat Immunol 2015;17:34–40.

18. Gomez Perdiguero E, Klapproth K, Schulz C, et al. Tissue-resident macrophages originate from yolk-sac-derived erythro-myeloid progenitors. Nature 2015;518:547–51.

19. Ginhoux F and Jung S. Monocytes and macrophages: developmental pathways and tissue homeostasis. Nat Rev Immunol 2014;14:392–404.

20. Tavian M and Peault B. Embryonic development of the human hematopoietic system. Int J Dev Biol 2003;49:243–50.

21. Golde DW, Byers LA, and Finley TN. Proliferative capacity of human alveolar macrophage. Nature 1974;247:373–5.

22. Chen BD, Mueller M, and Chou TH. Role of granulocyte/macrophage colony-stimulating factor in the regulation of murine alveolar macrophage proliferation and differentiation. J Immunol 1988;141:139–44.

23. Bitterman PB, Adelberg S, Goodman S, Saltzman L, and Crystal RG. Role of macrophage replication in modulating the increased number of alveolar macrophages in chronic inflammatory lung disorders. Am Rev Respir Dis Supplement 1983;127:A60.

24. Kennedy DW and Abkowitz JL. Kinetics of central nervous system microglial and macrophage engraftment: analysis using a transgenic bone marrow transplantation model. Blood 1997;90:986–93.

25. Maus UA, Janzen S, Wall G, et al. Resident alveolar macrophages are replaced by recruited monocytes in response to endotoxin-induced lung inflammation. Am J Respir Cell Mol Biol 2006;35:227–35.

26. Tarling JD, Lin HS, and Hsu S. Self-renewal of pulmonary alveolar macrophages: evidence from radiation chimera studies. J Leukoc Biol 1987;42:443–6.

27. Gordon S and Taylor PR. Monocyte and macrophage heterogeneity. Nat Rev Immunol 2005;5:953–64.

28. Gordon S. The macrophage. Bioessays 1995;17:977–86.

29. Gordon S. Alternative activation of macrophages. Nat Rev Immunol 2003;3:23–35.

30. Mosser DM and Edwards JP. Exploring the full spectrum of macrophage activation. Nat Rev Immunol 2008;8:958–69.

31. Martinez FO and Gordon S. The M1 and M2 paradigm of macrophage activation: time for reassessment. F1000Prime Rep 2014;6:13.

32. Murray PJ, Allen JE, Biswas SK, et al. Macrophage activation and polarization: nomenclature and experimental guidelines. Immunity 2014;41:14–20.

33. Verreck FA, Boer T de, Langenberg DM, et al. Human IL-23-producing type 1 macrophages promote but IL-10-producing type 2 macrophages subvert immunity to (myco)bacteria. Proc Natl Acad Sci U S A 2004;101:4560–5.

34. MacMicking JD, North RJ, LaCourse R, Mudgett JS, Shah SK, and Nathan CF. Identification of nitric oxide synthase as a protective locus against tuberculosis. Proc Natl Acad Sci U S A 1997;94:5243–8.

35. MacMicking J, Xie QW, and Nathan C. Nitric oxide and macrophage function. Annu Rev Immunol 1997;15:323–50.

36. Shaykhiev R, Krause A, Salit J, et al. Smoking-dependent reprogramming of alveolar macrophage polarization: implication for pathogenesis of chronic obstructive pulmonary disease. J Immunol 2009;183:2867–83.

37. Martinez VG, Escoda-Ferran C, Tadeu Simoes I, et al. The macrophage soluble receptor AIM/Api6/CD5L displays a broad pathogen recognition spectrum and is involved in early response to microbial aggression. Cell Mol Immunol 2014;11:343–54.

38. Chang NC, Hung SI, Hwa KY, et al. A macrophage protein, Ym1, transiently expressed during inflammation is a novel mammalian lectin. J Biol Chem 2001;276:17497–506.

39. Raes G, De Baetselier P, Noel W, Beschin A, Brombacher F, and Hassanzadeh Gh G. Differential expression of FIZZ1 and Ym1 in alternatively versus classically activated macrophages. J Leukoc Biol 2002;71:597–602.

40. Welch JS, Escoubet-Lozach L, Sykes DB, Liddiard K, Greaves DR, and Glass CK. TH2 cytokines and allergic challenge induce Ym1 expression in macrophages by a STAT6-dependent mechanism. J Biol Chem 2002;277:42821–9.

41. Giannetti N, Moyse E, Ducray A, et al. Accumulation of Ym1/2 protein in the mouse olfactory epithelium during regeneration and aging. Neuroscience 2004;123:907–17.

42. Nair MG, Gallagher IJ, Taylor MD, et al. Chitinase and Fizz family members are a generalized feature of nematode infection with selective upregulation of Ym1 and Fizz1 by antigen-presenting cells. Infect Immun 2005;73:385–94.

43. Arora M, Chen L, Paglia M, et al. Simvastatin promotes Th2-type responses through the induction of the chitinase family member Ym1 in dendritic cells. Proc Natl Acad Sci U S A 2006;103:7777–82.

44. Ferrante CJ, Pinhal-Enfield G, Elson G, et al. The adenosine-dependent angiogenic switch of macrophages to an M2-like phenotype is independent of interleukin-4 receptor alpha (IL-4Ralpha) signaling. Inflammation 2013;36:921–31.

45. Luo C, Chen M, Madden A, and Xu H. Expression of complement components and regulators by different subtypes of bone marrow-derived macrophages. Inflammation 2012;35:1448–61.

46. Mantovani A, Sica A, Sozzani S, Allavena P, Vecchi A, and Locati M. The chemokine system in diverse forms of macrophage activation and polarization. Trends Immunol 2004;25:677–86.

47. Li MO, Wan YY, Sanjabi S, Robertson AK, and Flavell RA. Transforming growth factor-beta regulation of immune responses. Annu Rev Immunol 2006;24:99–146.

48. Couper KN, Blount DG, Wilson MS, et al. IL-10 from CD4CD25Foxp3CD127 adaptive regulatory T cells modulates parasite clearance and pathology during malaria infection. PLoS Pathog 2008;4:e1000004.

49. Couper KN, Blount DG, and Riley EM. IL-10: the master regulator of immunity to infection. J Immunol 2008;180:5771–7.

50. Anders HJ and Ryu M. Renal microenvironments and macrophage phenotypes determine progression or resolution of renal inflammation and fibrosis. Kidney Int 2011;80:915–25.

51. Lugo-Villarino G, Verollet C, Maridonneau-Parini I, and Neyrolles O. Macrophage polarization: convergence point targeted by mycobacterium tuberculosis and HIV. Front Immunol 2011;2:43.

52. Zizzo G, Hilliard BA, Monestier M, and Cohen PL. Efficient clearance of early apoptotic cells by human macrophages requires M2c polarization and MerTK induction. J Immunol 2012;189:3508–20.

53. Duluc D, Delneste Y, Tan F, et al. Tumor-associated leukemia inhibitory factor and IL-6 skew monocyte differentiation into tumor-associated macrophage-like cells. Blood 2007;110:4319–30.

54. Duluc D, Corvaisier M, Blanchard S, et al. Interferon-gamma reverses the immunosuppressive and protumoral properties and prevents the generation of human tumor-associated macrophages. Int J Cancer 2009;125:367–73.

55. Jeannin P, Duluc D, and Delneste Y. IL-6 and leukemia-inhibitory factor are involved in the generation of tumor-associated macrophage: regulation by IFN-gamma. Immunotherapy 2011;3:23–6.

56. Birnie KA, Yip YY, Ng DC, et al. Loss of miR-223 and JNK signalling contribute to elevated Stathmin in malignant pleural mesothelioma. Mol Cancer Res 2015.

57. Christie C, Madsen SJ, Peng Q, and Hirschberg H. Macrophages as nanoparticle delivery vectors for photothermal therapy of brain tumors. Ther Deliv 2015;6:371–84.

58. Villalta SA, Rinaldi C, Deng B, Liu G, Fedor B, and Tidball JG. Interleukin-10 reduces the pathology of mdx muscular dystrophy by deactivating M1 macrophages and modulating macrophage phenotype. Hum Mol Genet 2011;20:790–805.

59. Kaczmarek M, Nowicka A, Kozlowska M, Zurawski J, Batura-Gabryel H, and Sikora J. Evaluation of the phenotype pattern of macrophages isolated from malignant and non-malignant pleural effusions. Tumour Biol 2011;32:1123–32.

60. Sharda DR, Yu S, Ray M, et al. Regulation of macrophage arginase expression and tumor growth by the Ron receptor tyrosine kinase. J Immunol 2011;187:2181–92.

61. Cassol E, Cassetta L, Alfano M, and Poli G. Macrophage polarization and HIV-1 infection. J Leukoc Biol 2010;87:599–608.

62. Dinarello CA. A clinical perspective of IL-1beta as the gatekeeper of inflammation. Eur J Immunol 2011;41:1203–17.

63. Guo Z, Wen Z, Qin A, et al. Antisense oligonucleotide treatment enhances the recovery of acute lung injury through IL-10-secreting M2-like macrophage-induced expansion of CD4+ regulatory T cells. J Immunol 2013;190:4337–48.

64. Ingham E and Fisher J. The role of macrophages in osteolysis of total joint replacement. Biomaterials 2005;26:1271–86.

65. Antonios JK, Yao Z, Li C, Rao AJ, and Goodman SB. Macrophage polarization in response to wear particles in vitro. Cell Mol Immunol 2013;10:471–82.

66. Nich C, Takakubo Y, Pajarinen J, et al. Macrophages-key cells in the response to wear debris from joint replacements. J Biomed Mater Res A 2013;101:3033–45.

67. Goodman SB, Gibon E, Pajarinen J, et al. Novel biological strategies for treatment of wear particle-induced periprosthetic osteolysis of orthopaedic implants for joint replacement. J R Soc Interface 2014;11:20130962.

68. Webb DC, McKenzie AN, and Foster PS. Expression of the Ym2 lectin-binding protein is dependent on interleukin (IL)-4 and IL-13 signal transduction: identification of a novel allergy-associated protein. J Biol Chem 2001;276:41969–76.

69. Migliaccio CT, Buford MC, Jessop F, and Holian A. The IL-4Rα pathway in macrophages and its potential role in silica-induced pulmonary fibrosis. J Leukoc Biol 2008;83:630–9.

70. Goerdt S, Politz O, Schledzewski K, et al. Alternative versus classical activation of macrophages. Pathobiology 1999;67:222–6.

71. Mosser DM. The many faces of macrophage activation. J Leukoc Biol 2003;73:209–12.

72. Spencer M, Yao-Borengasser A, Unal R, et al. Adipose tissue macrophages in insulin-resistant subjects are associated with collagen VI and fibrosis and demonstrate alternative activation. Am J Physiol Endocrinol Metab 2010;299:E1016–27.

73. Martinez FO, Sica A, Mantovani A, and Locati M. Macrophage activation and polarization. Front Biosci 2008;13:453–61.

74. Edwards JP, Zhang X, Frauwirth KA, and Mosser DM. Biochemical and functional characterization of three activated macrophage populations. J Leukoc Biol 2006;80:1298–307.

75. Zhang W, Xu W, and Xiong S. Macrophage differentiation and polarization via phosphatidylinositol 3-kinase/Akt-ERK signaling pathway conferred by serum amyloid P component. J Immunol 2011;187:1764–77.

76. Kobayashi T, Onodera S, Kondo E, et al. Impaired fracture healing in macrophage migration inhibitory factor-deficient mice. Osteoporos Int 2011;22:1955–65.

77. Asai A, Nakamura K, Kobayashi M, Herndon DN, and Suzuki F. CCL1 released from M2b macrophages is essentially required for the maintenance of their properties. J Leukoc Biol 2012;92:859–67.

78. Pradhan V, Patwardhan M, and Ghosh K. Fc gamma receptor polymorphisms in systemic lupus erythematosus and their correlation with the clinical severity of the disease. Indian J Hum Genet 2008;14:77–81.

79. Urbonaviciute V, Furnrohr BG, Meister S, et al. Induction of inflammatory and immune responses by HMGB1-nucleosome complexes: implications for the pathogenesis of SLE. J Exp Med 2008;205:3007–18.

80. Santoni M, Massari F, Amantini C, et al. Emerging role of tumor-associated macrophages as therapeutic targets in patients with metastatic renal cell carcinoma. Cancer Immunol Immunother 2013;62:1757–68.

81. Nagai H and Toyokuni S. Biopersistent fiber-induced inflammation and carcinogenesis: lessons learned from asbestos toward safety of fibrous nanomaterials. Arch Biochem Biophys 2010;502:1–7.

82. Jiang Y, Fei W, Cen X, Tang Y, and Liang X. Near-infrared light activatable multimodal gold nanostructures platform: an emerging paradigm for cancer therapy. Curr Cancer Drug Targets 2015;15:406–22.

83. Wang HY, Hua XW, Wu FG, et al. Synthesis of ultrastable copper sulfide nanoclusters via trapping the reaction intermediate: potential anticancer and antibacterial applications. ACS Appl Mater Interfaces 2015;7:7082–92.

84. Ley K, Miller YI, and Hedrick CC. Monocyte and macrophage dynamics during atherogenesis. Arterioscler Thromb Vasc Biol 2011;31:1506–16.

85. Bekkering S, Joosten LA, Meer JW van der, Netea MG, and Riksen NP. The epigenetic memory of monocytes and macrophages as a novel drug target in atherosclerosis. Clin Ther 2015;37:914–23.

86. Buttari B, Profumo E, and Rigano R. Crosstalk between red blood cells and the immune system and its impact on atherosclerosis. Biomed Res Int 2015;2015:616834.

87. Boyle JJ, Johns M, Kampfer T, et al. Activating transcription factor 1 directs Mhem atheroprotective macrophages through coordinated iron handling and foam cell protection. Circ Res 2012;110:20–33.

88. Gleissner CA. Macrophage phenotype modulation by CXCL4 in atherosclerosis. Front Physiol 2012;3:1.

89. Colin S, Chinetti-Gbaguidi G, and Staels B. Macrophage phenotypes in atherosclerosis. Immunol Rev 2014;262:153–66.

90. Ying Z, Kampfrath T, Thurston G, et al. Ambient particulates alter vascular function through induction of reactive oxygen and nitrogen species. Toxicol Sci 2009;111:80–8.

91. Brook RD, Rajagopalan S, Pope C. A. 3, et al. Particulate matter air pollution and cardiovascular disease: an update to the scientific statement from the American Heart Association. Circulation 2010;121:2331–78.

92. Rylance J, Fullerton DG, Scriven J, et al. Household air pollution causes dose-dependent inflammation and altered phagocytosis in human macrophages. Am J Respir Cell Mol Biol 2014;52:584–93.

93. Dittmar T and Zänker KS. Cell Fusion in Health and Disease - II: Cell Fusion in Disease. Advances in Experimental Medicine and Biology 950. Springer Netherlands, 2011. 204 pp. URL: http://www.springer.com/biomed/book/978-94-007-0781-8 (visited on 02/22/2015).

94. Alvarez-Dolado M, Pardal R, Garcia-Verdugo JM, et al. Fusion of bone-marrow-derived cells with Purkinje neurons, cardiomyocytes and hepatocytes. Nature 2003;425:968–73.

95. Lluis F and Cosma MP. Cell-fusion-mediated somatic-cell reprogramming: a mechanism for tissue regeneration. J Cell Physiol 2010;223:6–13.

96. Helming L and Gordon S. Macrophage fusion induced by IL-4 alternative activation is a multistage process involving multiple target molecules. Eur J Immunol 2007;37:33–42.

97. Maarsseveen TCMT van, Vos W, and Diest PJ van. Giant cell formation in sarcoidosis Cell fusion or proliferation with non-division. Clin Exp Immunol 2009;155:476–86.

98. Machlus KR and Italiano JE. The incredible journey: from megakaryocyte development to platelet formation. J Cell Biol 2013;201:785–96.

99. Langhans T. Ueber Riesenzellen mit wandständigen Kernen in Tuberkeln und die fibröse Form des Tuberkels. Virchows Arch Pathol Anat Physiol Klin Med 1868;42:382–404.

100. Aterman K, Remmele W, and Smith M. Karl Touton and his "xanthelasmatic giant cell." A selective review of multinucleated giant cells. Am J Dermatopathol 1988;10:257–69.

101. Touton K. Ueber das Xanthom, insbesondere dessen Histiologie und Histiogenese. Vierteljahresschrift f Dermatol u Syph 1885;17:3–53.

102. Fraser W, Haffejee Z, and Cooper K. Rheumatic Aschoff nodules revisited: an immunohistological reappraisal of the cellular component. Histopathology 1995;27:457–61.

103. Chopra P, Wanninang J, and Sampath Kumar A. Immunohistochemical and histochemical profile of Aschoff bodies in rheumatic carditis in excised left atrial appendages: an immunoperoxidase study in fresh and paraffin-embedded tissue. Int J Cardiol 1992;34:199–207.

104. Stehbens WE and Zuccollo JM. Anitschkow myocytes or cardiac histiocytes in human hearts. Pathology 1999;31:98–101.

105. Krueger D. Clinical impact of mTOR inhibitors on the management of subependymal giant cell astrocytomas in tuberous sclerosis complex. Int J Clin Rev 2011.

106. Rickert CH. Cortical dysplasia: neuropathological aspects. Childs Nerv Syst 2006;22:821–6.

107. Gómez-Mateo MdC and Monteagudo C. Nonepithelial skin tumors with multinucleated giant cells. Semin Diagn Pathol 2013;30:58–72.

108. Magro G, Amico P, Vecchio GM, et al. Multinucleated floret-like giant cells in sporadic and NF1-associated neurofibromas: a clinicopathologic study of 94 cases. Virchows Arch 2009;456:71–6.

109. Hassanein A, Telang G, Benedetto E, and Spielvogel R. Subungual myxoid pleomorphic fibroma. Am J Dermatopathol 1998;20:502–5.

110. Kim EJ, Park HS, Yoon HS, and Cho S. A case of perforating dermatofibroma with floret-like giant cells. Clin Exp Dermatol 2015;40:305–8.

111. Zhang L, Peeples ME, Boucher RC, Collins PL, and Pickles RJ. Respiratory syncytial virus infection of human airway epithelial cells is polarized, specific to ciliated cells, and without obvious cytopathology. J Virol 2002;76:5654–66.

112. Schoolmeester JK and Smyrk TC. Multinucleated epithelial giant cells in the duodenum. Int J Surg Pathol 2013;21:202–4.

113. Cohen PR, Paravar T, and Lee RA. Epidermal multinucleated giant cells are not always a histopathologic clue to a herpes virus infection: multinucleated epithelial giant cells in the epidermis of lesional skin biopsies from patients with acantholytic dermatoses can histologically mimic a herpes virus infection. Dermatol Pract Concept 2014;4:21–7.

114. Iolascon A, Heimpel H, Wahlin A, and Tamary H. Congenital dyserythropoietic anemias: molecular insights and diagnostic approach. Blood 2013;122:2162–6.

115. Holt DJ and Grainger DW. Multinucleated giant cells from fibroblast cultures. Biomaterials 2011;32:3977–87.

116. Devaney K, Goodman ZD, and Ishak KG. Postinfantile giant-cell transformation in hepatitis. Hepatology 1992;16:327–33.

117. Gábor L, Pál K, and Zsuzsa S. Giant cell hepatitis in adults. Pathol Oncol Res 1997;3:215–8.

118. Cohen LM. The starburst giant cell is useful for distinguishing lentigo maligna from photodamaged skin. J Am Acad Dermatol 1996;35:962–8.

119. Patino WD, Hutchens KA, Kapil J, Chiou Y, and Gottlieb GJ. Eosinophilic cytoplasmic inclusion bodies in vesicular multinucleated melanocytes: a clue to the diagnosis of benign melanocytic lesions. Am J Dermatopathol 2012;34:424–7.

120. Küppers R and Hansmann ML. The Hodgkin and Reed/Sternberg cell. Int J Biochem Cell Biol 2005;37:511–7.

121. Rengstl B, Rieger MA, and Newrzela S. On the origin of giant cells in Hodgkin lymphoma. Commun Integr Biol 2014;7:e28602.

122. Kamel OW, LeBrun DP, Berry GJ, Dorfman RF, and Warnke RA. Warthin-Finkeldey polykaryocytes demonstrate a T-cell immunophenotype. Am J Clin Pathol 1992;97:179–83.

123. Orenstein JM. The Warthin-Finkeldey-type giant cell in HIV infection, what is it? Ultrastruct Pathol 1998;22:293–303.

124. Papadimitriou JM, Sforsina D, and Papaelias L. Kinetics of multinucleate giant cell formation and their modification by various agents in foreign body reactions. Am J Pathol 1973;73:349–64.

125. Zhao QH, Anderson JM, Hiltner A, Lodoen GA, and Payet CR. Theoretical analysis on cell size distribution and kinetics of foreign-body giant cell formation in vivo on polyurethane elastomers. J Biomed Mater Res 1992;26:1019–38.

126. Honma T and Hamasaki T. Ultrastructure of multinucleated giant cell apoptosis in foreign-body granuloma. Virchows Arch 1996;428:165–76.

127. Anderson JM. Multinucleated giant cells. Curr Opin Hematol 2000;7:40–7.

128. McNally AK and Anderson JM. Macrophage fusion and multinucleated giant cells of inflammation. In: *Cell fusion in health and disease*. Ed. by Dittmar T and Zänker KS. Advances in experimental medicine and biology. Dordrecht: Springer Netherlands, 2011:97–111. DOI: 10.1007/978-94-007-0763-4_7. (Visited on 08/30/2018).

129. McInnes A and Rennick DM. Interleukin 4 induces cultured monocytes/macrophages to form giant multinucleated cells. J Exp Med 1988;167:598–611.

130. DeFife KM, Jenney CR, McNally AK, Colton E, and Anderson JM. Interleukin-13 induces human monocyte/macrophage fusion and macrophage mannose receptor expression. J Immunol 1997;158:3385–90.

131. Weinberg JB, Hobbs MM, and Misukonis MA. Recombinant human gamma-interferon induces human monocyte polykaryon formation. Proc Natl Acad Sci U S A 1984;81:4554–7.

132. McNally AK and Anderson JM. Interleukin-4 induces foreign body giant cells from human monocytes/macrophages. Differential lymphokine regulation of macrophage fusion leads to morphological variants of multinucleated giant cells. Am J Pathol 1995;147:1487–99.

133. Kondo Y, Yasui K, Yashiro M, Tsuge M, Kotani N, and Morishima T. Multi-nucleated giant cell formation from human cord blood monocytes in vitro, in comparison with adult peripheral blood monocytes. Clin Exp Immunol 2009;158:84–90.

134. Sakai H, Okafuji I, Nishikomori R, et al. The CD40–CD40L axis and IFN-γ play critical roles in Langhans giant cell formation. Int Immunol 2012;24:5–15.

135. McNally AK and Anderson JM. Foreign body-type multinucleated giant cell formation is potently induced by α-tocopherol and prevented by the diacylglycerol kinase inhibitor R59022. Am J Pathol 2003;163:1147–56.

136. Abe E, Miyaura C, Tanaka H, et al. 1 alpha,25-dihydroxyvitamin D3 promotes fusion of mouse alveolar macrophages both by a direct mechanism and by a spleen cell-mediated indirect mechanism. Proc Natl Acad Sci U S A 1983;80:5583–7.

137. Hassan NF, Kamani N, Meszaros MM, and Douglas SD. Induction of multinucleated giant cell formation from human blood-derived monocytes by phorbol myristate acetate in in vitro culture. J Immunol 1989;143:2179–84.

138. Takashima T, Ohnishi K, Tsuyuguchi I, and Kishimoto S. Differential regulation of formation of multinucleated giant cells from concanavalin A-stimulated human blood monocytes by IFN-gamma and IL-4. J Immunol 1993;150:3002–10.

139. Miyamoto T and Suda T. Molecules Regulating Macrophage Fusions. In: *Cell Fusions*. Springer, Dordrecht, 2011:233–48. DOI: 10.1007/978-90-481-9772-9_11. URL: https://link.springer.com/chapter/10.1007/978-90-481-9772-9_11 (visited on 04/20/2018).

140. Vignery A. Macrophage Fusion: The Making of a New Cell. In: *Cell Fusions*. Springer, Dordrecht, 2011:219–31. DOI: 10.1007/978-90-481-9772-9_10. URL: https://link.springer.com/chapter/10.1007/978-90-481-9772-9_10 (visited on 04/20/2018).

141. Helming L and Gordon S. Molecular mediators of macrophage fusion. Trends Cell Biol 2009;19:514–22.

142. Quinn MT and Schepetkin IA. Role of NADPH oxidase in formation and function of multinucleated giant cells. J Innate Immun 2009;1:509–26.

143. Aguilar PS, Baylies MK, Fleissner A, et al. Genetic basis of cell-cell fusion mechanisms. Trends Genet 2013;29:427–37.

144. MacLauchlan S, Skokos EA, Meznarich N, et al. Macrophage fusion, giant cell formation, and the foreign body response require matrix metalloproteinase 9. J Leukoc Biol 2009;85:617–26.

145. Moreno JL, Mikhailenko I, Tondravi MM, and Keegan AD. IL-4 promotes the formation of multinucleated giant cells from macrophage precursors by a STAT6-dependent, homotypic mechanism: contribution of E-cadherin. J Leukoc Biol 2007;82:1542–53.

146. Miyamoto T. STATs and macrophage fusion. JAKSTAT 2013;2:e24777.

147. Jay SM, Skokos E, Laiwalla F, Krady MM, and Kyriakides TR. Foreign body giant cell formation is preceded by lamellipodia formation and can be attenuated by inhibition of Rac1 activation. Am J Pathol 2007;171:632–40.

148. McNally AK, MacEwan SR, and Anderson JM. alpha subunit partners to beta1 and beta2 integrins during IL-4-induced foreign body giant cell formation. J Biomed Mater Res A 2007;82A:568–74.

149. Lemaire I, Falzoni S, and Adinolfi E. Purinergic signaling in giant cell formation. Front Biosci (Elite Ed) 2012;4:41–55.

150. Helming L, Winter J, and Gordon S. The scavenger receptor CD36 plays a role in cytokine-induced macrophage fusion. J Cell Sci 2009;122:453–9.

151. Schlesinger L, Musson RA, and Johnston RB. Functional and biochemical studies of multinucleated giant cells derived from the culture of human monocytes. J Exp Med 1984;159:1289–94.

152. Enelow RI, Sullivan GW, Carper HT, and Mandell GL. Cytokine-induced human multinucleated giant cells have enhanced candidacidal activity and oxidative capacity compared with macrophages. J Infect Dis 1992;166:664–8.

153. Lay G, Poquet Y, Salek-Peyron P, et al. Langhans giant cells from M. tuberculosis-induced human granulomas cannot mediate mycobacterial uptake. J Pathol 2007;211:76–85.

154. DeFife KM, Jenney CR, Colton E, and Anderson JM. Cytoskeletal and adhesive structural polarizations accompany IL-13-induced human macrophage fusion. J Histochem Cytochem 1999;47:65–74.

155. Zhao Q, Topham N, Anderson JM, Hiltner A, Lodoen G, and Payet CR. Foreign-body giant cells and polyurethane biostability: In vivo correlation of cell adhesion and surface cracking. J Biomed Mater Res 1991;25:177–83.

156. Zhu XW, Price NM, Gilman RH, Recarvarren S, and Friedland JS. Multinucleate giant cells release functionally unopposed matrix metalloproteinase-9 in vitro and in vivo. J Infect Dis 2007;196:1076–9.

157. Park JK, Rosen A, Saffitz JE, et al. Expression of cathepsin K and tartrate-resistant acid phosphatase is not confined to osteoclasts but is a general feature of multinucleated giant cells: systematic analysis. Rheumatology (Oxford) 2013;52:1529–33.

158. Lau YS, Sabokbar A, Gibbons CLMH, Giele H, and Athanasou N. Phenotypic and molecular studies of giant-cell tumors of bone and soft tissue. Hum Pathol 2005;36:945–54.

159. Cowan RW and Singh G. Giant cell tumor of bone: a basic science perspective. Bone 2013;52:238–46.

160. Kawanami O, Basset F, Barrios R, Lacronique JG, Ferrans VJ, and Crystal RG. Hypersensitivity pneumonitis in man. Light- and electron-microscopic studies of 18 lung biopsies. Am J Pathol 1983;110:275–89.

161. Castonguay MC, Ryu JH, Yi ES, and Tazelaar HD. Granulomas and giant cells in hypersensitivity pneumonitis. Hum Pathol 2015;46:607–13.

162. Prieditis H and Adamson IYR. Alveolar macrophage kinetics and multinucleated giant cell formation after lung injury. J Leukoc Biol 1996;59:534–8.

163. Warheit DB, Sayes CM, Frame SR, and Reed KL. Pulmonary exposures to Sepiolite nanoclay particulates in rats: Resolution following multinucleate giant cell formation. Toxicol Lett 2010;192:286–93.

164. Beno M, Hurbankova M, Dusinska M, et al. Multinucleate cells (MNC) as sensitive semiquantitative biomarkers of the toxic effect after experimental fibrous dust and cigarette smoke inhalation by rats. Exp Toxicol Pathol 2005;57:77–87.

165. Silva RM, Xu J, Saiki C, et al. Short versus long silver nanowires: a comparison of in vivo pulmonary effects post instillation. Part Fibre Toxicol 2014;11:52.

166. Porter DW, Hubbs AF, Mercer RR, et al. Mouse pulmonary dose- and time course-responses induced by exposure to multi-walled carbon nanotubes. Toxicology 2010;269:136–47.

167. Nemery B and Abraham JL. Hard metal lung disease: still hard to understand. Am J Respir Crit Care Med 2007;176:2–3.

168. Tanaka J, Moriyama H, Terada M, et al. An observational study of giant cell interstitial pneumonia and lung fibrosis in hard metal lung disease. BMJ Open 2014;4:e004407.

169. Freiman DG and Hardy HL. Beryllium disease: The relation of pulmonary pathology to clinical course and prognosis based on a study of 130 cases from the U.S. Beryllium Case Registry. Hum Pathol 1970;1:25–44.

170. Limas C. The spectrum of primary cutaneous elastolytic granulomas and their distinction from granuloma annulare: a clinicopathological analysis. Histopathology 2004;44:277–82.

171. Mahadeva U, Martin JP, Patel NK, and Price AB. Granulomatous ulcerative colitis: a re-appraisal of the mucosal granuloma in the distinction of Crohn's disease from ulcerative colitis. Histopathology 2002;41:50–5.

172. Favara BE and Jaffe R. The histopathology of Langerhans cell histiocytosis. Br J Cancer Suppl 1994;23:S17–23.

173. Koizumi F, Matsuno H, Wakaki K, Ishii Y, Kurashige Y, and Nakamura H. Synovitis in rheumatoid arthritis: scoring of characteristic histopathological features. Pathol Int 1999;49:298–304.

174. Hunder GG, Bloch DA, Michel BA, et al. The American College of Rheumatology 1990 criteria for the classification of giant cell arteritis. Arthritis Rheum 1990;33:1122–8.

175. Kim KR and Scully RE. Peritoneal keratin granulomas with carcinomas of endometrium and ovary and atypical polypoid adenomyoma of endometrium a clinicopathological analysis of 22 cases. Am J Surg Pathol 1990;14:925–32.

176. Bayliss OB. The giant cell in cholesterol resorption. Br J Exp Pathol 1976;57:610–8.

177. Lai S and Zhou X. Inflammatory Cells in Tissues of Gout Patients and Their Correlations with Comorbidities. Open Rheumatol J 2013;7:26–31.

178. Anderson JM, Rodriguez A, and Chang DT. Foreign body reaction to biomaterials. Semin Immunol 2008;20:86–100.

179. Krewski D, Yokel RA, Nieboer E, et al. Human health risk assessment for aluminium, aluminium oxide, and aluminium hydroxide. J Toxicol Environ Health B Crit Rev sup1 2007;10:1–269.

180. Black MM and Epstein WL. Formation of multinucleate giant cells in organized epithelioid cell granulomas. Am J Pathol 1974;74:263–74.

181. Nemery B, Verbeken EK, and Demedts M. Giant cell interstitial pneumonia (hard metal lung disease, cobalt lung). Semin Respir Crit Care Med 2001;22:435–48.

182. Takemura T, Rom WN, Ferrans VJ, and Crystal RG. Morphologic characterization of alveolar macrophages from subjects with occupational exposure to inorganic particles. Am Rev Respir Dis 1989;140:1674–85.

183. Marchiori E, Lourenço S, Gasparetto TD, Zanetti G, Mano CM, and Nobre LF. Pulmonary talcosis: imaging findings. Lung 2010;188:165–71.

184. Ko CJ and Glusac EJ. Chapter 14 Noninfectious Granulomas of the Skin. In: *Lever's Histopathology of the Skin*. 11th ed. Lippincott Williams & Wilkins, 2014:1544. URL: https://www.lww.com/Product/9781451190373 (visited on 04/13/2015).

185. Hunt AC and Bothwell PW. Histological findings in human brucellosis. J Clin Pathol 1967;20:267–72.

186. Rosado FG, Stratton CW, and Mosse CA. Clinicopathologic correlation of epidemiologic and histopathologic features of pediatric bacterial lymphadenitis. Arch Pathol Lab Med 2011;135:1490–3.

187. Lockwood DN, Lucas SB, Desikan KV, Ebenezer G, Suneetha S, and Nicholls P. The histological diagnosis of leprosy type 1 reactions: identification of key variables and an analysis of the process of histological diagnosis. J Clin Pathol 2008;61:595–600.

188. Barrett AW, Villarroel Dorrego M, Hodgson TA, et al. The histopathology of syphilis of the oral mucosa. J Oral Pathol Med 2004;33:286–91.

189. Fungal Infections. In: *Dermatopathology*. Ed. by Elston DM, Peckham S, High WA, DiCaudo DJ, and Ko CJ. 2nd ed. Elsevier Health Sciences, 2014:270–85.

190. Das R, Dey P, Chakrabarti A, and Ray P. Fine-needle aspiration biopsy in fungal infections. Diagn Cytopathol 1997;16:31–4.

191. Shibuya K, Hirata A, Omuta J, et al. Granuloma and cryptococcosis. J Infect Chemother 2005;11:115–22.

192. Araya J, Kawabata Y, Tomichi N, et al. Allergic inflammatory reaction is involved in necrosis of human pulmonary dirofilariasis. Histopathology 2007;51:484–90.

193. Gatrill AJ, Mackenzie CD, McMahon JE, Williams JF, and Guderian RH. A histocytochemical study of the macrophages present in tissue responses to adult Onchocerca volvulus. Histochem J 1987;19:509–19.

194. Mehregan DR, Mehregan AH, and Mehregan DA. Histologic diagnosis of cutaneous leishmaniasis. Clin Dermatol 1999;17:297–304.

195. Geboes K, el-Dosoky I, el-Wahab A, and Abou Almagd K. The immunopathology of Schistosoma mansoni granulomas in human colonic schistosomiasis. Virchows Arch A Pathol Anat Histopathol 1990;416:527–34.

196. McNally AK and Anderson JM. Phenotypic expression in human monocyte-derived interleukin-4-induced foreign body giant cells and macrophages in vitro: dependence on material surface properties. J Biomed Mater Res A 2015;103A:1380–90.

197. Jay SM, Skokos EA, Zeng J, Knox K, and Kyriakides TR. Macrophage fusion leading to foreign body giant cell formation persists under phagocytic stimulation by microspheres in vitro and in vivo in mouse models. J Biomed Mater Res A 2010;93A:189–99.

198. Lemaire I, Falzoni S, Zhang B, Pellegatti P, and Virgilio FD. The P2X7 receptor and Pannexin-1 are both required for the promotion of multinucleated macrophages by the inflammatory cytokine GM-CSF. J Immunol 2011;187:3878–87.

199. Yagi M, Ninomiya K, Fujita N, et al. Induction of DC-STAMP by alternative activation and downstream signaling mechanisms. J Bone Miner Res 2007;22:992–1001.

200. Warfel AH. Macrophage fusion and multinucleated giant cell formation, surface morphology. Exp Mol Pathol 1978;28:163–76.

201. Tambuyzer BR and Nouwen EJ. Inhibition of microglia multinucleated giant cell formation and induction of differentiation by GM-CSF using a porcine in vitro model. Cytokine 2005;31:270–9.

202. Ikeda T, Ikeda K, Sasaki K, et al. IL-13 as well as IL-4 induces monocytes/macrophages and a monoblastic cell line (UG3) to differentiate into multinucleated giant cells in the presence of M-CSF. Biochem Biophys Res Commun 1998;253:265–72.

203. Xu Y, Zhan Y, Lew AM, Naik SH, and Kershaw MH. Differential development of murine dendritic cells by GM-CSF versus Flt3 ligand has implications for inflammation and trafficking. J Immunol 2007;179:7577–84.

204. Akagawa KS, Takasuka N, Nozaki Y, et al. Generation of CD1+RelB+ dendritic cells and tartrate-resistant acid phosphatase-positive osteoclast-like multinucleated giant cells from human monocytes. Blood 1996;88:4029–39.

205. Lacey DC, Achuthan A, Fleetwood AJ, et al. Defining GM-CSF– and macrophage-CSF–dependent macrophage responses by in vitro models. J Immunol 2012;188:5752–65.

206. Dong R, Moulding D, Himoudi N, et al. Cells with dendritic cell morphology and immunophenotype, binuclear morphology, and immunosuppressive function in dendritic cell cultures. Cell Immunol 2011;272:1–10.

207. Oh Y, Oh I, Morimoto J, Uede T, and Morimoto A. Osteopontin has a crucial role in osteoclast-like multinucleated giant cell formation. J Cell Biochem 2014;115:585–95.

208. Rivollier A, Mazzorana M, Tebib J, et al. Immature dendritic cell transdifferentiation into osteoclasts: a novel pathway sustained by the rheumatoid arthritis microenvironment. Blood 2004;104:4029–37.

209. Pegoraro G, Eaton BP, Ulrich RL, et al. A high-content imaging assay for the quantification of the Burkholderia pseudomallei induced multinucleated giant cell (MNGC) phenotype in murine macrophages. BMC Microbiol 2014;14:98.

210. Yagi M, Miyamoto T, Sawatani Y, et al. DC-STAMP is essential for cell–cell fusion in osteoclasts and foreign body giant cells. J Exp Med 2005;202:345–51.

211. Dutta DK, Potnis PA, Rhodes K, and Wood SC. Wear particles derived from metal hip implants induce the generation of multinucleated giant cells in a 3-dimensional peripheral tissue-equivalent model. PLoS One 2015;10:e0124389.

212. Luttikhuizen D.T., Dankers P.Y.W., Harmsen M.C., and van Luyn M.J.A. Material dependent differences in inflammatory gene expression by giant cells during the foreign body reaction. J Biomed Mater Res A 2007;83A:879–86.

213. Seitzer U, Scheel-Toellner D, Toellner K, et al. Properties of multinucleated giant cells in a new in vitro model for human granuloma formation. J Pathol 1997;182:99–105.

214. Solari F, Domenget C, Gire V, et al. Multinucleated cells can continuously generate mononucleated cells in the absence of mitosis: a study of cells of the avian osteoclast lineage. J Cell Sci 1995;108:3233–41.

215. Dickson BC, Li SQ, Wunder JS, et al. Giant cell tumor of bone express p63. Mod Pathol 2008;21:369–75.

216. Tezuka Ki, Sato T, Kamioka H, et al. Identification of osteopontin in isolated rabbit osteoclasts. Biochem Biophys Res Commun 1992;186:911–7.

217. Collin-Osdoby P and Osdoby P. Isolation and culture of primary chicken osteoclasts. In: *Bone Research Protocols*. Ed. by Helfrich MH and Ralston SH. Methods in Molecular Biology. Totowa, NJ: Humana Press, 2012:119–43. DOI: 10.1007/978-1-61779-415-5_9. URL: https://doi.org/10.1007/978-1-61779-415-5_9 (visited on 08/31/2018).

218. Xu M, Song ZG, Xu CX, et al. IL-17A stimulates the progression of giant cell tumors of bone. Clin Cancer Res 2013;19:4697–705.

219. Milde R, Ritter J, Tennent GA, et al. Multinucleated giant cells are specialized for complement-mediated phagocytosis and large target destruction. Cell Rep 2015;13:1937–48.

220. Sissons JR, Peschon JJ, Schmitz F, Suen R, Gilchrist M, and Aderem A. Cutting edge: microRNA regulation of macrophage fusion into multinucleated giant cells. J Immunol 2012;189:23–7.

221. Helming L, Tomasello E, Kyriakides TR, et al. Essential role of DAP12 signaling in macrophage programming into a fusion-competent state. Sci Signal 2008;1:ra11.

222. Sheikh F, Dickensheets H, Pedras-Vasconcelos J, et al. The interleukin-13 receptor-α1 chain is essential for induction of the alternative macrophage activation pathway by IL-13 but not IL-4. J Innate Immun 2015;7:494–505.

223. Yu M, Qi X, Moreno JL, Farber DL, and Keegan AD. NF-κB signaling participates in both RANKL- and IL-4–induced macrophage fusion: receptor cross-talk leads to alterations in NF-κB pathways. J Immunol 2011;187:1797–806.

224. Moore LB, Sawyer AJ, Saucier-Sawyer J, Saltzman WM, and Kyriakides TR. Nanoparticle delivery of miR-223 to attenuate macrophage fusion. Biomaterials 2016;89:127–35.

225. Moore LB, Sawyer AJ, Charokopos A, Skokos EA, and Kyriakides TR. Loss of monocyte chemoattractant protein-1 alters macrophage polarization and reduces NFκB activation in the foreign body response. Acta Biomater 2015;11:37–47.

226. Skokos EA, Charokopos A, Khan K, Wanjala J, and Kyriakides TR. Lack of TNF-α–induced MMP-9 production and abnormal E-Cadherin redistribution associated with compromised fusion in MCP-1–null macrophages. Am J Pathol 2011;178:2311–21.

227. Katsuyama E, Miyamoto H, Kobayashi T, et al. Interleukin-1 receptor-associated kinase-4 (IRAK4) promotes inflammatory osteolysis by activating osteoclasts and inhibiting formation of foreign body giant cells. J Biol Chem 2015;290:716–26.

228. Miyamoto H, Katsuyama E, Miyauchi Y, et al. An essential role for STAT6-STAT1 protein signaling in promoting macrophage cell-cell fusion. J Biol Chem 2012;287:32479–84.

229. Miyamoto H, Suzuki T, Miyauchi Y, et al. Osteoclast stimulatory transmembrane protein and dendritic cell–specific transmembrane protein cooperatively modulate cell–cell fusion to form osteoclasts and foreign body giant cells. J Bone Miner Res 2012;27:1289–97.

230. Oya A, Katsuyama E, Morita M, et al. Tumor necrosis factor receptor-associated factor 6 is required to inhibit foreign body giant cell formation and activate osteoclasts under inflammatory and infectious conditions. J Bone Miner Metab 2017:1–12.

231. Khan UA, Hashimi SM, Bakr MM, Forwood MR, and Morrison NA. CCL2 and CCR2 are essential for the formation of osteoclasts and foreign body giant cells. J Cell Biochem 2016;117:382–9.

232. Khan UA, Hashimi SM, Bakr MM, Forwood MR, and Morrison NA. Foreign body giant cells and osteoclasts are TRAP positive, have podosome-belts and both require OC-STAMP for cell fusion. J Cell Biochem 2013;114:1772–8.

233. Binder F, Hayakawa M, Choo MK, Sano Y, and Park JM. Interleukin-4-induced β-catenin regulates the conversion of macrophages to multinucleated giant cells. Mol Immunol 2013;54:157–63.

234. Wang HY, Jia HR, Lu X, et al. Imaging plasma membranes without cellular internalization: multisite membrane anchoring reagents based on glycol chitosan derivatives. J Mater Chem B Mater Biol Med 2015;3:6165–73.

235. Faust JJ, Christenson W, Doudrick K, Ros R, and Ugarova TP. Development of fusogenic glass surfaces that impart spatiotemporal control over macrophage fusion: direct visualization of multinucleated giant cell formation. Biomaterials 2017;128:160–71.

236. Medicine I of. Immunology of silicone. In: *Safety of Silicone Breast Implants*. Ed. by Bondurant S, Ernster V, and Herdman R. Washington, DC: National Academies Press, 1999. DOI: 10.17226/9602. URL: http://www.nap.edu/catalog/9602 (visited on 02/28/2019).

237. Vignery A, Niven-Fairchild T, and Shepard MH. Recombinant murine interferon-γ inhibits the fusion of mouse alveolar macrophages in vitro but stimulates the formation of osteoclastlike cells on implanted syngeneic bone particles in mice in vivo. J Bone Miner Res 1990;5:637–44.

238. Gharun K, Senges J, Seidl M, et al. Mycobacteria exploit nitric oxide-induced transformation of macrophages into permissive giant cells. EMBO Rep 2017;18:2144–59.

239. Kern I, Kecelj P, Košnik M, and Mermolja M. Multinucleated giant cells in bronchoalveolar lavage. Acta Cytol 2003;47:426–30.

240. Davison AG, Haslam PL, Corrin B, et al. Interstitial lung disease and asthma in hard-metal workers: bronchoalveolar lavage, ultrastructural, and analytical findings and results of bronchial provocation tests. Thorax 1983;38:119–28.

241. Kamp DW, Israbian VA, Yeldandi AV, Panos RJ, Graceffa P, and Weitzman SA. Phytic acid, an iron chelator, attenuates pulmonary inflammation and fibrosis in rats after intratracheal instillation of asbestos. Toxicol Pathol 1995;23:689–95.

242. Lemaire I. Characterization of the bronchoalveolar cellular response in experimental asbestosis. Different reactions depending on the fibrogenic potential. Am Rev Respir Dis 1985;131:144–9.

243. Lemaire I. Selective differences in macrophage populations and monokine production in resolving pulmonary granuloma and fibrosis. Am J Pathol 1991;138:487–95.

244. Murphy FA, Poland CA, Duffin R, and Donaldson K. Length-dependent pleural inflammation and parietal pleural responses after deposition of carbon nanotubes in the pulmonary airspaces of mice. Nanotoxicology 2012;7:1157–67.

245. Kinaret P, Ilves M, Fortino V, et al. Inhalation and oropharyngeal aspiration exposure to rod-like carbon nanotubes induce similar airway inflammation and biological responses in mouse lungs. ACS Nano 2017;11:291–303.

246. Moriyama H, Kobayashi M, Takada T, et al. Two-dimensional analysis of elements and mononuclear cells in hard metal lung disease. Am J Respir Crit Care Med 2007;176:70–7.

247. Biswas R, Trout KL, Jessop F, Harkema JR, and Holian A. Imipramine blocks acute silicosis in a mouse model. Part Fibre Toxicol 2017;14:36.

248. Hamilton Jr RF, Wu N, Porter D, Buford M, Wolfarth M, and Holian A. Particle length-dependent titanium dioxide nanomaterials toxicity and bioactivity. Part Fibre Toxicol 2009;6:35.

249. Porter D, Sriram K, Wolfarth M, et al. A biocompatible medium for nanoparticle dispersion. Nanotoxicology 2008;2:144–54.

250. Xia T, Hamilton Jr RF, Bonner JC, et al. Interlaboratory evaluation of in vitro cytotoxicity and inflammatory responses to engineered nanomaterials: the NIEHS Nano GO consortium. Environ Health Perspect 2013;121:683–90.

251. Thakur SA, Hamilton Jr R, Pikkarainen T, and Holian A. Differential binding of inorganic particles to MARCO. Toxicol Sci 2009;107:238–46.

252. Hamilton Jr RF, Buford M, Xiang C, Wu N, and Holian A. NLRP3 inflammasome activation in murine alveolar macrophages and related lung pathology is associated with MWCNT nickel contamination. Inhal Toxicol 2012;24:995–1008.

253. Blake DJ, Bolin CM, Cox DP, Cardozo-Pelaez F, and Pfau JC. Internalization of Libby amphibole asbestos and induction of oxidative stress in murine macrophages. Toxicol Sci 2007;99:277–88.

254. Girtsman TA, Beamer CA, Wu N, Buford M, and Holian A. IL-1R signalling is critical for regulation of multi-walled carbon nanotubes-induced acute lung inflammation in C57Bl/6 mice. Nanotoxicology 2014;8:17–27.

255. Jessop F, Hamilton Jr RF, Rhoderick JF, Fletcher P, and Holian A. Phagolysosome acidification is required for silica and engineered nanoparticle-induced lysosome membrane permeabilization and resultant NLRP3 inflammasome activity. Toxicol Appl Pharmacol 2017;318:58–68.

256. Whiteley L, Meffert T, Haug M, et al. Entry, intracellular survival and multinucleated giant cell-forming activity of Burkholderia pseudomallei in human primary phagocytic and non-phagocytic cells. Infect Immun 2017;85:e00468–17.

257. Bracq L, Xie M, Lambelé M, et al. T cell-macrophage fusion triggers multinucleated giant cell formation for HIV-1 spreading. J Virol 2017;91:e01237–17.

258. Nakanishi-Matsui M, Yano S, Matsumoto N, and Futai M. Lipopolysaccharide induces multinuclear cell from RAW264.7 line with increased phagocytosis activity. Biochem Biophys Res Commun 2012;425:144–9.

259. Franz S, Rammelt S, Scharnweber D, and Simon JC. Immune responses to implants – A review of the implications for the design of immunomodulatory biomaterials. Biomaterials 2011;32:6692–709.

260. Helming L and Gordon S. The molecular basis of macrophage fusion. Immunobiology 2008;212:785–93.

261. Harkel B ten, Schoenmaker T, Picavet DI, Davison NL, Vries TJ de, and Everts V. The foreign body giant cell cannot resorb bone, but dissolves hydroxyapatite like osteoclasts. PLoS One 2015;10:e0139564.

262. Bühling F, Reisenauer A, Gerber A, et al. Cathepsin K – a marker of macrophage differentiation? J Pathol 2001;195:375–82.

263. Khan UA, Hashimi SM, Khan S, et al. Differential expression of chemokines, chemokine receptors and proteinases by foreign body giant cells (FBGCs) and osteoclasts. J Cell Biochem 2014;115:1290–8.

264. Jones JA, Chang DT, Meyerson H, et al. Proteomic analysis and quantification of cytokines and chemokines from biomaterial surface-adherent macrophages and foreign body giant cells. J Biomed Mater Res A 2007;83A:585–96.

265. McNally AK and Anderson JM. Foreign body-type multinucleated giant cells induced by interleukin-4 express select lymphocyte co-stimulatory molecules and are phenotypically distinct from osteoclasts and dendritic cells. Exp Mol Pathol 2011;91:673–81.

266. Gerrard TL, Dyer DR, and Mostowski HS. IL-4 and granulocyte-macrophage colony-stimulating factor selectively increase HLA-DR and HLA-DP antigens but not HLA-DQ antigens on human monocytes. J Immunol 1990;144:4670–4.

267. Madel MB, Ibáñez L, Rouleau M, Wakkach A, and Blin-Wakkach C. A novel reliable and efficient procedure for purification of mature osteoclasts allowing functional assays in mouse cells. Front Immunol 2018;9:2567.

268. Drachman JG, Jarvik GP, and Mehaffey MG. Autosomal dominant thrombocytopenia: incomplete megakaryocyte differentiation and linkage to human chromosome 10. Blood 2000;96:118–25.

269. Lombardo E, Alvarez-Barrientos A, Maroto B, Boscá L, and Knaus UG. TLR4-mediated survival of macrophages is MyD88 dependent and requires TNF-α autocrine signalling. J Immunol 2007;178:3731–9.

270. Oppong-Nonterah GO, Lakhdari O, Yamamura A, Hoffman HM, and Prince LS. TLR activation alters bone marrow-derived macrophage differentiation. J Innate Immun 2019;11:99–108.

271. Brown TA, Holian A, Pinkerton KE, Lee JW, and Cho YH. Early life exposure to environmental tobacco smoke alters immune response to asbestos via a shift in inflammatory phenotype resulting in increased disease development. Inhal Toxicol 2016;28:349–56.

272. Perkins RC, Scheule RK, Hamilton R, Gomes G, Freidman G, and Holian A. Human alveolar macrophage cytokine release in response to in vitro and in vivo asbestos exposure. Exp Lung Res 1993;19:55–65.

273. Youn MY, Takada I, Imai Y, Yasuda H, and Kato S. Transcriptionally active nuclei are selective in mature multinucleated osteoclasts. Genes Cells 2010;15:1025–35.

274. Boissy P, Saltel F, Bouniol C, Jurdic P, and Machuca-Gayet I. Transcriptional activity of nuclei in multinucleated osteoclasts and its modulation by calcitonin. Endocrinology 2002;143:1913–21.